NASA CR-159425

# DUCT WALL IMPEDANCE CONTROL AS AN ADVANCED CONCEPT FOR ACOUSTIC SUPPRESSION

BY
PETER D. DEAN

OCTOBER 1978

(NASA-CR-159425) DUCT WALL IMPEDANCE CONTROL AS AN ADVANCED CONCEPT FOR ACOUSTIC SUPPRESSION ENHANCEMENT Final Report (Lockheed-Georgia Co., Marietta.) 115 p HC A06/MF A01 CSCL 20A G3/71

N79-10842

Unclas 33840

THE LOCKHEED-GEORGIA COMPANY
MARIETTA, GEORGIA

LG78ER0243

PREPARED FOR
NATIONAL AERONAUTICS AND SPACE ADMINISTRATION

NASA-LEWIS RESEARCH CENTER
CONTRACT NAS3-20071

| 1. Report No. | 2. Government Accession No. | 3. Recipient's Catalog No. |
|---|---|---|
| CR-159425 | | LG78ER0243 |

| 4. Title and Subtitle | 5. Report Date |
|---|---|
| VARIABLE IMPEDANCE DUCT LINERS AS AN ADVANCED CONCEPT FOR ACOUSTIC SUPPRESSION ENHANCEMENT | May 1978 |
| | 6. Performing Organization Code |

| 7. Author(s) | 8. Performing Organization Report No. |
|---|---|
| Peter D. Dean | |
| | 10. Work Unit No. |

| 9. Performing Organization Name and Address | 11. Contract or Grant No. |
|---|---|
| Lockheed-Georgia Company<br>A Division of the Lockheed Corporation<br>86 South Cobb Drive<br>Marietta, Georgia 30063 | NAS3-20071 |
| | 13. Type of Report and Period Covered |
| 12. Sponsoring Agency Name and Address | Final Contract Report |
| National Aeronautics and Space Administration<br>Washington, D. C. 20548 | 14. Sponsoring Agency Code |

15. Supplementary Notes

Project Manager: Dr. Kenneth Baumeister, V/STOL and Noise Division
NASA Lewis Research Center, Cleveland, Ohio 44135

16. Abstract

This report describes a systems concept procedure for the optimization of acoustic duct liner design for both uniform and multi-segment types. The concept was implemented by the use of a double reverberant chamber flow duct facility coupled with sophisticated computer control and acoustic analysis systems. The optimization procedure for liner insertion loss was based on the concept of variable liner impedance produced by "bias" air flow through a multi-layer, resonant cavity liner. A multiple microphone technique for in situ wall impedance measurements was used and successfully adapted to produce automated measurements for all liner configurations tested. The complete validation of the systems concept was prevented by the inability to optimize the insertion loss using bias flow induced wall impedance changes. This inability appeared to be a direct function of the presence of higher-order energy carrying modes which were not influenced significantly by the wall impedance changes.

| 17. Key Words (Suggested by Author(s)) | 18. Distribution Statement |
|---|---|
| Flow Duct Acoustics<br>Acoustic Treatment Optimization<br>Engine Duct Noise Suppression<br>Sound Absorbent Duct Liners | Unclassified - Unlimited |

| 19. Security Classif. (of this report) | 20. Security Classif. (of this page) | 21. No. of Pages | 22. Price* |
|---|---|---|---|
| UNCLASSIFIED | UNCLASSIFIED | 110 | |

*For sale by the National Technical Information Service, Springfield, Virginia 22161

# VARIABLE IMPEDANCE DUCT LINERS AS AN ADVANCED CONCEPT FOR ACOUSTIC SUPPRESSION ENHANCEMENT

by

Peter D. Dean

May 1978

Prepared under Contract NAS3-20071 by
LOCKHEED-GEORGIA COMPANY

for
NATIONAL AERONAUTICS AND SPACE ADMINISTRATION
Lewis Research Center
Cleveland, Ohio

## SUMMARY

This report describes a systems concept procedure for the optimization of acoustic duct liner design for both uniform and multi-segment types. The concept was implemented by use of a double reverberant chamber flow duct facility coupled with sophisticated computer control and acoustic analysis systems. The optimization procedure for liner insertion loss was based on the concept of variable liner impedance produced by "bias" air flow through a multi-layer, resonant cavity liner. A multiple microphone technique for in-situ wall impedance measurements was used and successfully adapted to produce automated measurements for all liner configurations tested. The complete validation of the systems concept was prevented by the inability to optimize the insertion loss using bias flow induced wall impedance changes. This inability appeared to be a direct function of the presence of higher-order energy carrying modes which were not influenced significantly by the wall impedance changes.

# CONTENTS

# 1. INTRODUCTION

The ultimate goal of the NASA aircraft noise reduction program is to reduce further the noise impact on the observer on the ground. A specific identifiable noise component is that generated internally within a gas turbine engine and propagating to the far field through the intake and bypass duct work. The work described in this report concerns the attenuation of this noise component by means of sound absorbent duct linings. In this context the application of duct linings has invariably concentrated on the quest for an "optimum" design.

It is a fair statement to say that through a proper combination of analytical models (as described in ref. 1) with empirical qualifications the aerospace industry can successfully produce duct liner designs for particular application to commercial turbo-fan engines. However, these "optimum" designs are inherently a compromise, being governed by factors which are dependent on the basic characteristics of actual engine application and operation, i.e. variable source distributions due to variable operating range, variable mean flow environments, and severe weight, size, engine performance degradation and cost constraints. It is these variables which limit the degree of optimization or efficiency of a practical lining design and the accepted methodology of design currently centers around time-consuming and expensive tests of alternative liners in reduced or full-scale versions of the engine. Since the attenuation performance of a liner is characterized by its acoustic impedance, it appears entirely feasible that an enormous amount of experimental time could be saved by the use of the variable impedance liner concept, as described in reference 2, which would enable in-situ changes and their resulting effects on attenuation to be immediately evaluated.

The advantages of this approach becomes more obvious if one considers the underlying basic characteristics of the state of the art of the liner design as follows:

(1) Acoustic theory of mode propagation in lined ducts with flow has been accepted as valid.

(2) The proper specification, in terms of modal content of what constitutes the actual source structure is debatable, as is the relative modal importance.

(3) The optimum liner design procedure is thus a direct function of the designer himself, who must face the decisions of optimum criteria, mode number, and frequency content to be analyzed theoretically; this is a possibly mammoth computational task.

(4) Multi-element liner approaches which are currently in vogue offer promise of improved attenuations over a uniform liner design with a large increase in the design analysis required.

(5) Liner hardware designs from impedance models of liner configurations perform reasonably well in zero grazing flow situations for small mode orders and noncritical impedance applications (i.e. where attenuation is not very sensitive to liner impedance).

(6) Nearly optimum impedance designs in grazing flow situations are unreliable due to inadequacies in modal formulations and in practical hardware manufacturing tolerances.

Thus, the traditional approach for impedance specification to a real life situation is a time-consuming complex analytical task coupled to the inherent practical difficulties and uncertainties of realization of this specified impedance into hardware.

With these characteristics in mind, the work described in this report centers on a systems concept which attempts to circumvent the above inherent problems of design; the aim being to provide a means of arriving at an optimum liner configuration using the concept of variable, in-situ liner impedance control. In essence, this concept utilizes the effect of steady air flow through a multi-layer, locally reacting, resonant cavity absorber. The effect of this "bias" flow through the resistive facing sheets of each layer is to change the layer acoustic resistance in a quasi-linear* manner. Since the liner cavity depths dominate the acoustic reactance, bias air induced reactive changes are accomplished by the decoupling of the intermediate layer cavity depths with a suitable choice of higher flow resistive sheets facing those layers. A more complete discussion of this concept is given in reference 2, however, its successful implementation is an essential component of the overall systems concept proposed in this work.

The systems concept embodies three basic objectives:

(1) To prove the application of the variable impedance (or bias flow) concept as a design tool for acoustic suppression in flow ducts.

(2) To determine the feasibility of using the variable impedance concept as a means of evaluating the effectiveness of multi-element liners.

(3) To measure the liner impedance in-situ once optimization has been achieved.

The first objective embodies the definition of the systems concept, its build-up and operation and is the major task in this report being a prerequisite for the remaining objectives.

*In this context quasi-linear refers to the dominant part of the relationship between acoustic resistance and incident bias flow velocity.

# 2. SYSTEMS CONCEPT

The system design concept centers around the development of an active control system which will control the impedance (by means of bias flow) of acoustic liner segments in such a way that the attenuation or insertion loss of the system will be maximized automatically for any given source structure and duct flow condition.

On attainment of this "optimum" condition, the wall impedance will be measured "in-situ" thus defining explicitly the "optimum" wall impedance for that particular source/flow situation. Thus, in principle, a complete locus map of optimum wall impedance versus source and flow conditions would be obtained extremely rapidly. In addition, the principle could be easily extended to segmented liners in the form of a multiple degree of freedom control system.

## 2.1 SYSTEM LOGIC

A block diagram of the concept control logic can be seen in figure 1. Once the source and duct flow parameters are set, the control loop will measure the insertion loss, perturb the bias flow (and thus the wall impedance), deduce the gradient of bias motion to maximize the insertion loss and predict the new values of bias flow based on a parabolic curve-fitting procedure. On reaching the peak value, the control loop will terminate and proceed to the wall impedance measurement.

The implementation of this logic is based on the following fundamental premises:

(1) The source modal content is not known exactly but is assumed to carry energy predominately in low order acoustic modes.

(2) For each given source type, there exists at least one or more values of wall impedance which results in a defined measurable maximum of insertion loss.

(3) These impedance values lie within the available range of the variable impedance liner.

The first two assumptions are linked in the sense that for the case of one propagating mode a well-defined maximum attenuation point will certainly exist (the branch point in the classical impedance plane or bulls-eye plot, as shown, for example, in figure 2, of the mode attenuation contours). For the case of the first two modes, again the classical Cremer optimum will exist. However, in the case of multiple modes of equal energy, it is not at all clear that a definable and physically measurable optimum impedance for energy attenuation will exist, hence, the necessity for the above assumptions. In addition, the complexity of finite length liner segments of variable impedance could result in multiple optimum solutions which are spaced in the

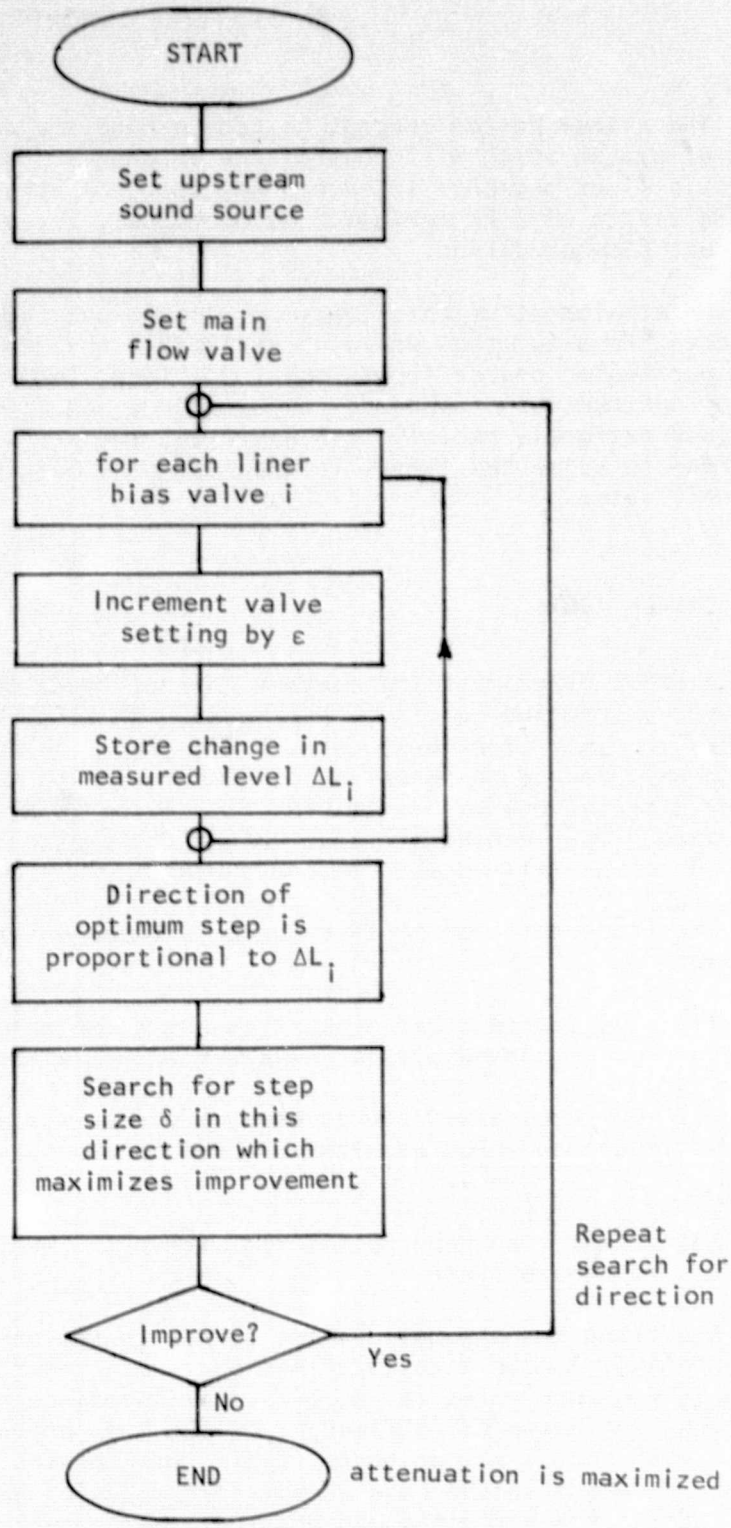


Figure 1. CONTROL CONCEPT SYSTEM LOGIC FLOW CHART

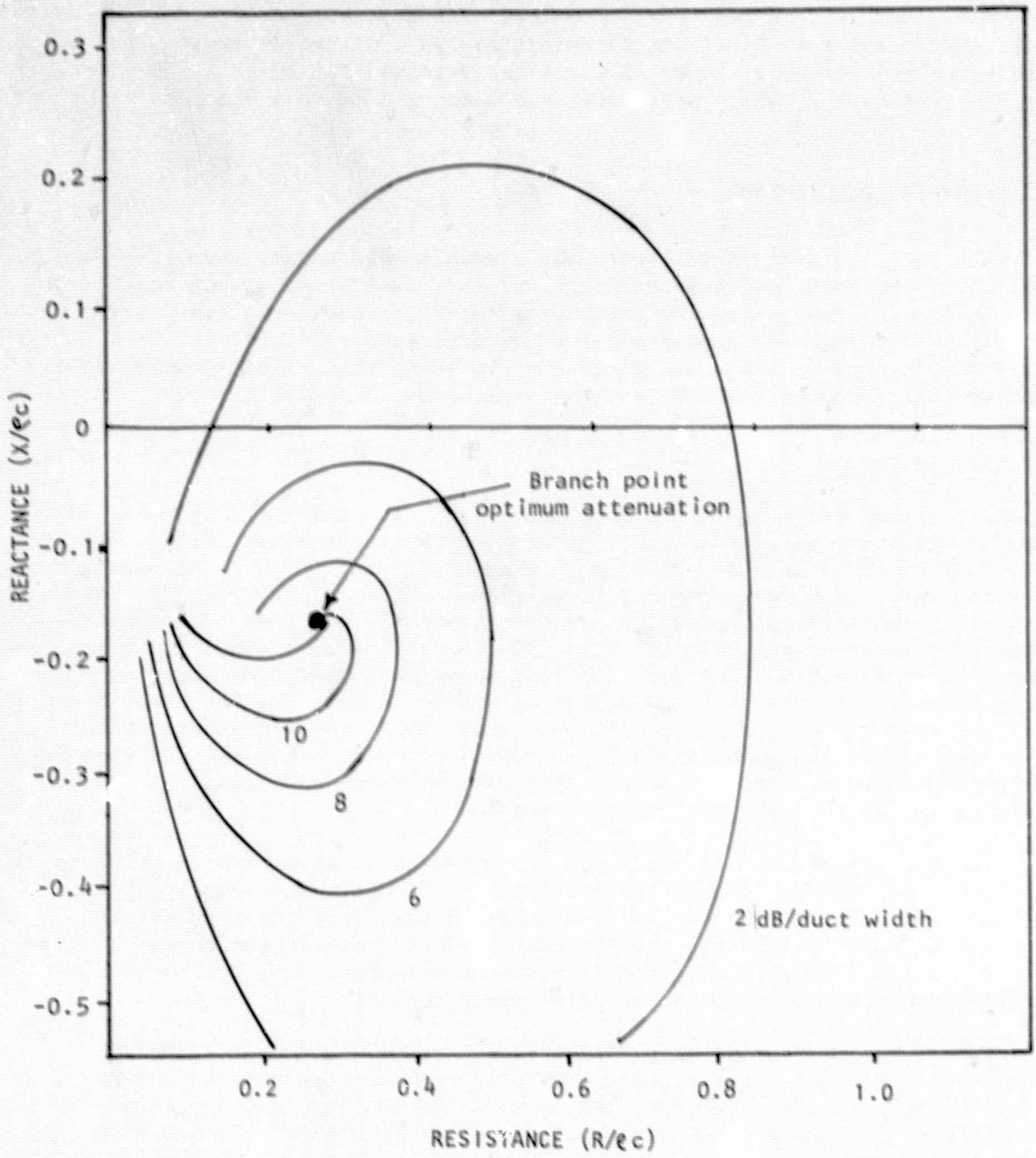


Figure 2. TYPICAL CLASSICAL SINGLE MODE ATTENUATION CONTOURS

impedance plane such that the control system resolving power is inadequate. This aspect of extreme peakiness of attenuation response could tend to "smear out", in the real case of finite bandwidth analysis of random excitation, leading to the ill-conditioned (i.e. rather insensitive) attenuation isogram example of figure 3, which would not be amenable to the optimization procedure.

## 2.2 FACILITY DESCRIPTION

The facility used in this work was a double reverberant chamber flow duct facility. The principal characteristic of this type of flow duct configuration is the ability to measure the energy insertion loss of a liner system, relatively easily, with a multiple-mode acoustic source structure. This source structure is, however, uncontrollable in the sense that relative modal amplitude and phase content at any arbitrary frequency cannot be changed.

### 2.2.1 Duct Layout

The double reverberation chamber duct facility is shown in figures 4(a) and (b). The test section is rectangular in cross-section and was reduced from 75.2 cm × 31.1 cm (30" × 15") to 76.2 cm × 17.8 cm (30" × 7"), by means of a dividing wall, in order to reduce the air consumption for a given duct flow velocity. The test configuration was such that only one side of the duct was lined, the liner height being 76.2 cm (30"). Provision for mounting three lined segments each 30.5 cm (12") in length was made, all other duct surfaces being acoustically "hard". The design is unique in that the air inlet diffuser to the source chamber acts as a broad band acoustic generator in itself, with additional provision being made for mounting acoustic drivers in the source chamber, should discrete tone excitation or additional source augmentation at low duct air flows be desired.

The downstream chamber rear wall is connected to an exhaust duct, with absorbent splitters to reduce the externally radiated noise levels and is faced on the chamber side with a steel plate offset from the rear wall to provide the maximum possible reverberant conditions within the chamber. Each chamber is provided with a system of microphone support rods for sound field sampling in order to estimate the total power content.

In addition to the primary flow duct air supply system, a secondary regulated supply with acoustically treated plenum was constructed to feed the liner bias air supply control valves (as shown in fig. 5) in order to prevent flow inconsistencies and noise contamination of the bias air flow within the test liners.

### 2.2.2 Facility Instrumentation

Two basic instrumentation systems were required: one for acoustic measurements and the other for air supply controls. These systems were linked by a Texas Instruments 990/4 micro-computer whose function was to acquire data, control the air supplies, and record all relevant results for later analysis (by listing and magnetic tape) upon facility operator command. Due to the

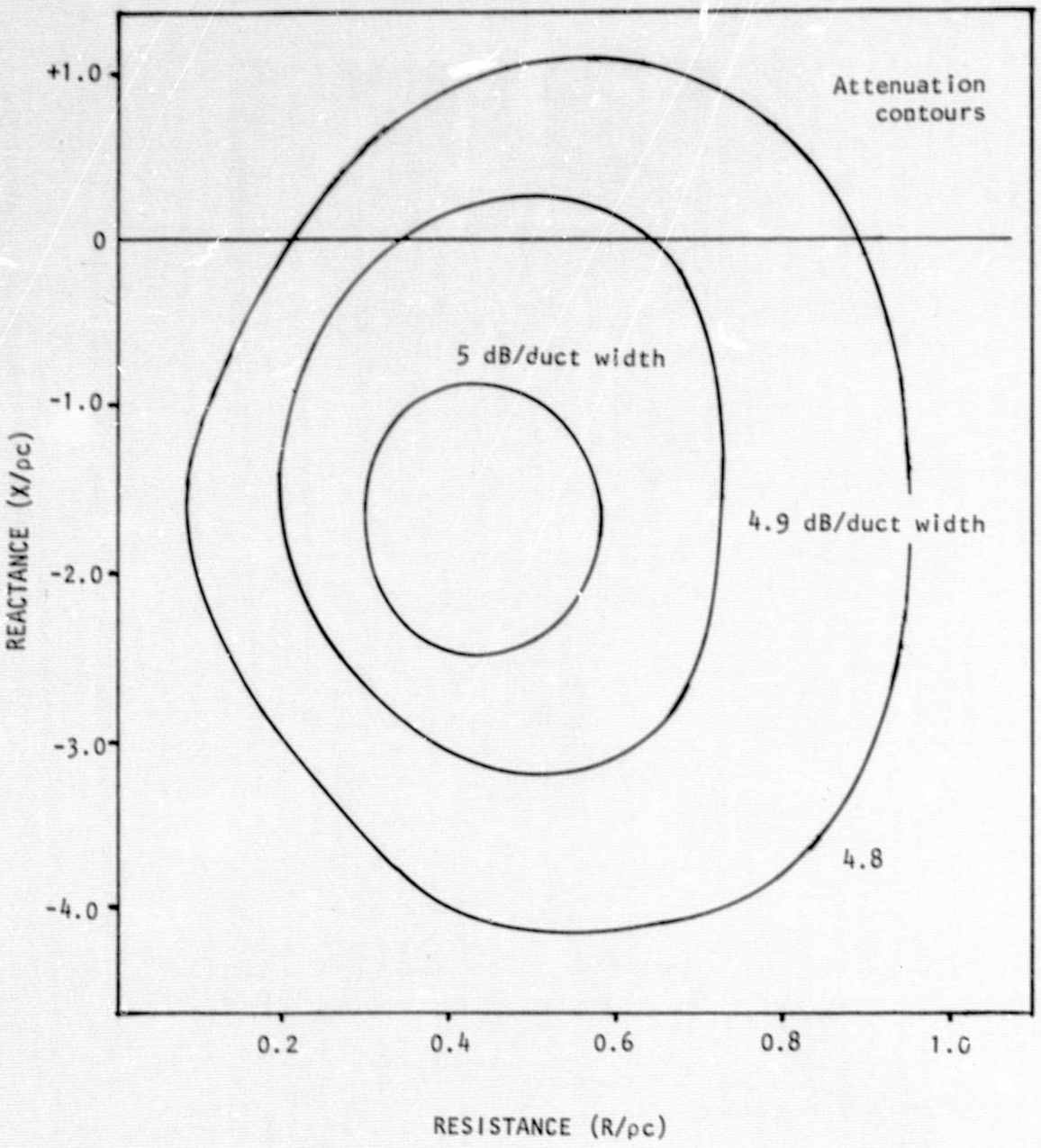


Figure 3. EXAMPLE OF POSSIBLE ILL-CONDITIONED MULTI-MODE (OR MULTI-SEGMENT) ATTENUATION ISOGRAM


Figure 4(a). OVERALL VIEW OF DOUBLE REVERBERANT CHAMBER FLOW DUCT FACILITY

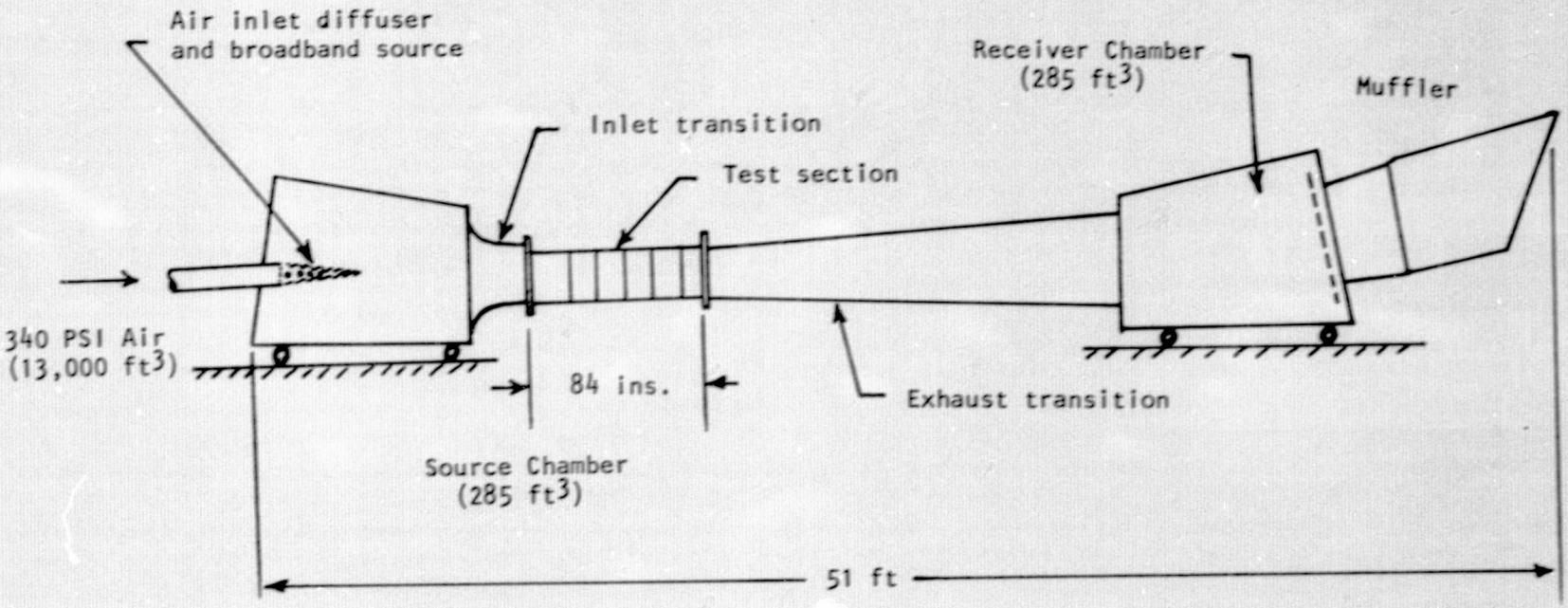


Figure 4(b). DOUBLE REVERBERANT CHAMBER FLOW DUCT FACILITY

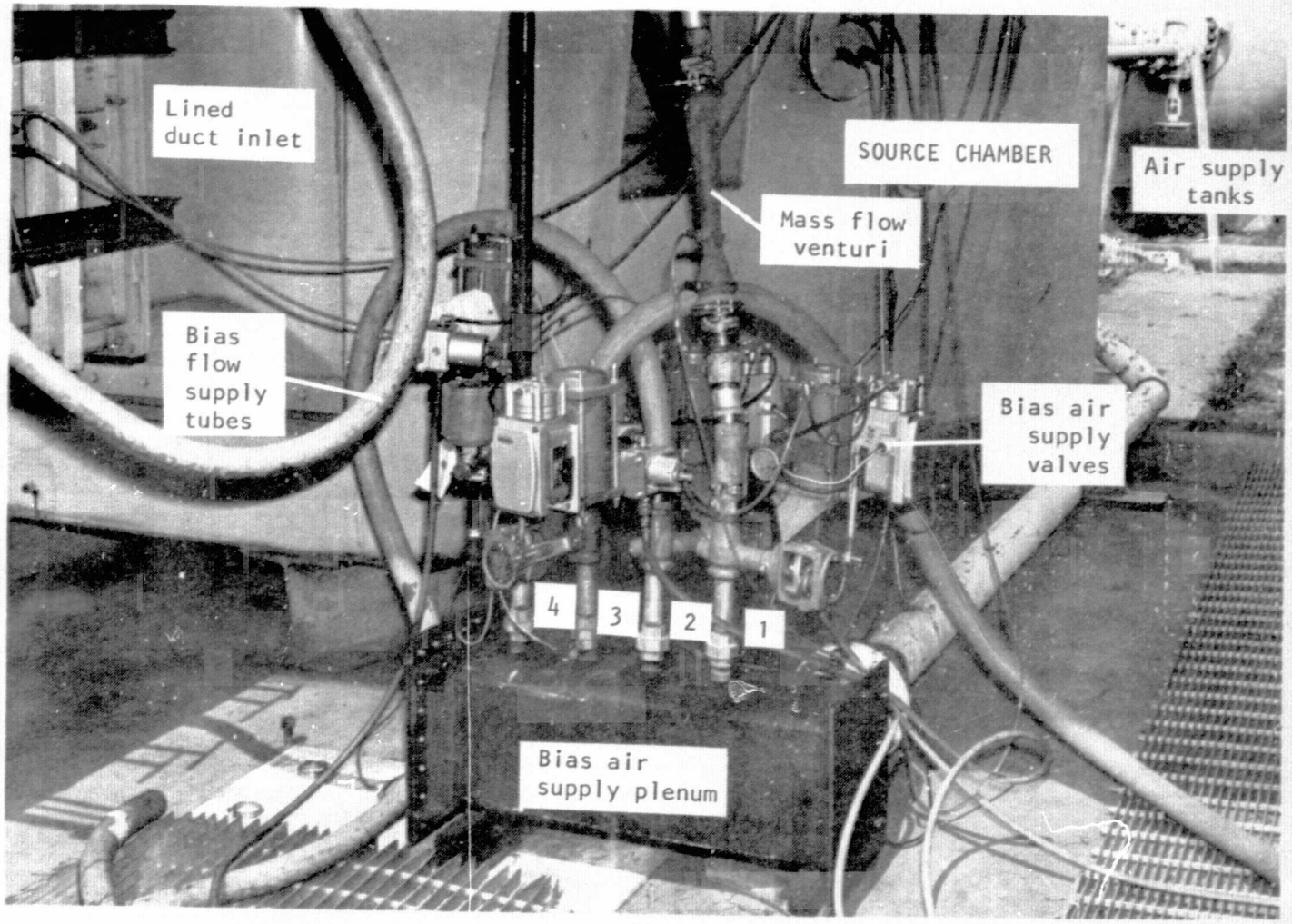


Figure 5. BIAS AIR SUPPLY VALVES & MUFFLED SUPPLY PLENUM

critical crosslinking nature of the control and analysis elements required for real-time operation, a considerable portion of the total work effort was concentrated on this system (the functional components are shown in figs. 6 and 7).

2.2.2.1 Source generation

The upstream source requirements for discrete tone and random excitation were met by use of a sine-random signal generator feeding four Altec 100-watt electrodynamic driver units placed at the corners of the floor of the source chamber. This placement ensured high efficiency of source chamber mode excitation.

2.2.2.2 Insertion loss measurement system

The parameter to be maximized in the duct lining control system is the energy Insertion Loss (I.L.). This is represented as the difference between upstream and downstream chamber reverberant sound pressures with the duct lining present, compared to those measured with the lining absent (i.e. hard wall condition).

The layout used to measure these reverberant sound pressures is shown in figure 8. Four microphones are fixed in each chamber at "random" locations at least 20 cm from any wall surface and out of the direct airflow path of the duct. The outputs of these four microphones (B&K type #4133) using broadband random excitation are multiplexed by an electronic scanner at a 200 kHz rate and bandpass filtered before being analyzed. The filter bandwidth was set to be between 50 Hz and 10 kHz, the lower limit set to remove possible wind noise components and the upper to remove all multiplexer switching transients as well as unwanted spectral information. The resultant signal was fed to both an analog to digital converter attached to the T.I. computer, and the Spectral Dynamics F.F.T. analyzer (SD360). The A/D inputs to the computer calculated the R.M.S. of each signal and this difference was used as the I.L. maximization parameter in the control loop. The spectrum analyzer (a 500-line constant bandwidth type) was set up to compute the ratio of the spectral component amplitudes (i.e. the transmissibility) such that changes in the I.L. spectra could be evaluated and recorded, if required, either on an X-Y plot, magnetic tape or printed paper output format.

2.2.2.3 Wall impedance measurement system

The in-situ wall impedance measurement technique is based on the two-microphone technique modified for a multi-layer resonant cavity type absorber. The analytical formulation for the measurement of impedance for the three layer liner design used in this work is developed fully in reference 2. The technique requires the measurement of relative S.P.L. and phase at the duct side of each resistive layer and the rear hard wall of the liner, a total of four points.

This measurement is most easily accomplished by means of a probe microphone which is traversed through the liner from the rear hard wall to the duct itself. The probe is positioned at each of the four measurement points

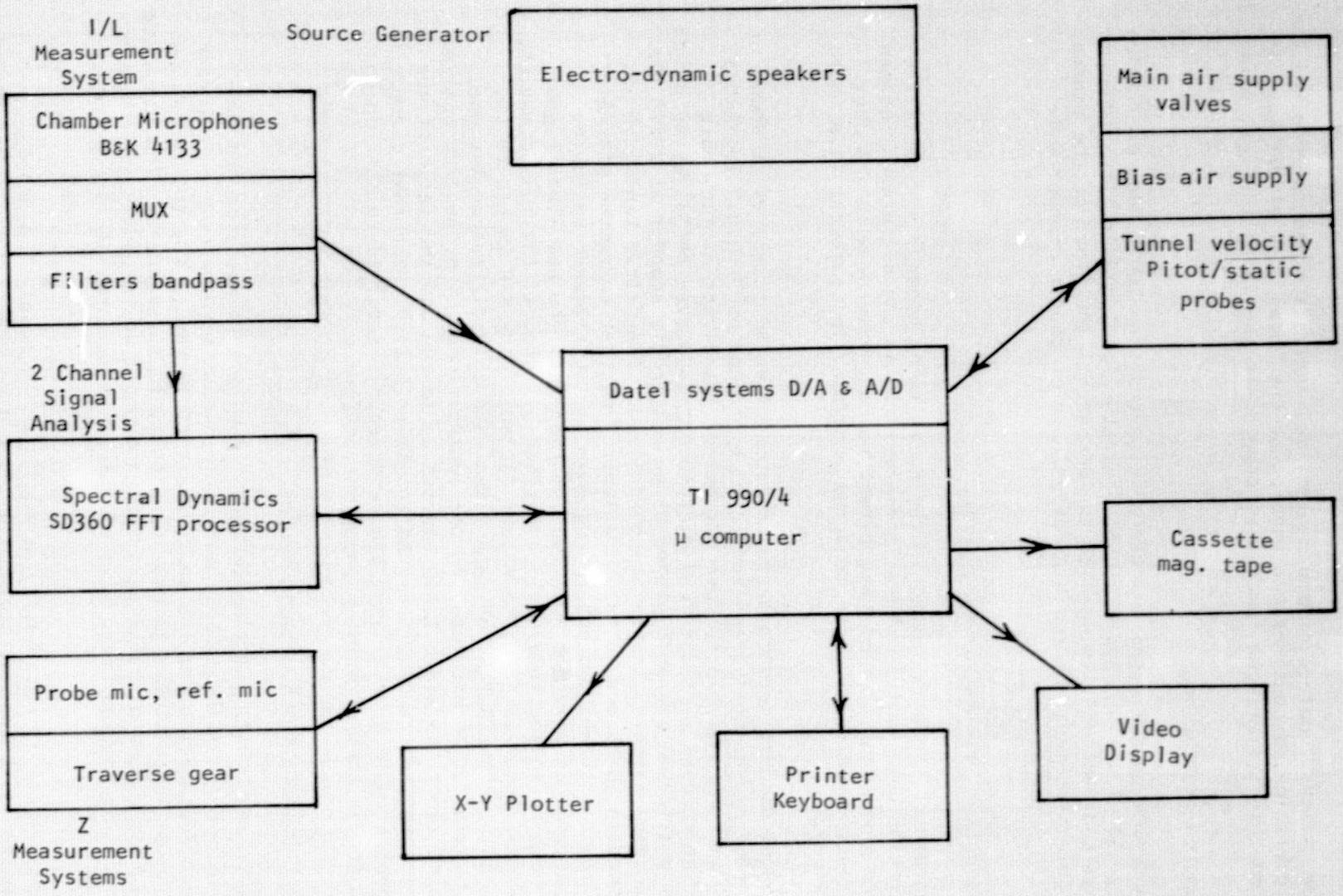


Figure 6. MEASUREMENT SYSTEM FUNCTIONAL COMPONENTS


Figure 7. ANALYSIS AND CONTROL SYSTEM HARDWARE

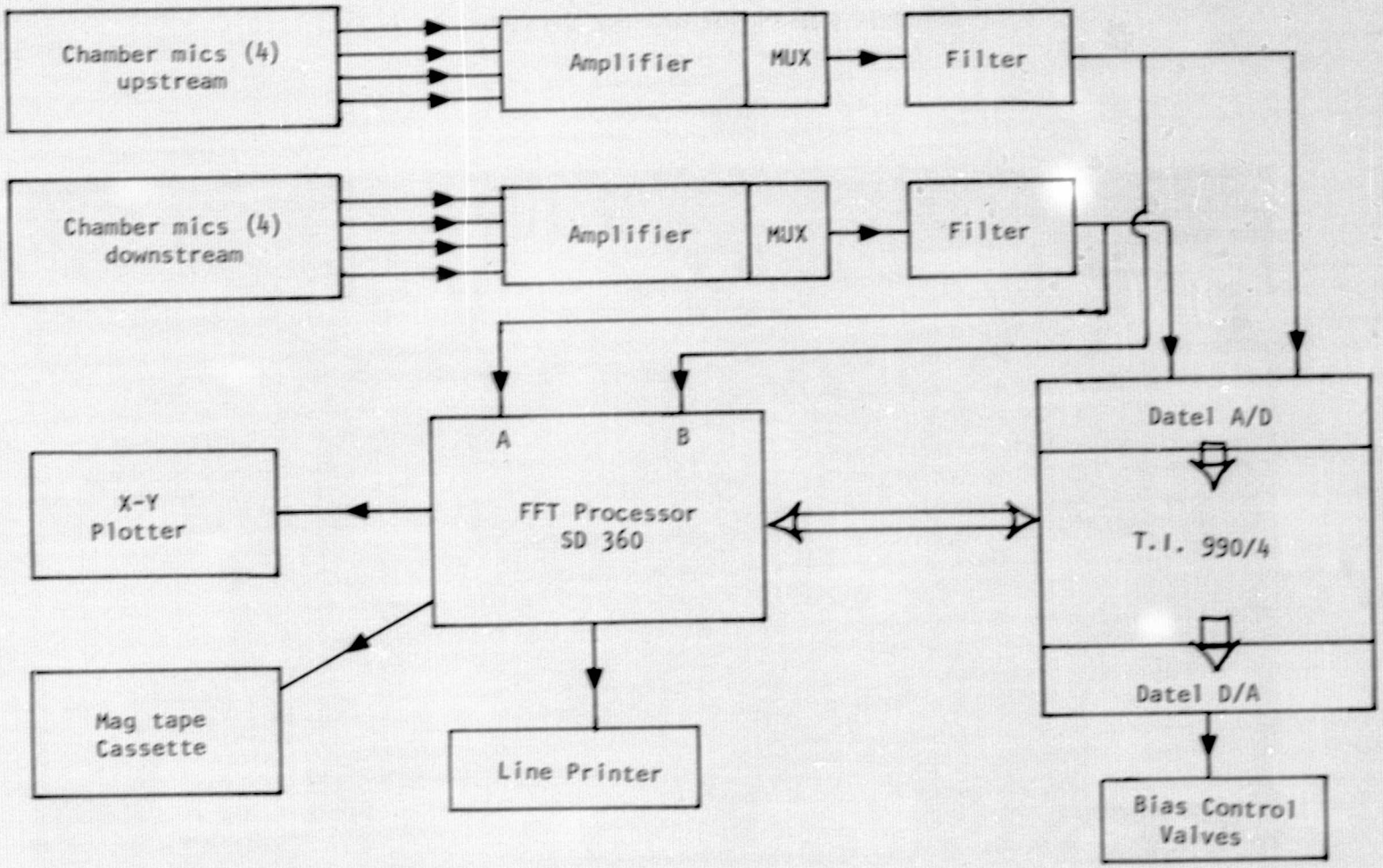


Figure 8. INSERTION LOSS MEASUREMENT SYSTEM

and the sound field measured with respect to a second microphone (used as a reference) located at the facing sheet of the liner.

In order to facilitate this measurement, a special probe traverse was built (shown in fig. 9) such that any arbitrary probe location or sequence of locations could be accurately set by means of a stepper motor drive under computer control. The possible traverse length was set to 45 cm such that complete probe cross-mapping of the liner and the duct could be done, if necessary. The probe itself was 2.5 mm in diameter and 0.3 mm wall thickness and some 90 cm in length. The sensing holes were located 45 cm from the microphone, the extreme length being required to enable the probe to be always supported by the opposite duct wall, and in addition, also provided a convenient means of anechoically terminating the probe tube with a long sliver of acoustic foam.

The relative amplitude and phase measurements were accomplished using a dual channel F.F.T. analyzer (SD360) in the coherent transfer function mode. That is to say, with random noise excitation at each probe measurement point, all frequencies of interest (512 to be exact) could be analyzed simultaneously on a constant bandwidth basis, thus providing an order of magnitude improvement in experimental time and resolution over discrete frequency tests.

For each test condition and probe measurement point, the amplitude and phase for each frequency was recorded on magnetic tape for subsequent playback and use in the determination of the wall impedance. A block diagram of the complete system is given in figure 10.

#### 2.2.2.4 Air supply control system

Two separate control systems were required, one for the duct grazing air supply, the other for the variable impedance liner bias air supply. Both systems were set up for computer control with manual overrides. The centerline tunnel velocity was the control parameter in the first case, via a pitot/static probe and differential pressure transducer. This input voltage was digitized by a Datel Systems A/D (and D/A) converter and the computer-generated control signal was fed back through the D/A system to an electro-pneumatic transducer to control the main air supply valve.

Four identical control paths were used for the bias air supply (as shown in fig. 11) such that the bias flow control parameter was the measured insertion loss. In addition, a venturi system for mass flow measurement was installed in series with one bias flow supply line.

## 2.3 OPERATIONAL PROCEDURE - WORK PLAN

In this program a great deal of stress has been placed on automated systems as demanded by the objectives and the work program cost constraints. Consequently, a great deal of thought was given to the structure of the computer programs, their linking and the facility operator interfacing. Four distinct software tasks were identified and programmed as distinct but linkable

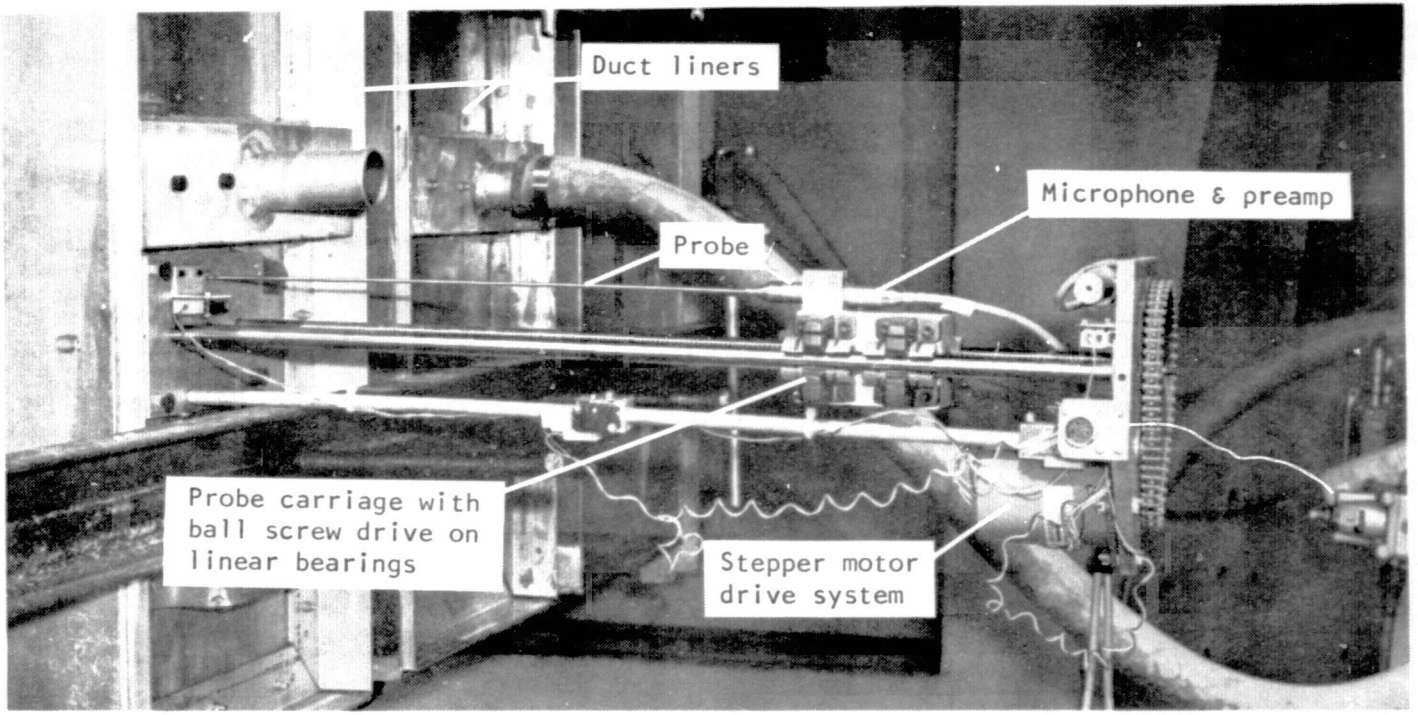


Figure 9. PROBE MICROPHONE TRAVERSE GEAR FOR WALL IMPEDANCE MEASUREMENTS

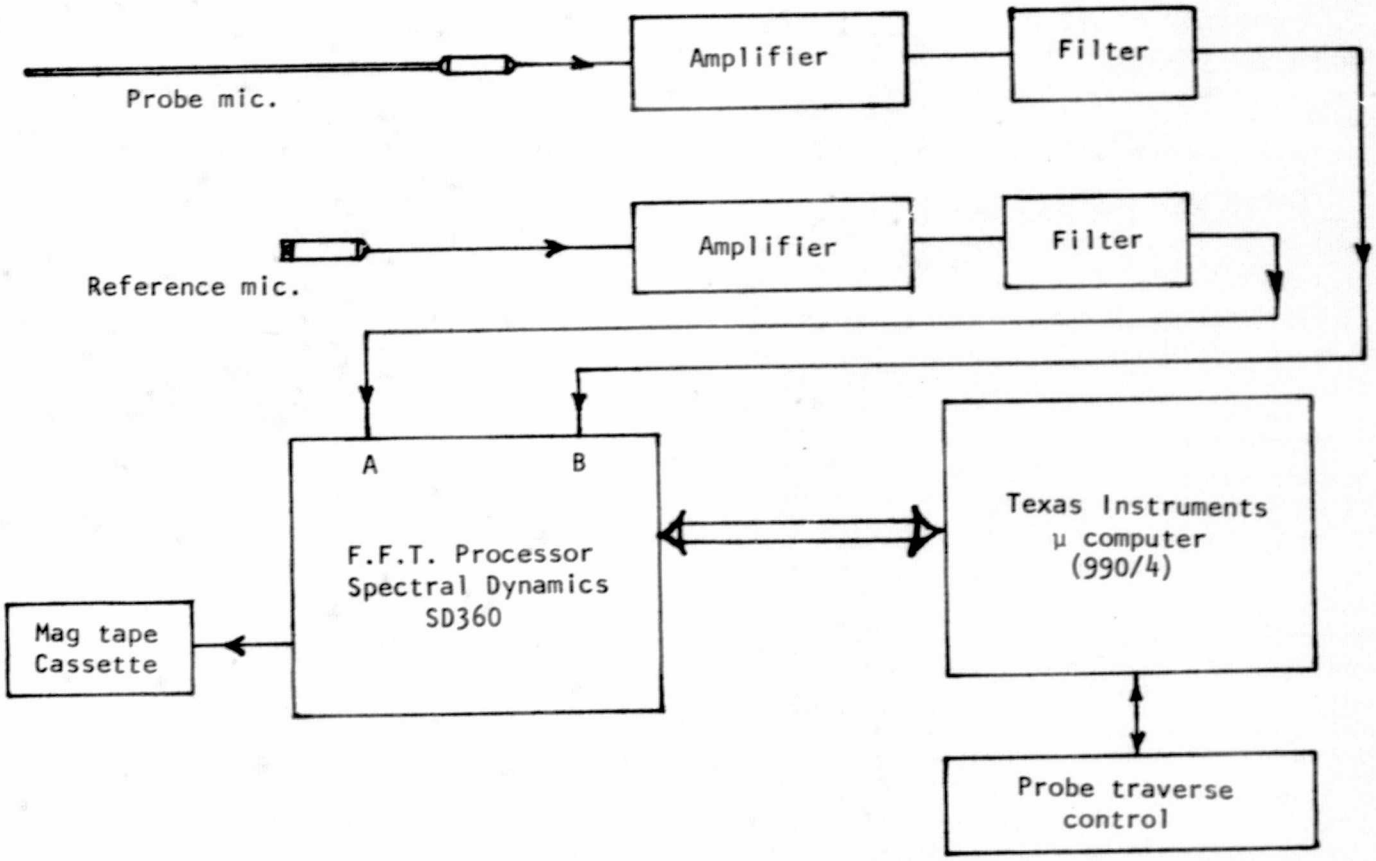


Figure 10. IMPEDANCE MEASUREMENT SYSTEM

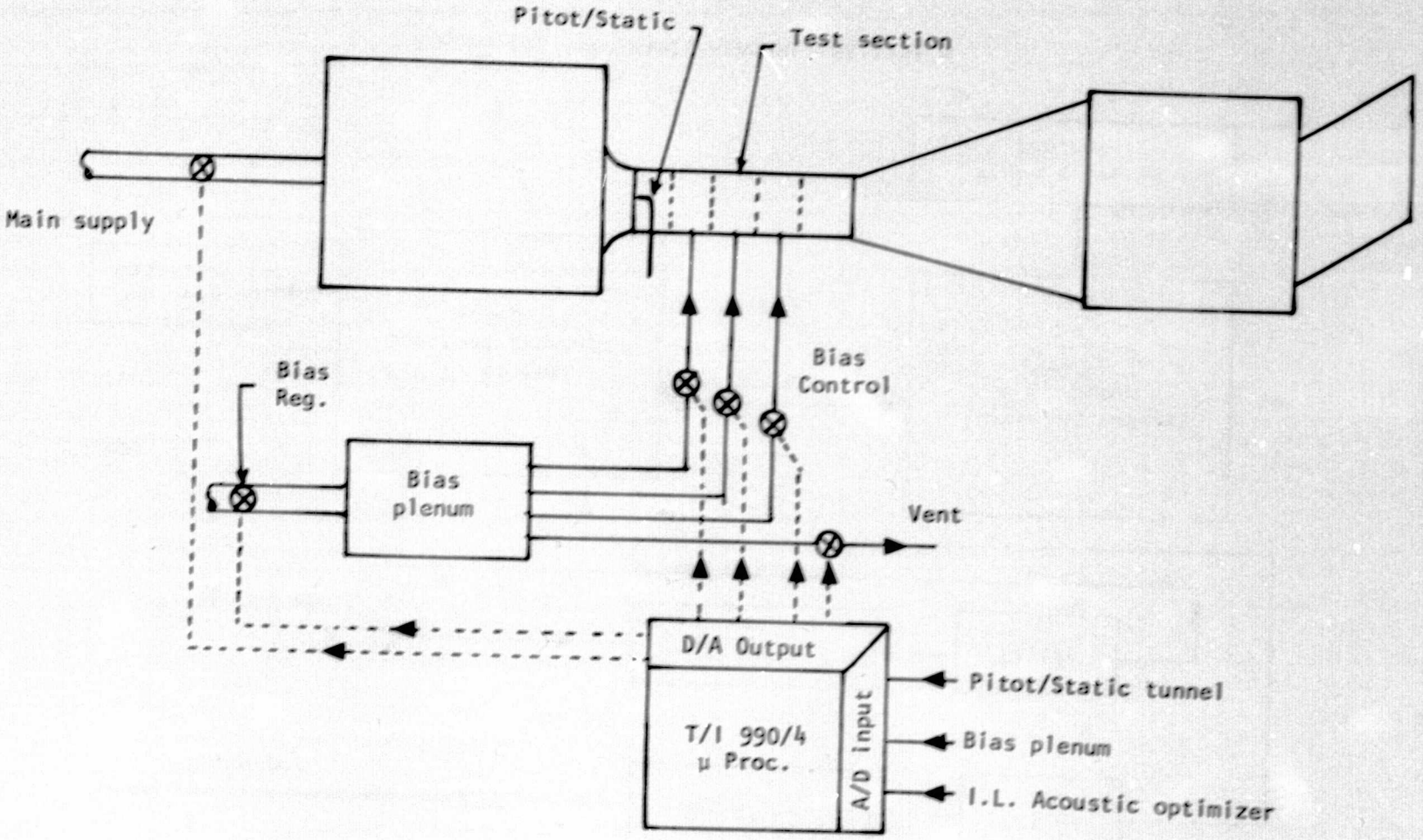


Figure 11. AIR SUPPLY CONTROL SYSTEM

entities. These were: (1) the air supply valve control system, (2) the insertion loss optimization algorithms, (3) the probe microphone drive system, and (4) the Spectral Dynamics SD360 digital interface and data logging system. Of these, the last proved the most time consuming due to inaccurate and incomplete manufacturer's documentation.

The work plan was designed to satisfy the original objectives in terms of three distinct tasks: (1) the facility calibration, (2) the insertion loss measurements and optimization, and (3) the wall impedance measurement. Of these three, the calibration phase was designed to exercise all the software routines and define the operation procedures in an optimum manner.

### 2.3.1 Facility Calibration

#### 2.3.1.1 Duct mean flow

The flow duct was calibrated by means of a pitot/static probe traverse across the duct upstream of the test liners. The resulting contours of flow velocity showed no intake flow separations to be present over the range of duct velocities of interest (up to Mach 0.2). The average mean flow velocity was calculated and plotted in terms of the duct centerline velocity as measured by a fixed pitot/static probe. The differential pressure on this probe was the valve control parameter for duct mean flow.

#### 2.3.1.2 Bias flow

Since each liner type was constructed with different perforate porosities, their flow resistances were different, thus mass flow and consequently bias flow velocities were different for constant valve openings and upstream supply pressure. Thus, a calibration was necessary in order to correlate bias flow velocities with percentage valve opening (the controlled parameter) for each liner type. This was achieved by the use of a venturi flow meter (as shown in fig. 5) which measured total mass flows for each liner as a function of valve opening. These were converted to bias flow approach velocities and the results are presented in figure 12 for each liner configuration. The upstream pressure to the bias flow valves was regulated by the computer to 138 KPa (20 psi) (with the exception of two 40 psi points shown) irrespective of bias flow loading to the liners.

#### 2.3.1.3 Insertion loss

The double reverberant chamber system has some energy loss even with "hard" duct walls. This insertion loss was considered as a baseline value to which the attenuation characteristics of each liner configuration were referenced (i.e. the difference between the measured transmissibility with a liner in place and the transmissibility with hard walls was defined as the liner insertion loss). With a hard duct wall, the multiplexed output of each set of four microphones in the upstream and downstream chambers was fed to the SD360 analyzer and the transmissibility (ratio of downstream to upstream amplitudes) recorded in 20 Hz bands from zero to 10 kHz using broadband

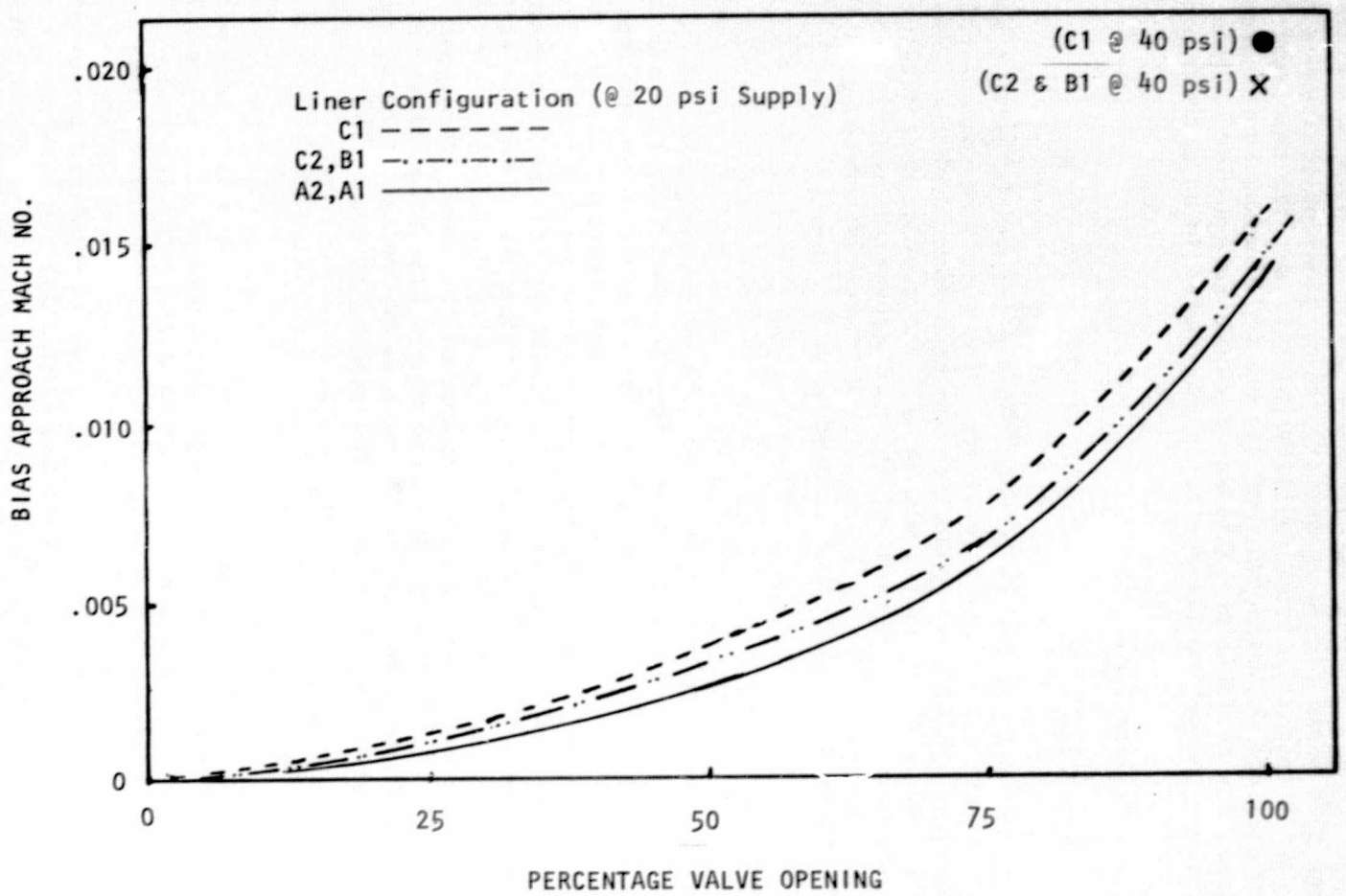


Figure 12. BIAS FLOW APPROACH VELOCITIES VERSUS VALVE OPENING FOR VARIOUS LINER TYPES

random noise excitation for four values of duct mean velocity. These results (for mean flow Mach numbers of zero, 0.05, 0.10, and 0.2) are shown in figure 13.

2.3.1.4 Probe microphone

The wall impedance measurement technique required the use of a probe microphone (described earlier in section 2.2.2.3). However, the characteristic frequency response of a probe microphone shows a marked drop-off at high frequencies with superimposed resonant peaks and valleys. It was necessary to damp the probe in order to keep the deviation of the resonant valleys from the mean to a minimum, thus maintaining adequate signal-to-noise ratios. The calibration of the damped probe was achieved using a random noise source in a small chamber surrounding the probe sensing holes and a 1/2" B&K reference microphone. The transfer function between the reference microphone and the probe is the desired calibration curve (as shown in fig. 14).

2.3.2 Initial Work Plan: Insertion Loss Optimization and Impedance Measurements

Two grazing flow velocities were called for, zero and a Mach number of 0.2. The frequency range for all experiments covered from 300 Hz to 5 kHz. For the zero flow tests electrodynamic drivers were used as the sound source (with random noise excitation), whereas for the flow tests, the inlet diffuser itself generated sufficient levels of broadband random noise within the test frequency band.

The work plan initially called for optimization of the insertion loss for each liner configuration for two classifications of frequency analysis: (1) wide band overall and (2) narrow band (in one-third octave bands). Two liner configurations were to be tested, specifically: (1) all test panels to be operated with bias flow in parallel, i.e. a uniform liner configuration and (2) two or three independently controlled panels. Three nondimensional frequencies were chosen by NASA with specified impedances for both uniform and multi-segment operation and are summarized in Table I. The liner design details and construction, necessary to achieve these impedance specifications are given in Section 3.

Thus, six liner configurations were to be tested for two duct velocities and fourteen frequency bands (one overall and thirteen one-third octave). The test plan logic embodied five basic procedural steps. These were: (1) setting and maintaining the duct flow, (2) setting and maintaining the bias flow air supply, (3) selecting the desired spectral analysis band, (4) setting the initial values for bias flow, and activating the optimization routine, and (5) after attainment of convergence to measure the wall impedance and record all data. When this sequence of events was complete, the next spectral band would be set up.

This systems concept routine would be exercised some 168 times in all. However, as discussed in Section 4, the application of this procedure revealed

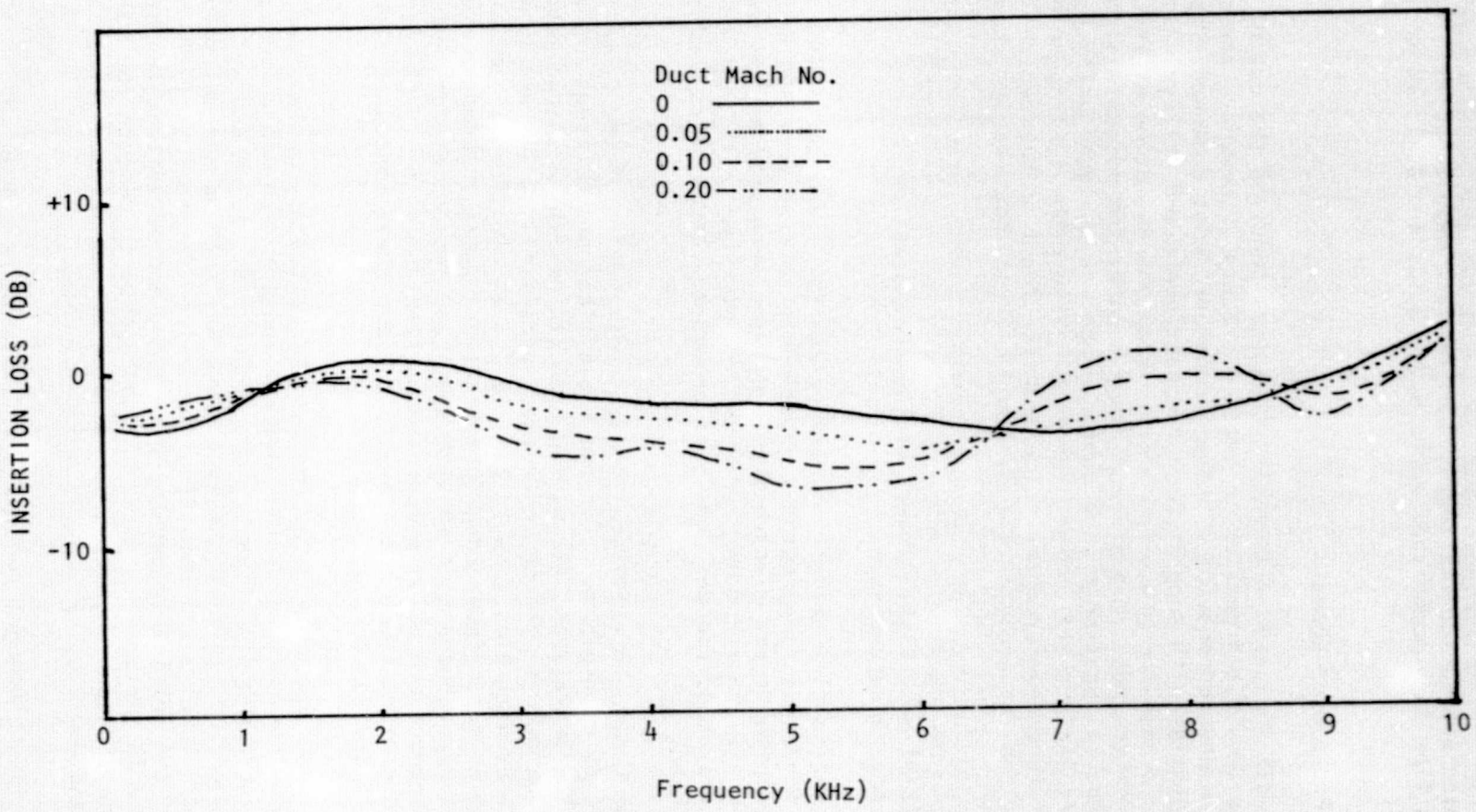


Figure 13. INSERTION LOSS OF HARDWALL BASELINE FOR VARIOUS DUCT MEAN FLOWS

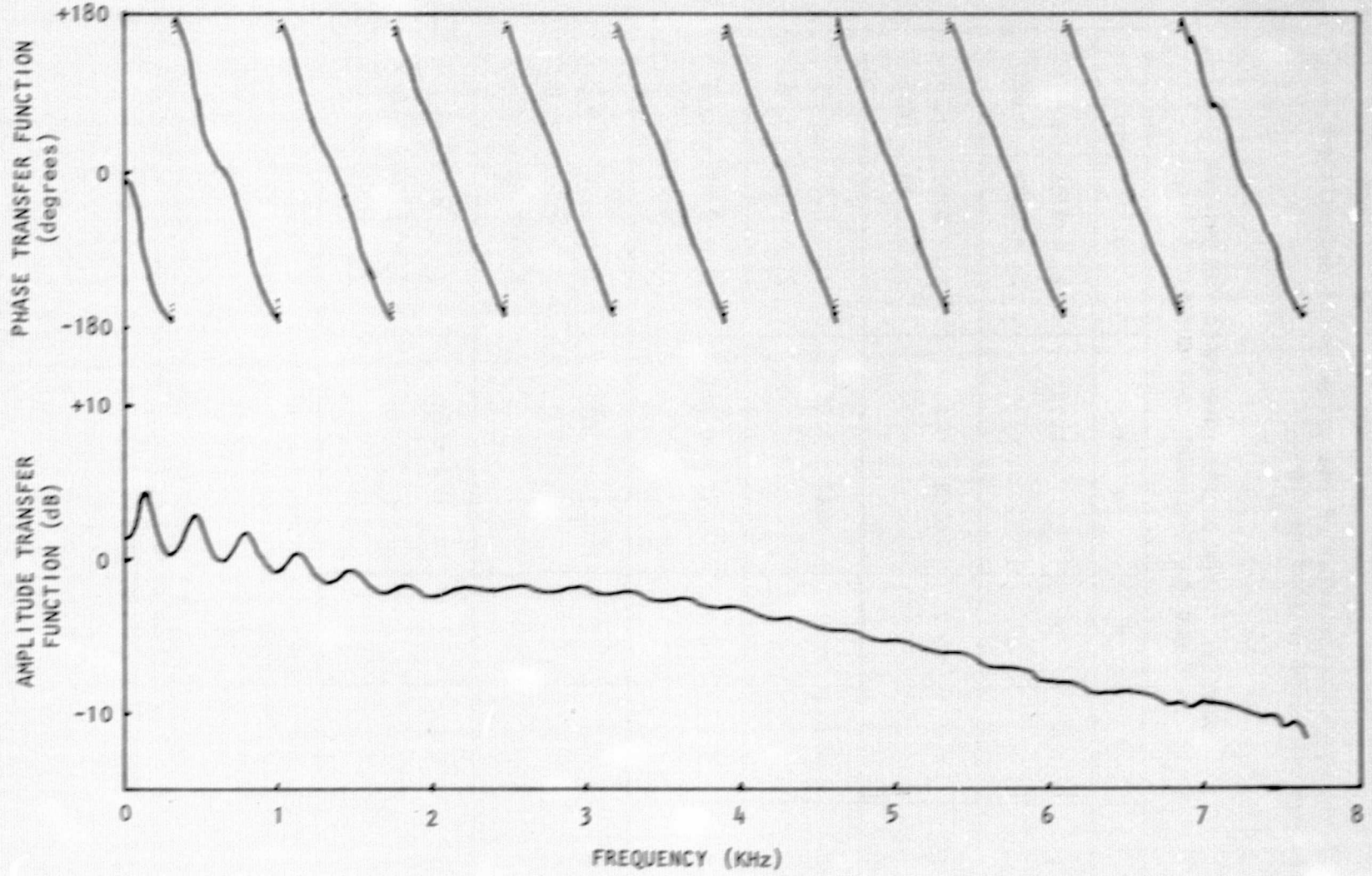


Figure 14. PROBE MICROPHONE AMPLITUDE & PHASE CALIBRATION

some operational characteristics of the system which necessitated work plan modifications discussed in that section.

TABLE I. LINER DESIGN IMPEDANCES FOR UNIFORM AND MULTI-SEGMENT CONFIGURATIONS

| $\eta^*$ | K | M | Uniform | Multi-Segment |
|---|---|---|---|---|
| 0.25 | 1.6 | 0 | 0.11 - 0.15j | $Z_1$ = 0.05 - 0.15j<br>$Z_2$ = 0.27 + 0.03j |
| 0.25 | 1.6 | 0.2 | 0.08 - 0.10j | $Z_1$ = 0.03 - 0.10j<br>$Z_2$ = 0.18 + .02j |
| 1.0 | 6.3 | 0 | 0.61 - 1.05j | $Z_1$ = 0.31 - 1.2j<br>$Z_2$ = 0.36 - 0.15j |
| 1.0 | 6.3 | 0.2 | 0.42 - 0.72j | $Z_1$ = 0.21 - .83j<br>$Z_2$ = 0.25 - .10j |
| 1.6 | 9.6 | 0 | 1.3 - 2.03j | $Z_1$ = 1.20 - .97j<br>$Z_2$ = 1.57 - 2.32j<br>$Z_3$ = 0.63 - .56j |
| 1.6 | 9.6 | 012 | .89 - 1.40j | $Z_1$ = .83 - .67<br>$Z_2$ = 1.08 - 1.6j<br>$Z_3$ = 0.43 - .39j |

*$\eta$ = frequency x duct height/speed of sound*
*K = reduced frequency = wave number x duct height = $2\pi\eta$*

**Note the $\eta$ = 0.25 values were supplied from NASA while the $\eta$ = 1.0 and 1.6 were taken from reference 4.*

# 3. ANALYTICAL WORK

## 3.1 LINER DESIGN

Three basic frequency parameter values were chosen ($\eta = 0.25$, 1.0 and 1.6) which, for an 18 cm (7 in.) duct width, corresponding to frequencies of about 500 Hz, 2 kHz, and 3 kHz, respectively. Table I lists the desired optimum impedances which were specified by NASA both for uniform and multi-segment liner configurations. These impedances were specified for zero duct mean flow and thus for the case of arbitrary mean flow were modified by the classical relationship.*

$$Z_M = Z_o \times \frac{1}{(1+M)^2}$$

where M equals Mach number of grazing mean flow with respect to the direction of sound propagation. For the case of $M = 0.2$, then the desired impedances are equal to 0.69 times the values of zero flow. A summary figure of the design impedances plotted on the impedance plane is given in figure 15.

The basic construction of the liner is similar to that used in reference 2, being simply a locally reacting multi-cavity resonant absorber liner as shown in figure 16. The front and intermediate cavity facing sheets are perforated sheet material, while the bias air supply cavity facing sheet is a high flow resistive fiber metal material in order to provide both an even supply of bias air and a relatively hard acoustic backing.

The design procedure was based entirely on the impedance model developed in reference 2 which requires as input, cavity depths, perforated sheet porosities, hole diameters and sheet thickness. The design philosophy was to vary the bias flow from an approach Mach number of zero to 0.02 and choose the liner physical parameters such that the design impedance was reached with a bias flow of approximately 0.01. This allowed the maximum possible impedance variation with bias flow changes, both increasing and decreasing.

It is desirable to have the variable impedance operating range below the second resonance point in order to use the less sensitive frequency characteristics of the multi-cavity type of liner design. In addition, if the design impedance points are very close to modal branch points with consequent possibilities of attenuation ambiguities, it is preferable to design a liner with resistances some 10% higher and reactances some 10% lower. Some difficulties were experienced, particularly for the $\eta$ values of 0.25, in obtaining sufficiently low resistances, since either the cavity depths would need to be very small or the sheet porosities very large. This would result in reactances that would be both too negative in value and that would be virtually unaffected by bias flow and thus not suitable for concept application. Thus, a compromise in design had to be reached in this case. In addition, the following constructional characteristics had to be taken into account:

*This relationship does not hold for very low $\eta$ values or near modal cut-off.

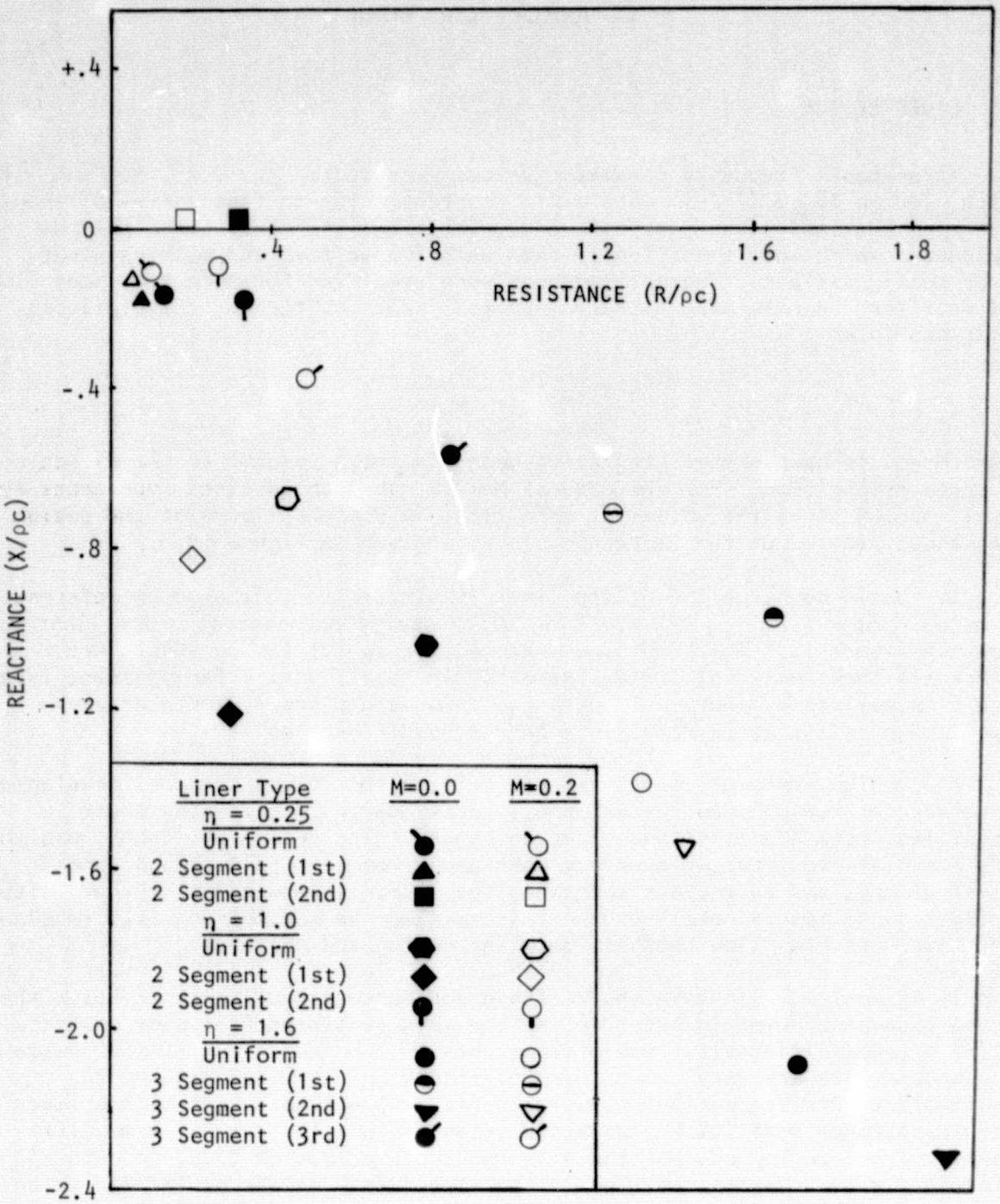


Figure 15. DESIGN IMPEDANCE REQUIREMENTS

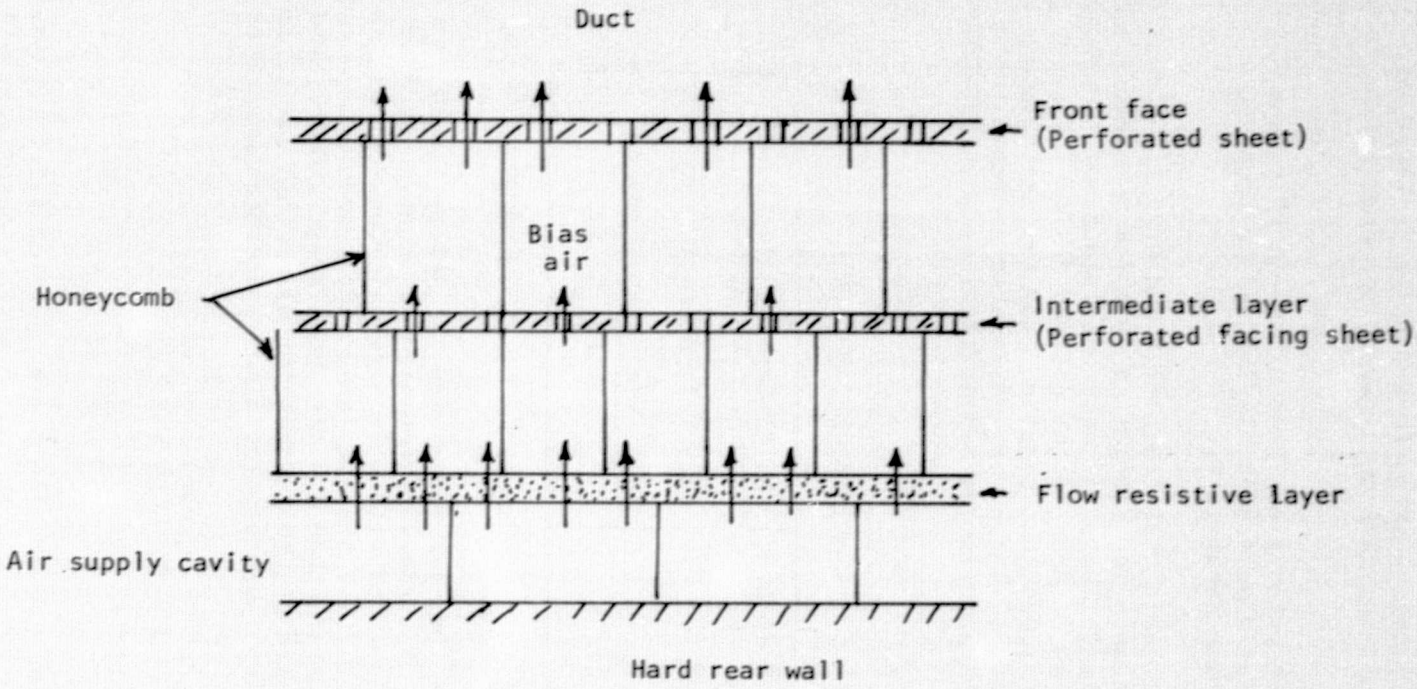


Figure 16. MULTI-CAVITY RESONANT ABSORBER LINER CONSTRUCTION

(1) Approximately 10% blockage of perforate holes is likely to occur on bonding of honeycomb cell cavity supports to the perforate sheets.

(2) The perforate sheet porosities, hole sizes and thickness, which are commercially available, is limited to discrete step changes in those parameters.

An inspection of figure 15 reveals that the $\eta = 1.6$ and 0.25 liner designs lie on lines of increasing resistance for increasing negative reactance. Thus, a reduction in the number of test liners was made possible by using a bias flow characteristic which passes on or near to the desired design frequency points. Thus, seven liner design configurations resulted from the design study which covered the entire test program. These were designated as shown in Table II with associated bias flow characteristics and physical geometries shown in figure 17.

TABLE II. LINER DESIGNATIONS

| $\eta$ | Uniform Z | Multi-Segment Z1, Z2, Z3 |
|---|---|---|
| 0.25 | A1 | A1, A2 |
| 1.0 | B1 | B2, B3 |
| 1.6 | C1 | C1, C1, C2 |

It should be noted that the air supply cavity ideally should be faced with a fiber metal of about 80 rayls flow resistance. However, due to the manufacturing tolerances associated with this material, considerable variation (order of ±20%) is possible. Thus, the available sample sheets were spot tested with a flow bench apparatus and the most consistent samples used in construction. The liner design procedure does not allow this cavity and facing sheet to be a variable, thus measured flow resistances were used in the impedance estimations.

## 3.2 LINER CONSTRUCTION

The liner panel sizes were 70 cm (30 in.) by 30.5 cm (12 in.), thus the most challenging problem was to obtain an even distribution of bias air flow from the 3 cm I.D. flexible hose supply line from the bias control valve. The system used consisted of a distribution plenum across the rear hard wall (or backplate) of the liner (seen in fig. 18) inside of which an inverted "V" of 20% porosity perforated plate was placed to act as a crude diffuser. Nine slots were then cut through the back plate and covered by nine inverted lengths

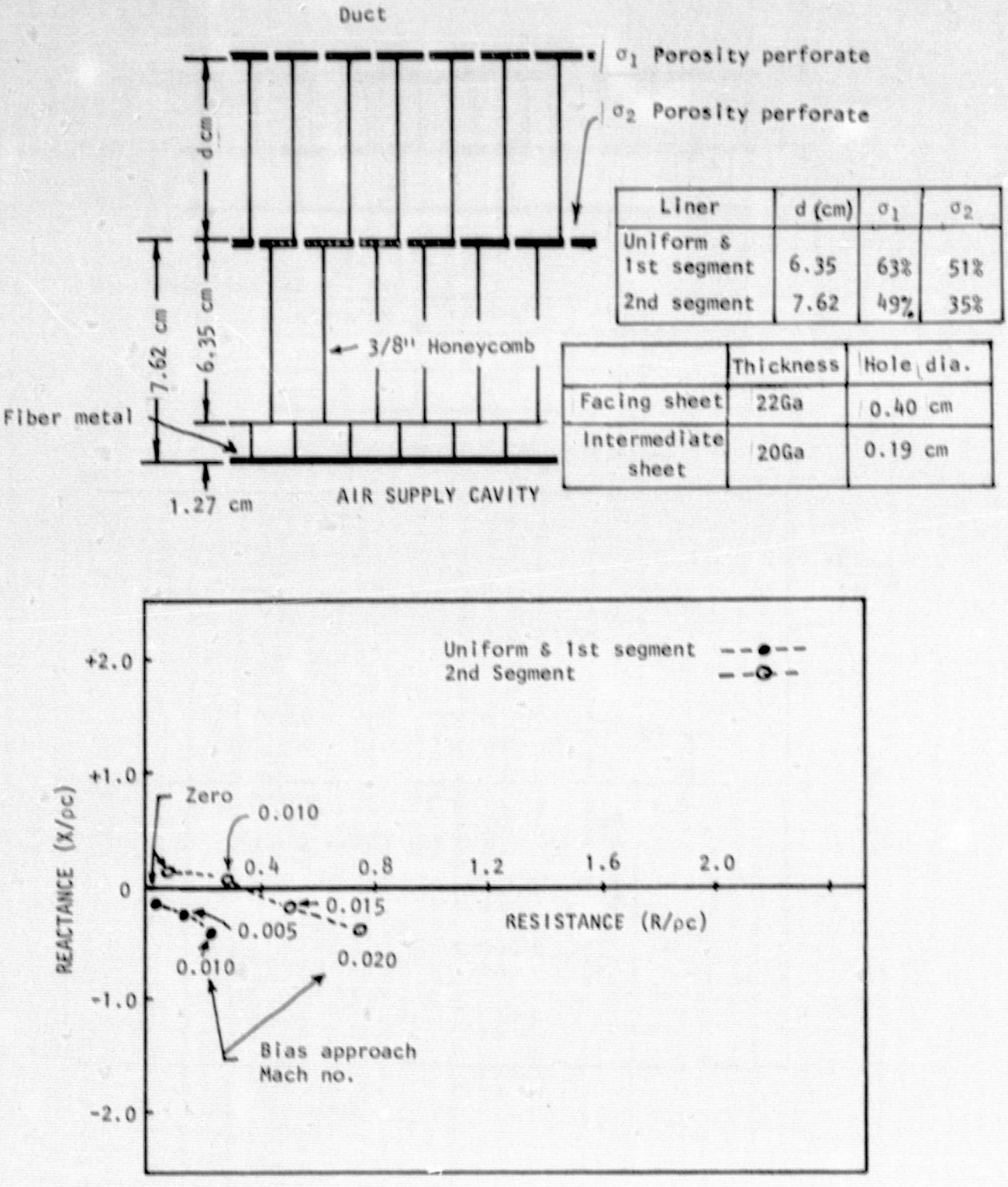


| Liner | d (cm) | $\sigma_1$ | $\sigma_2$ |
|---|---|---|---|
| Uniform & 1st segment | 6.35 | 63% | 51% |
| 2nd segment | 7.62 | 49% | 35% |

| | Thickness | Hole dia. |
|---|---|---|
| Facing sheet | 22Ga | 0.40 cm |
| Intermediate sheet | 20Ga | 0.19 cm |

Figure 17(a). BASIC CONSTRUCTION AND BIAS FLOW CHARACTERISTIC $\eta$ = 0.25 LINER (UNIFORM AND 2-SEGMENT DESIGNS)

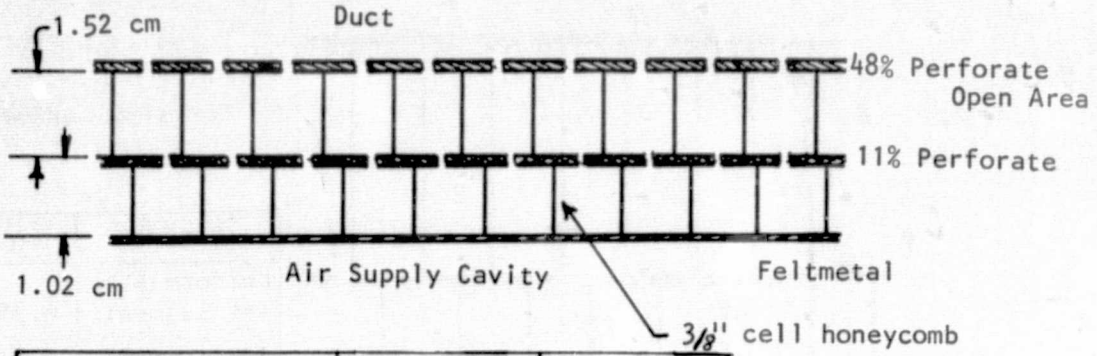


| | Thickness | Hole dia. |
|---|---|---|
| Facing sheet | 20Ga | 0.19 cm |
| Intermediate sheet | 20Ga | 0.16 cm |

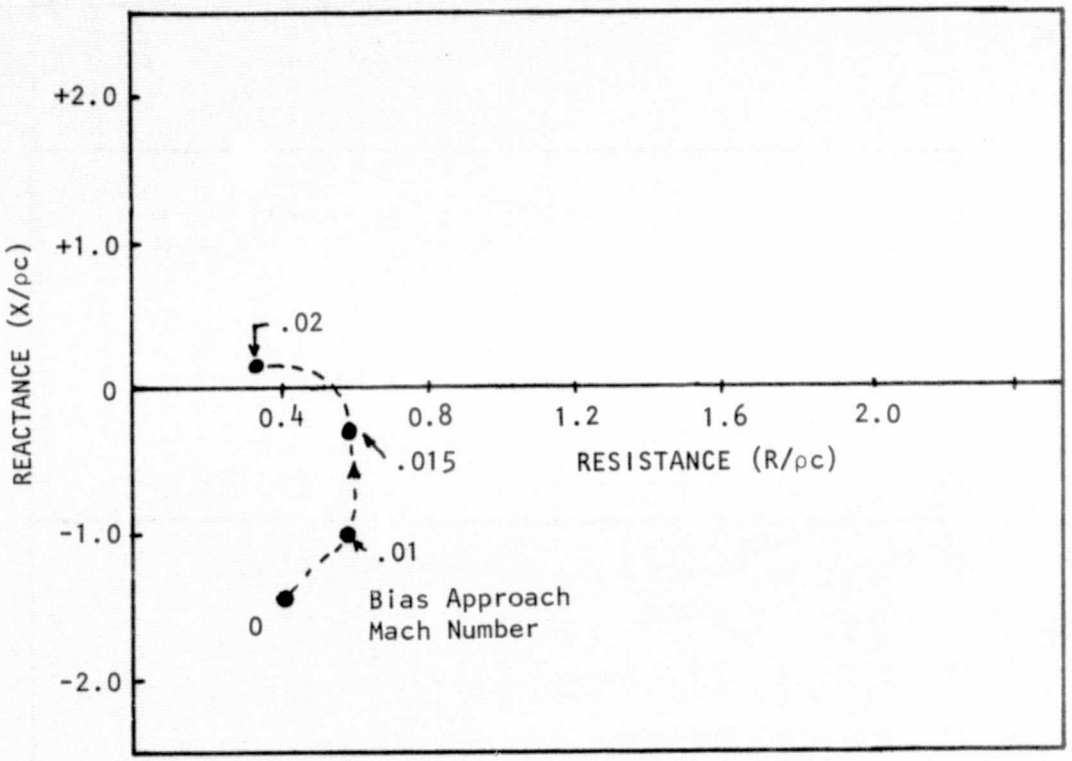


Figure 17(b). BASIC CONSTRUCTION AND BIAS FLOW CHARACTERISTICS OF $\eta$ = 1.0 LINER (UNIFORM DESIGN)

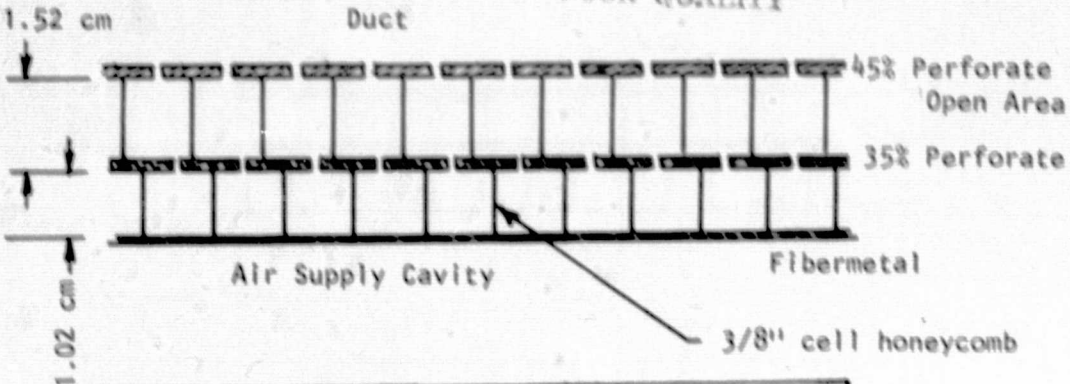


| | Thickness | Hole dia. |
|---|---|---|
| Facing sheet | 22Ga | 0.16 cm |
| Intermediate sheet | 24Ga | 0.10 cm |

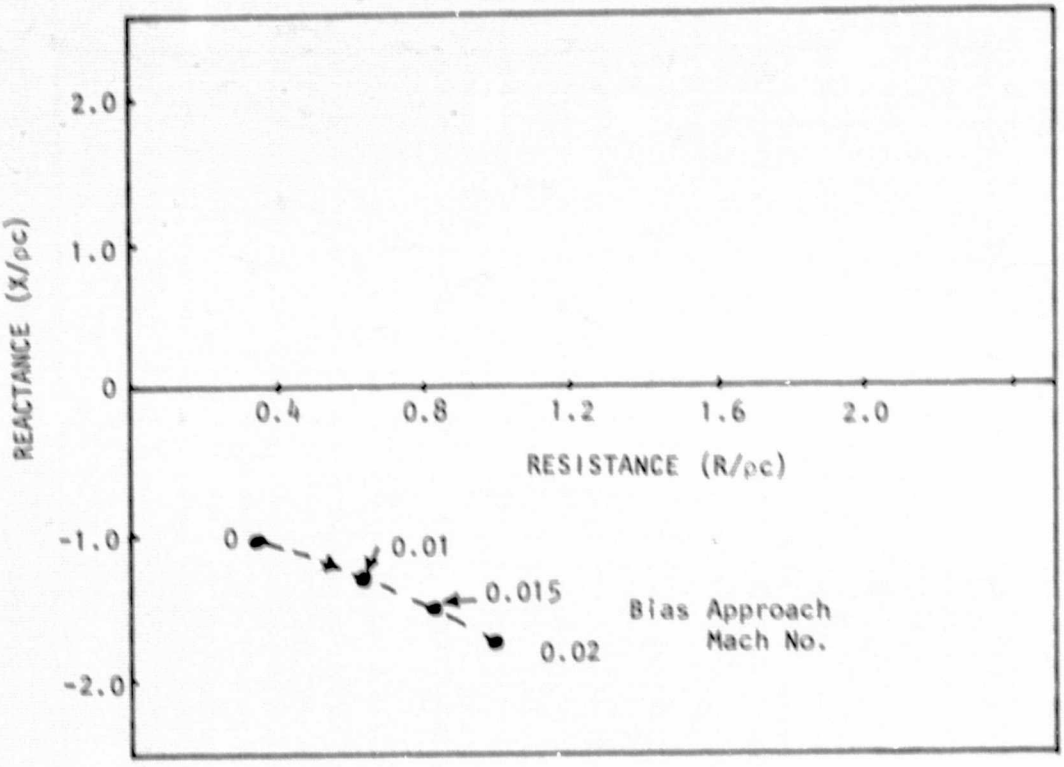


Figure 17(c). BASIC CONSTRUCTION AND BIAS FLOW CHARACTERISTICS OF $\eta$ = 1.0 LINER (FIRST SEGMENT OF 2-SEGMENT DESIGN)

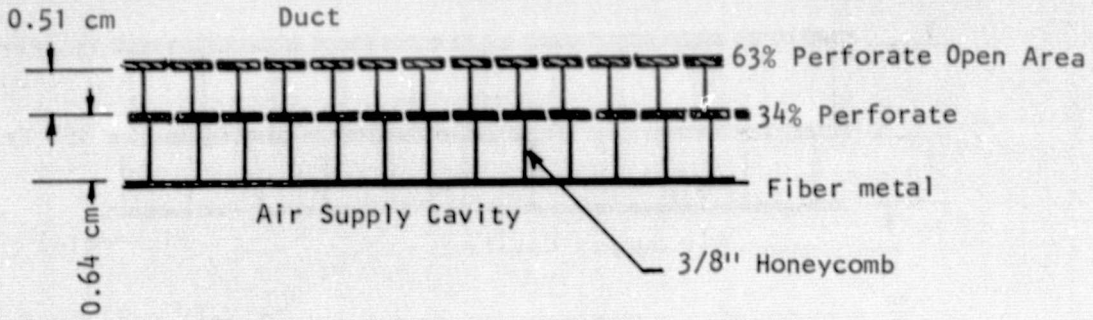


| | Thickness | Hole dia. |
|---|---|---|
| Facing sheet | 22Ga | 0.40 cm |
| Intermediate sheet | 22Ga | 0.20 cm |

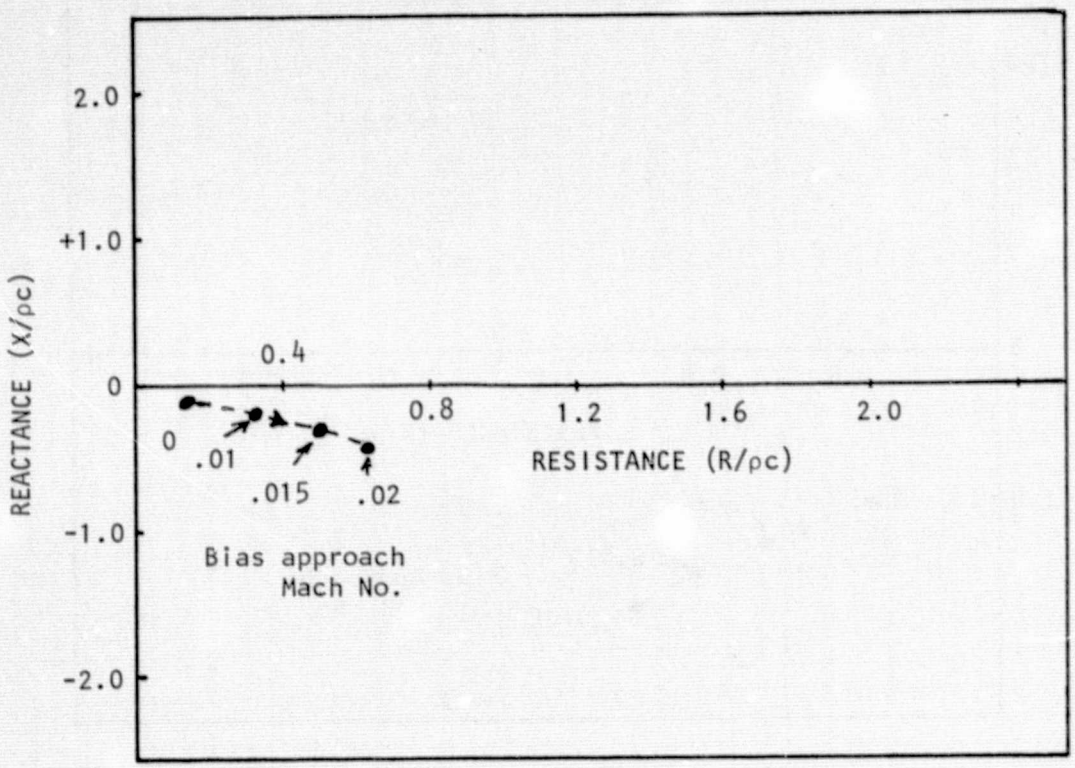


Figure 17(d). BASIC CONSTRUCTION AND BIAS FLOW CHARACTERISTIC OF $\eta$ = 1.0 LINER (SECOND SEGMENT OF 2-SEGMENT DESIGN)

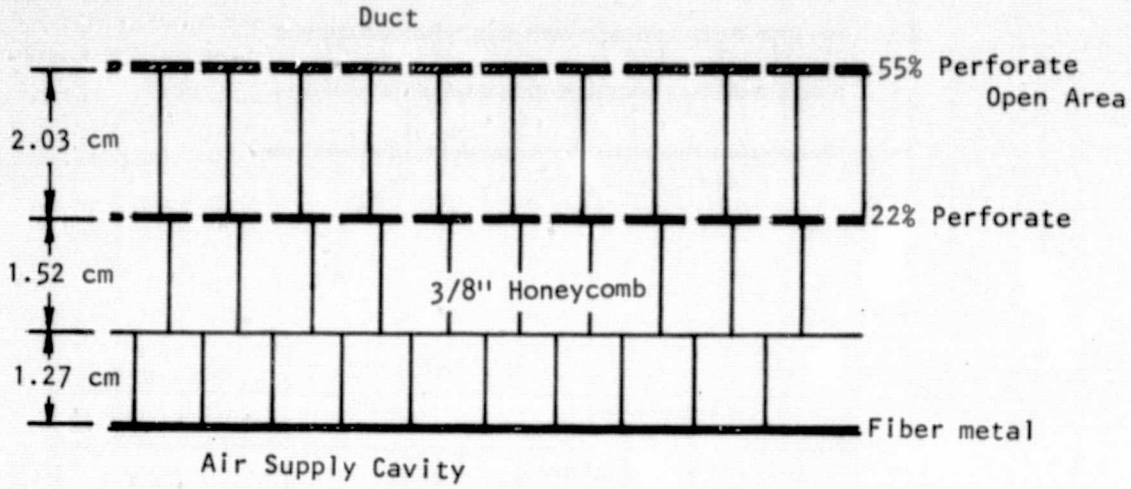


| | Thickness | Hole dia. |
|---|---|---|
| Facing sheet | 24Ga | 0.36 cm |
| Intermediate sheet | 24Ga | 0.16 cm |

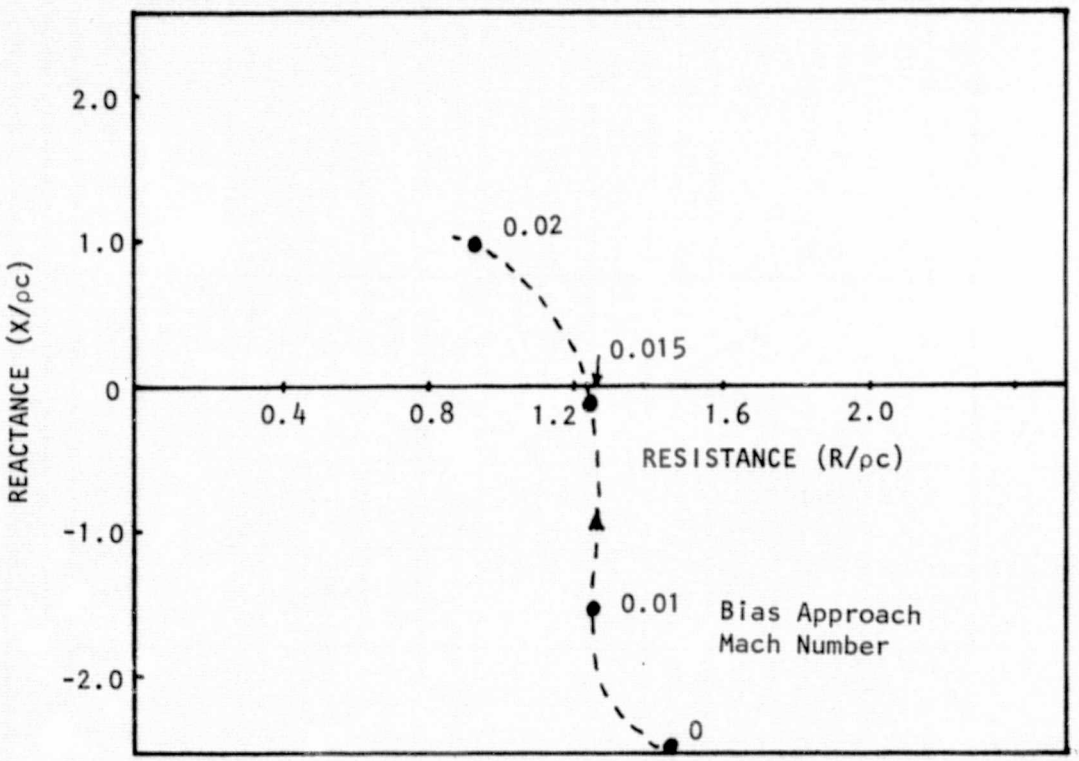


Figure 17(e). BASIC CONSTRUCTION AND BIAS FLOW CHARACTERISTIC FOR $\eta$ = 1.6 LINER (UNIFORM AND 1ST & 2ND SEGMENT OF 3-SEGMENT DESIGN)

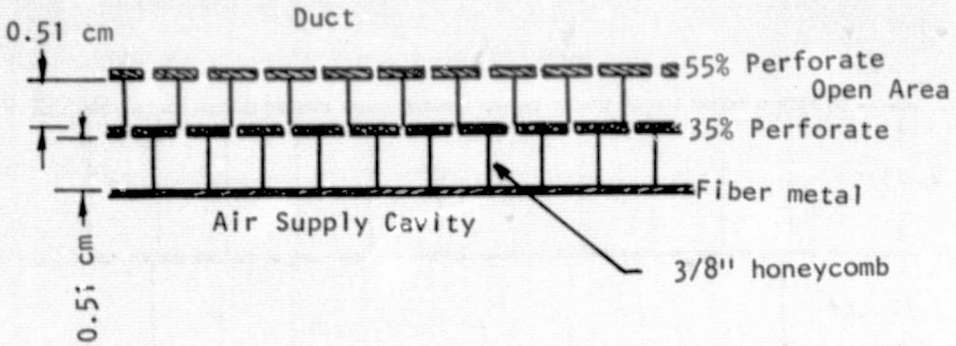


| | Thickness | Hole dia. |
|---|---|---|
| Facing sheet | 24Ga | 0.36 cm |
| Intermediate sheet | 22Ga | 0.2 cm |

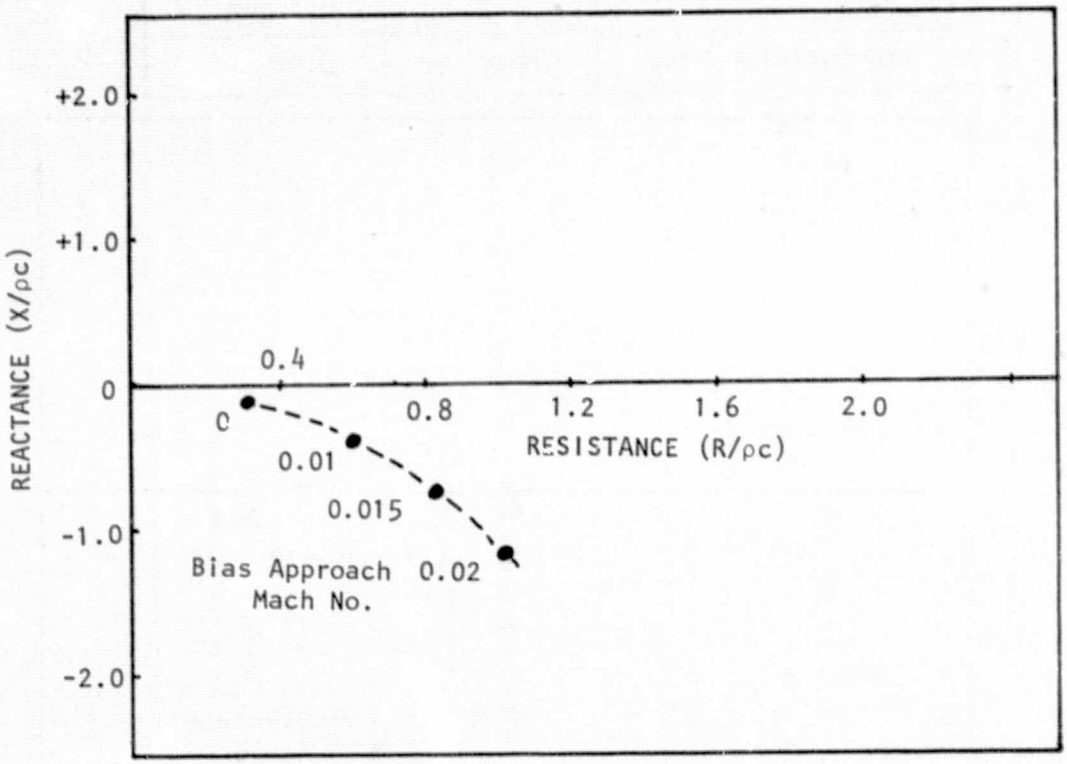


Figure 17(f). BASIC CONSTRUCTION AND BIAS FLOW CHARACTERISTIC FOR $\eta$ = 1.6 LINER (THIRD SEGMENT OF 3-SEGMENT DESIGN)

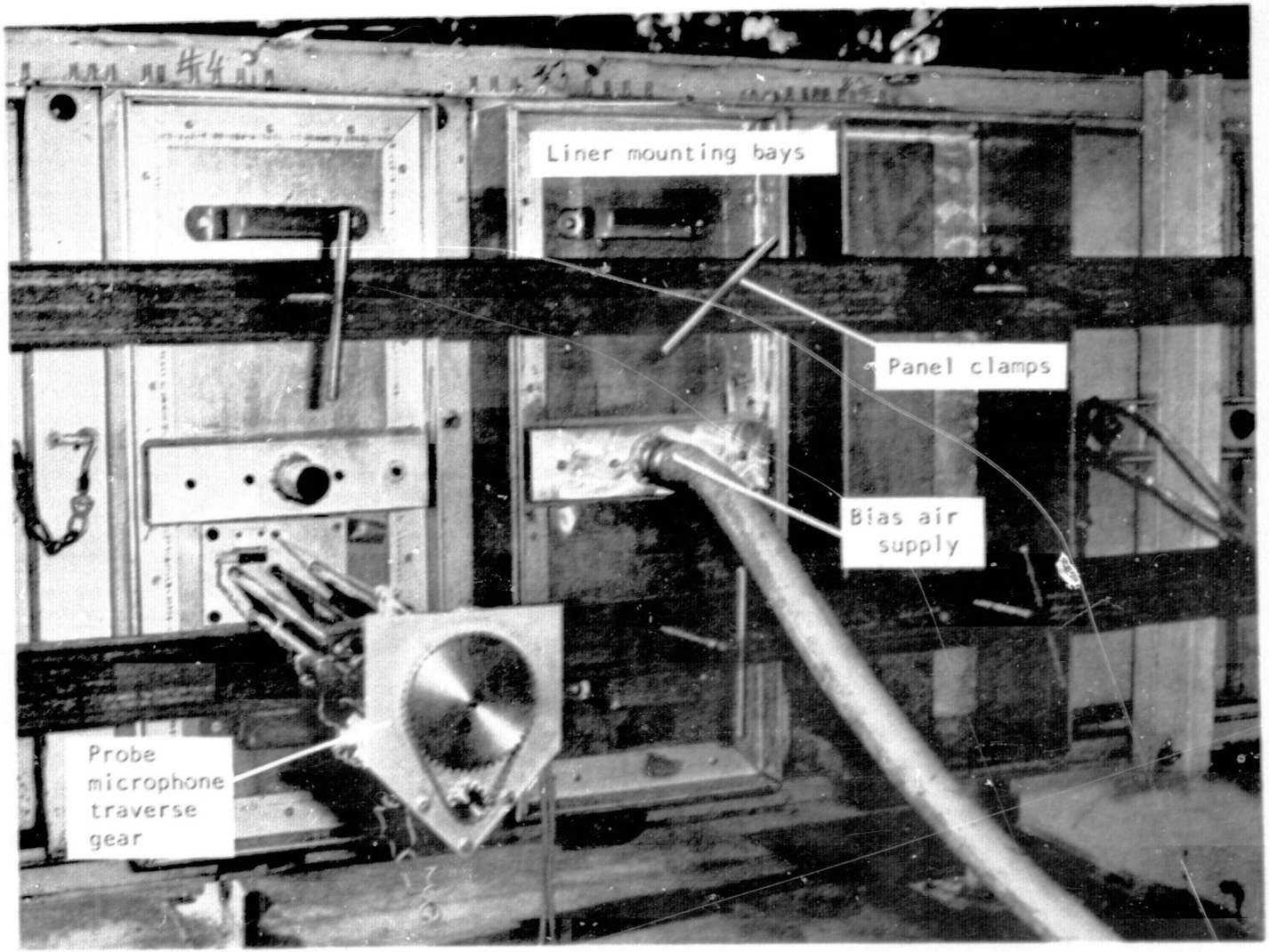


Figure 18. EXTERIOR VIEW OF TEST LINER MOUNTING AND PROBE MICROPHONE TRAVERSE ASSEMBLY

of aluminum angle as shown in figure 19. These angles act as secondary plenums, the bias air bleeding out through 28 slots 3 mm long and 0.3 mm wide on each side of the angle.

The back plate air supply cavity was common for all liner configurations, the facing and intermediate cavity sections being mounted against the back plate, as indicated in figure 20. The whole assembly was sleeved inside a rectangular frame mounted in each duct test bay and clamped from the rear as shown in figure 18.

The intermediate and facing sheet configurations were built up using standard epoxy bonding techniques for aluminum or Nomex 1 cm cell size honeycomb to the perforated sheet panels. The three uniform liner panels, A1, B1 and C1 configurations are shown in figure 21.

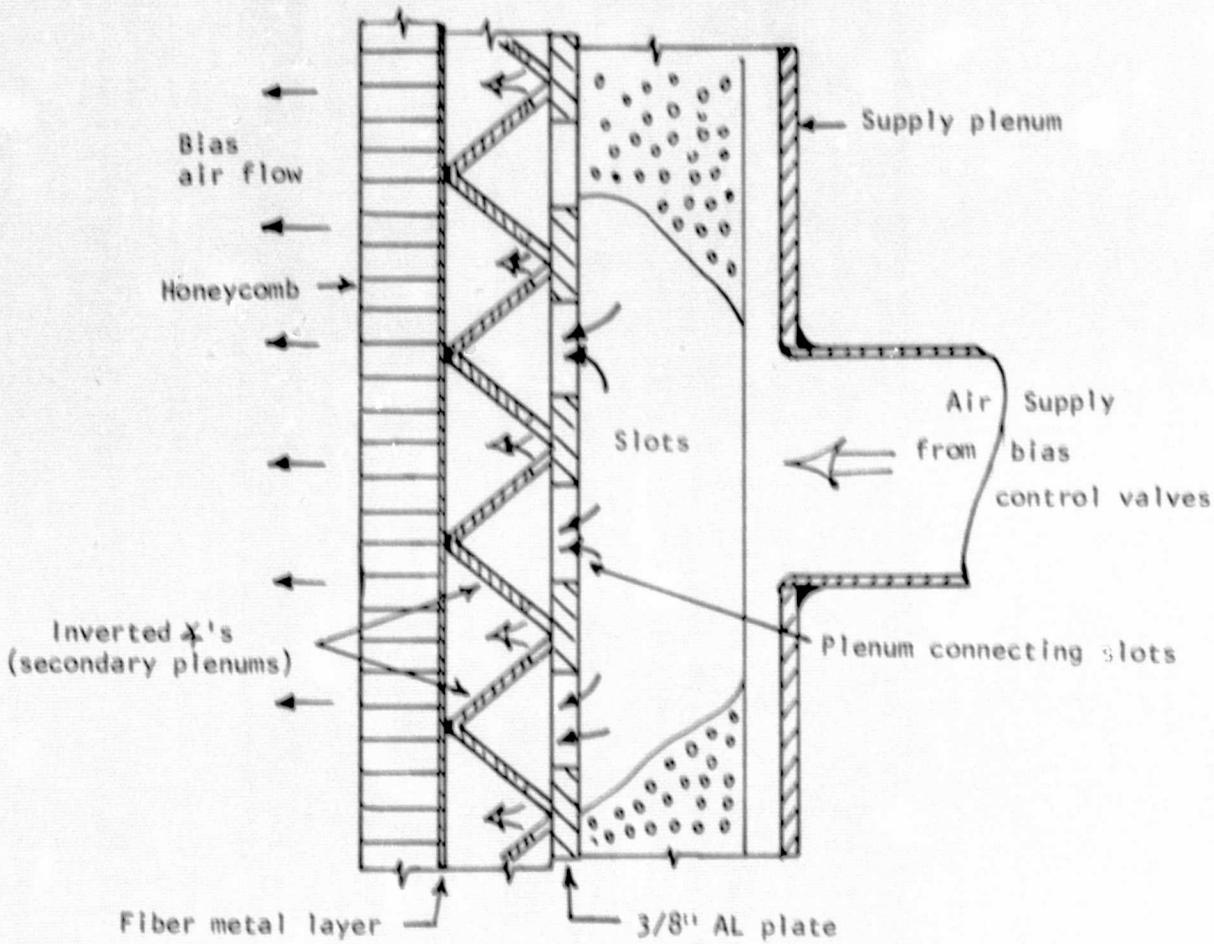


Figure 19(a). CONSTRUCTIONAL DETAILS OF LINER HARDWALL BACK PLATE

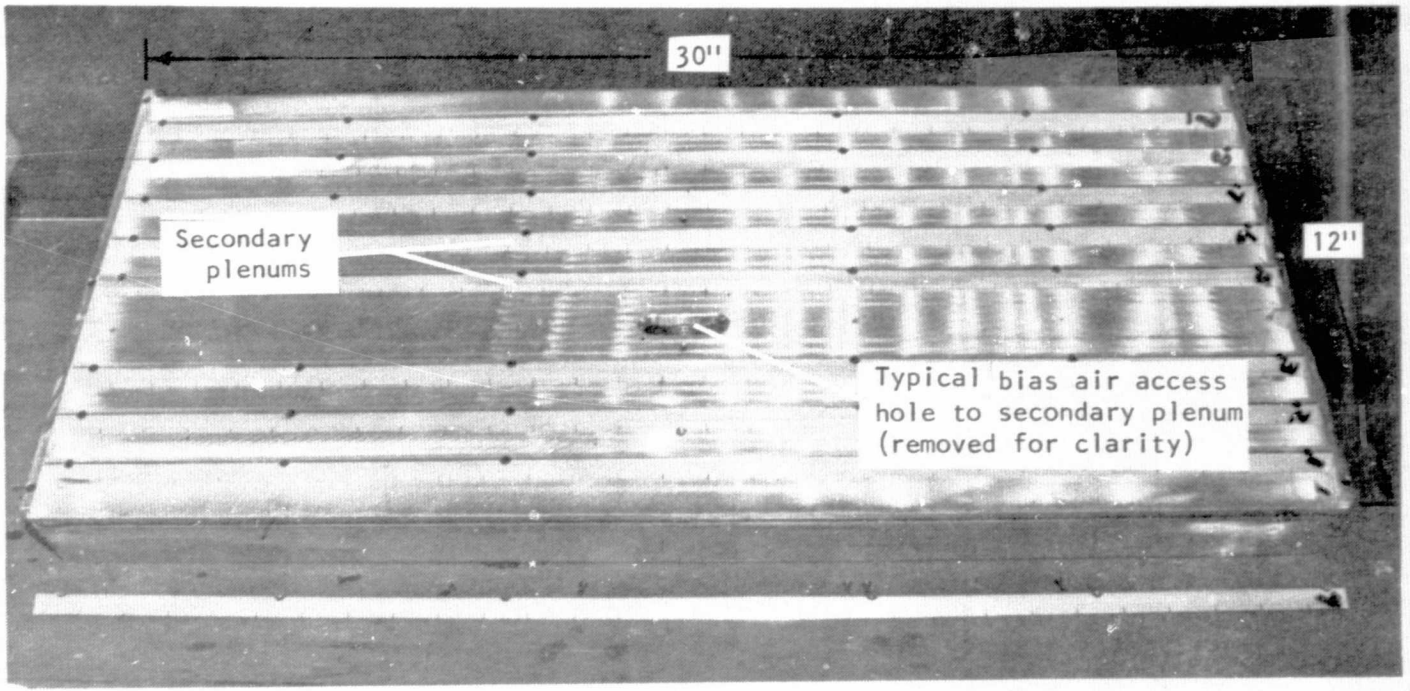


Figure 19(b). LINER BACKPLATE AND SECONDARY SUPPLY PLENUMS ON DUCT SIDE

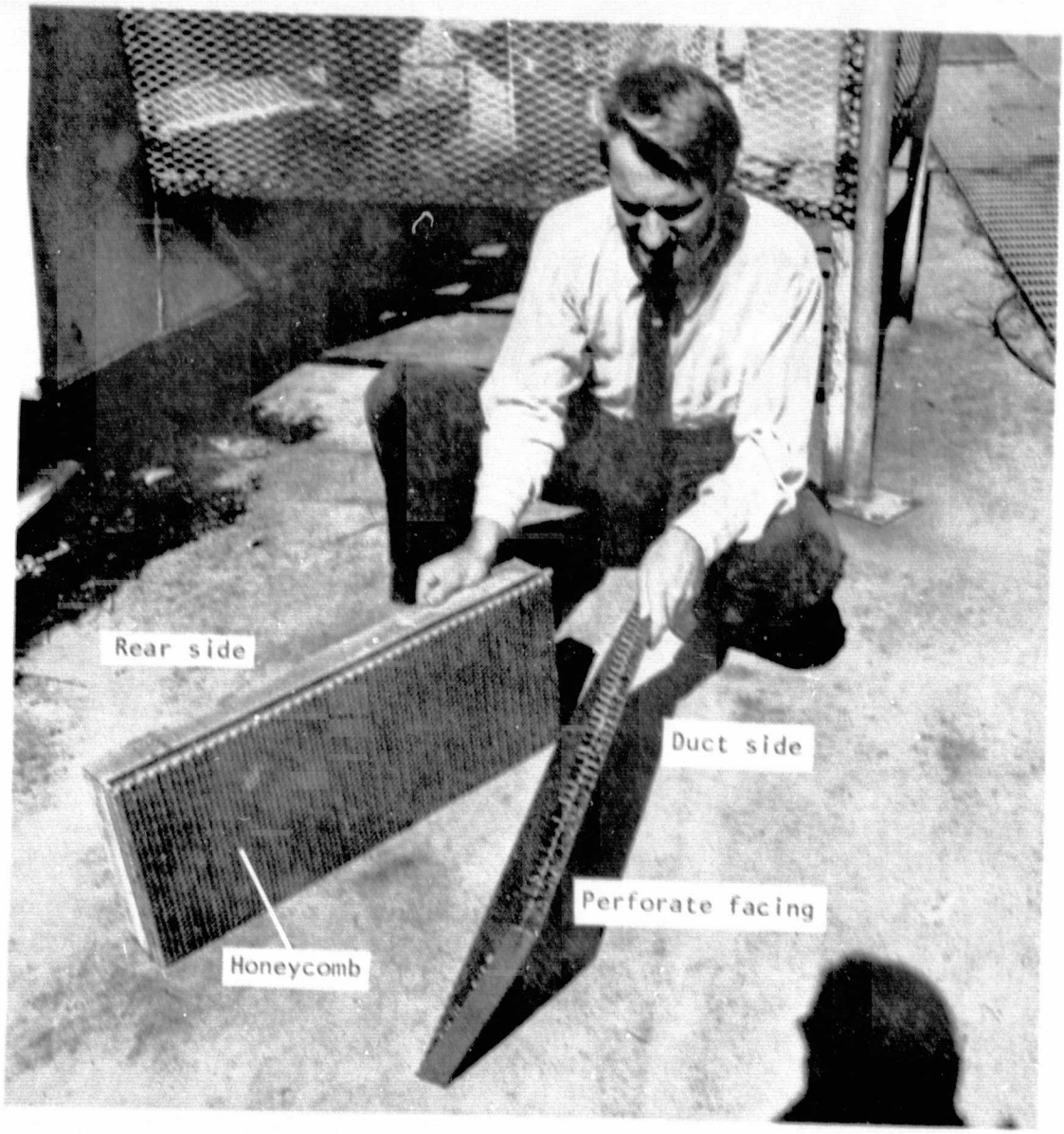


Figure 20. LINER BACKPLATE AND INTERMEDIATE FACING CAVITY ASSEMBLY

Figure 21. UNIFORM LINER PANELS: A1, B1 AND C1 CONFIGURATIONS

# 4. EXPERIMENTAL WORK

## 4.1 PRELIMINARY TESTS: MODIFIED WORK PLAN

The prerequisite to the success of the optimization routine is that an insertion loss maxima should exist within the range of liner impedance changes induced by the bias flow for the frequency band of interest. Consequently, the first test involved manual changes of bias flow from zero to the maximum possible for each liner for each frequency condition of interest (overall and 1/3-octave band).

It thus became evident that this prerequisite did not exist. On an overall basis, no discernable insertion loss maxima could be detected at any bias flow operating condition. Even on a 1/3-octave basis, changes of 2 dB with bias flow could be detected but were not repeatable between successive runs. These characteristics did not change with type of broadband source (either from inlet diffuser or acoustic drivers) or with the presence of flow. On the contrary, flow appeared to accentuate the nonrepeatability, possibly due in part to duct air temperature changes (which effect modal wavenumbers). These changes were induced by the upstream air source supply pressure and temperature changes with time in the blow-down holding tanks.

Thus, activation of the optimization control system even with a uniform liner did not result in proper convergence. Subsequently, narrow band analysis (to 10 Hz) was done on the insertion loss signal with various combinations of bias flow and it was evident that in any one narrow frequency band typical changes of +4 dB could be induced, however, the next narrow band could be -4 dB at the same bias flow condition. Thus, a broader bandwidth (1/3-octave) would average this behavior and show little, if any, change.

In the extreme case of discrete frequency excitation, bias flow changes resulted in as much as 10 dB differences in "insertion loss." However, it must be remembered that since the microphones are spatially fixed, a discrete frequency excitation will produce a fixed phase relationship between each microphone (i.e. high coherence), thus multiplexing between them will not result in an equivalent spatial averaging of the sound field (which is required for total energy representation). Thus, insertion loss measured under discrete tone excitation is not a true insertion loss, such as would be measured under random excitation conditions with total incoherency between microphones. Indeed, if 4 more microphones were placed in different locations in a discrete frequency situation, the 10 dB "insertion loss" variations would probably not be seen. Consequently, random excitation is the only valid method which can be used with this microphone configuration.

There are five possible effects which could result in the lack of detection of an insertion loss maxima with changes in bias flow. The first and perhaps most obvious reason is that the bias flow was not changing the wall impedance as the liner model predicted it should. Secondly, it is possible that the specified wall impedances were nowhere near the optimum (i.e., changes in wall impedance were following lines of essentially constant attenuation

contours on the impedance plane). The third possibility is that there existed other energy carrying modes in the duct that were insensitive to the changes in wall impedance and had low attenuation rates. The fourth possibility is an extension to the third in that the modal attenuation optima for adjacent modes might be so scattered throughout the impedance plane that no overall defined optimum solution exists within the entire liner impedance plane. Finally the fifth possibility is that bias flow changes the duct mean flow conditions significantly. For long lined ducts, this effect could be significant, however for the test configuration used here, changes in mean flow of less than 1% could only be detected at the rearmost liner exit position.

Of these five possible causes, the third seems the most likely. Table III lists the hard wall cut-on frequencies and respective mode orders for the test duct. It can be seen that the plane mode exists in isolation only below about 220 Hz. Thus, at the design $\eta$ of values of 0.25, 1.0, and 1.6 (which correspond to 500, 2 kHz and 3 kHz, respectively) many higher modes could exist and effectively carry energy even if the lower mode orders were highly attenuated. This aspect is further elaborated on later in Section 4.4.

As a result of the preliminary tests and performance appraisal, the original work plan was modified such that the automatic optimization control system was de-emphasized, while the insertion loss measurements and impedance measurements were expanded to cover all values of bias flows (not just the optimum values) with a much finer frequency resolution (10 Hz bandwidth not 1/3 octave). These changes were considered necessary in the fundamental sense that any user of the resultant data base would have a comprehensive set of measurements from which to work. In addition, the extra work required in collecting this data necessitated the deletion of the flow tests, since, in the fundamental sense, they did not constitute an essential requirement of the system concept evaluation.

TABLE III. CUT-ON FREQUENCIES FOR HARD WALL MODES IN TEST DUCT (First 22 Higher Modes)

| Mode Order | $f_c$ (Hz) | Mode Order | $f_c$ (Hz) |
|---|---|---|---|
| (0,1) | 224 | (1,5) | 1475 |
| (0,2) | 448 | (0,7) | 1568 |
| (0,3) | 672 | (1,6) | 1652 |
| (0,4) | 896 | (0,8 | 1792 |
| (1,0) | 960 | (1,7) | 1838 |
| (1,1) | 986 | (2,0) | 1920 |
| (1,2) | 1060 | (2,1) | 1933 |
| (0,5) | 1120 | (2,2) | 1971 |
| (1,3) | 1172 | (0,9) | 2016 |
| (1,4) | 1313 | (1,8) | 2032 |
| (0,6) | 1344 | (2,3) | 2034 |

The modified work plan thus defined the two experimental tasks to be as follows:

(1) The insertion loss would be measured for (a) three sets of uniform liners (designated A1, B1, and C1) at five values of liner bias flows (zero, 25%, 50%, 75%, and 100%), and (b) one set of two independently controlled liner panels (designated A1 and A2) at three independently set values of bias flow (zero, 50%, and 100%).

(2) The wall impedance will be measured in-situ for each of the liner designations A1, A2, B1, and C1 at five levels of bias flow (zero, 25%, 50%, 75% and 100%).

The results of these two measurement tasks are given below in Sections 4.2 and 4.3.

## 4.2 INSERTION LOSS MEASUREMENTS

The insertion loss measurements were done using the technique and procedure described in Section 2. All plots presented here are the result of subtraction of the base line hard wall insertion loss, from the insertion loss measured with the test liner configuration in place. Since the basic narrow band analysis technique inevitably produced large scatter between adjacent bands (as shown in Figure 22, for example) an eleven-point spectral smoothing technique (based on Simpson's rule) was applied to the raw data before subtraction took place. The result of this was the much cleaner plot of Figure 23. Final enhancement of all the following insertion loss (I.L.) plots was achieved by a five-point smoothing of the I.L. spectrum itself (shown in figure 24, for example). Four liner configurations were tested as per the modified work plan; three uniform and one two-segment system, at five levels of bias flow: zero, 25, 50, 75 and 100%, with the results presented below.

### 4.2.1 Characteristics of $\eta = 1.6$ Uniform Liner

The basic shape of the i.L. at zero bias flow can be seen in figure 24 to consist of two major valleys (equivalent to attenuation peaks) one at 1 kHz of about 12 dB, the other around 3.1 kHz of about 11 dB. The latter valley is very near the design frequency of 3 kHz for this liner (designation C1). As bias flow is increased up to 100% (figures 25 to 28), little change is initially observed at 25%, perhaps ±1 dB difference with respect to the zero bias flow case. At 50% bias, a definite improvement of +1 dB in the I.L. valleys can be seen. With 75% bias, little change is observed. If the bias flow is increased to 100%, the total observed improvement is eroded completely, in fact, the I.L. valleys are 1 dB less than the zero bias flow case. As a further check on this trend, one extra measurement was done which involved increasing the bias supply pressure from 138 KPa (20 psi) to 276 KPa (40 Psi) with 100% bias flow valve opening. The result of this test (shown in figure 29) confirmed the continuing decrease in I.L., as the attenuation then became 3-4 dB less than the zero bias case over the whole frequency range tested above 500 Hz.

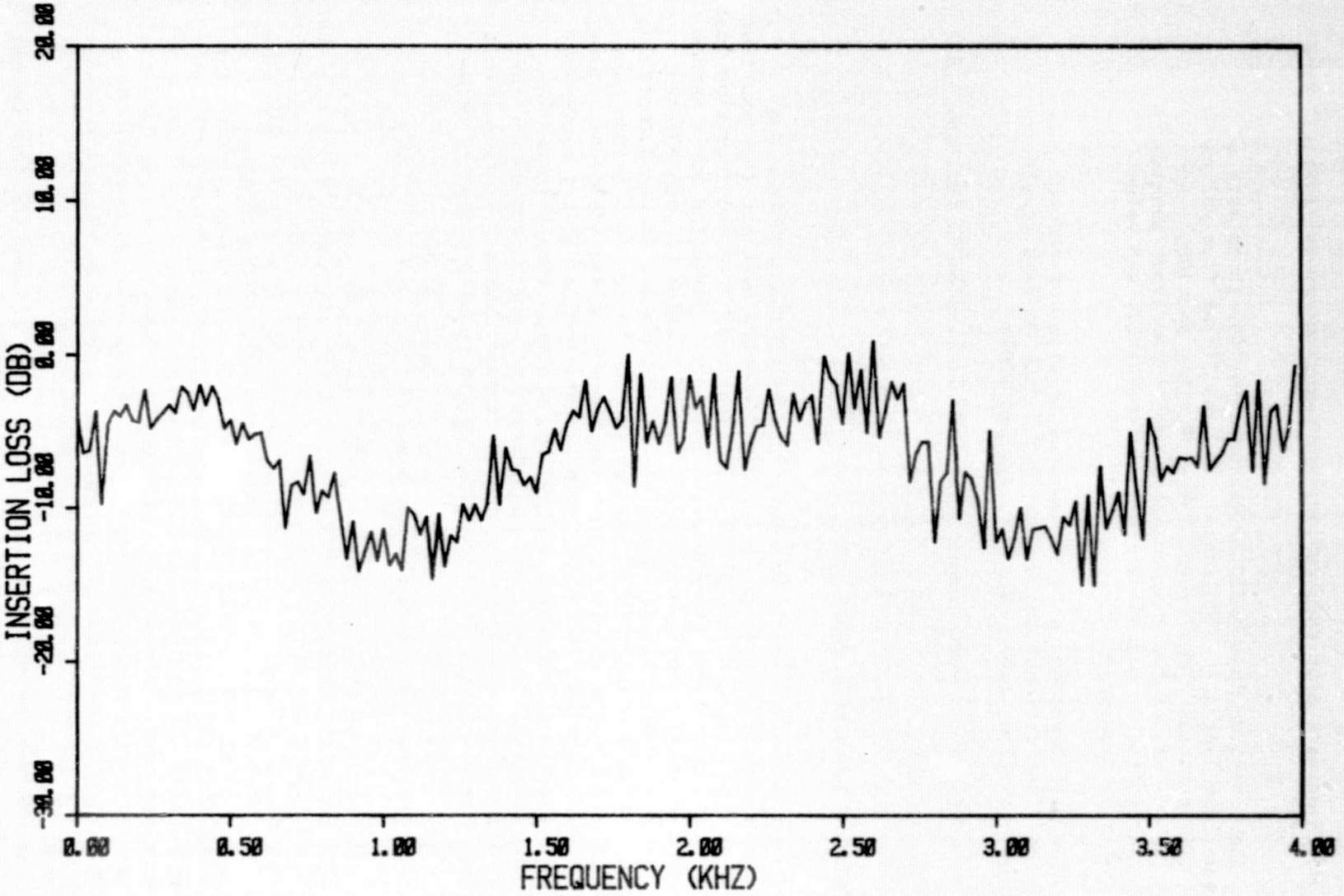


FIG. 22 INSERTION LOSS OF LINER SEGMENTS C1, C1, C1 WITH BIAS FLOWS OF 0 %, 0 %, 0 % RESPECTIVELY.
(EXAMPLE OF RAW DATA MEASUREMENT)

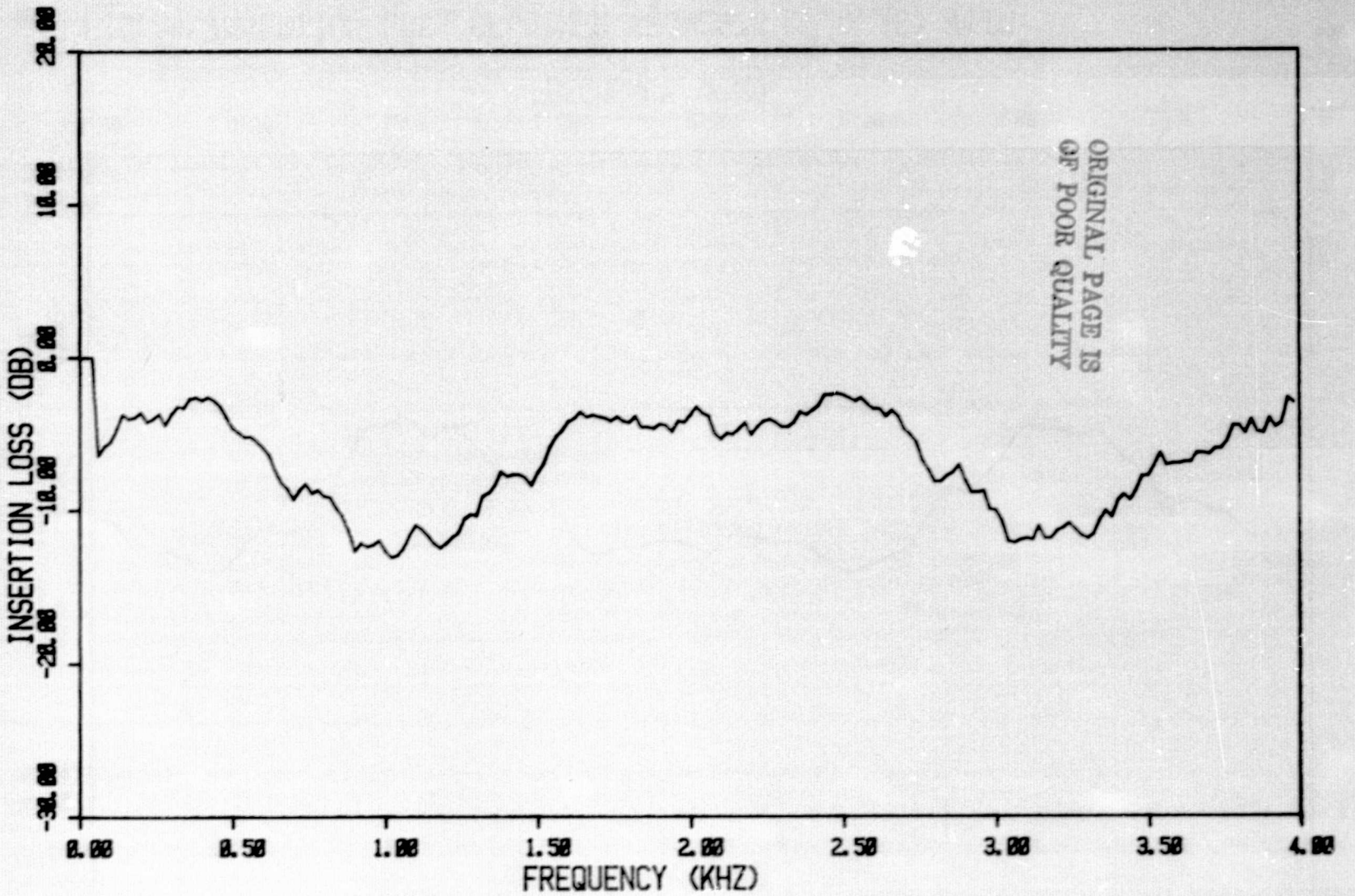




FIG. 23 INSERTION LOSS OF LINER SEGMENTS C1, C1, C1 WITH BIAS FLOWS OF 0 %, 0 %, 0 % RESPECTIVELY.
(EXAMPLE OF 11 PT SMOOTHING OF RAW DATA)

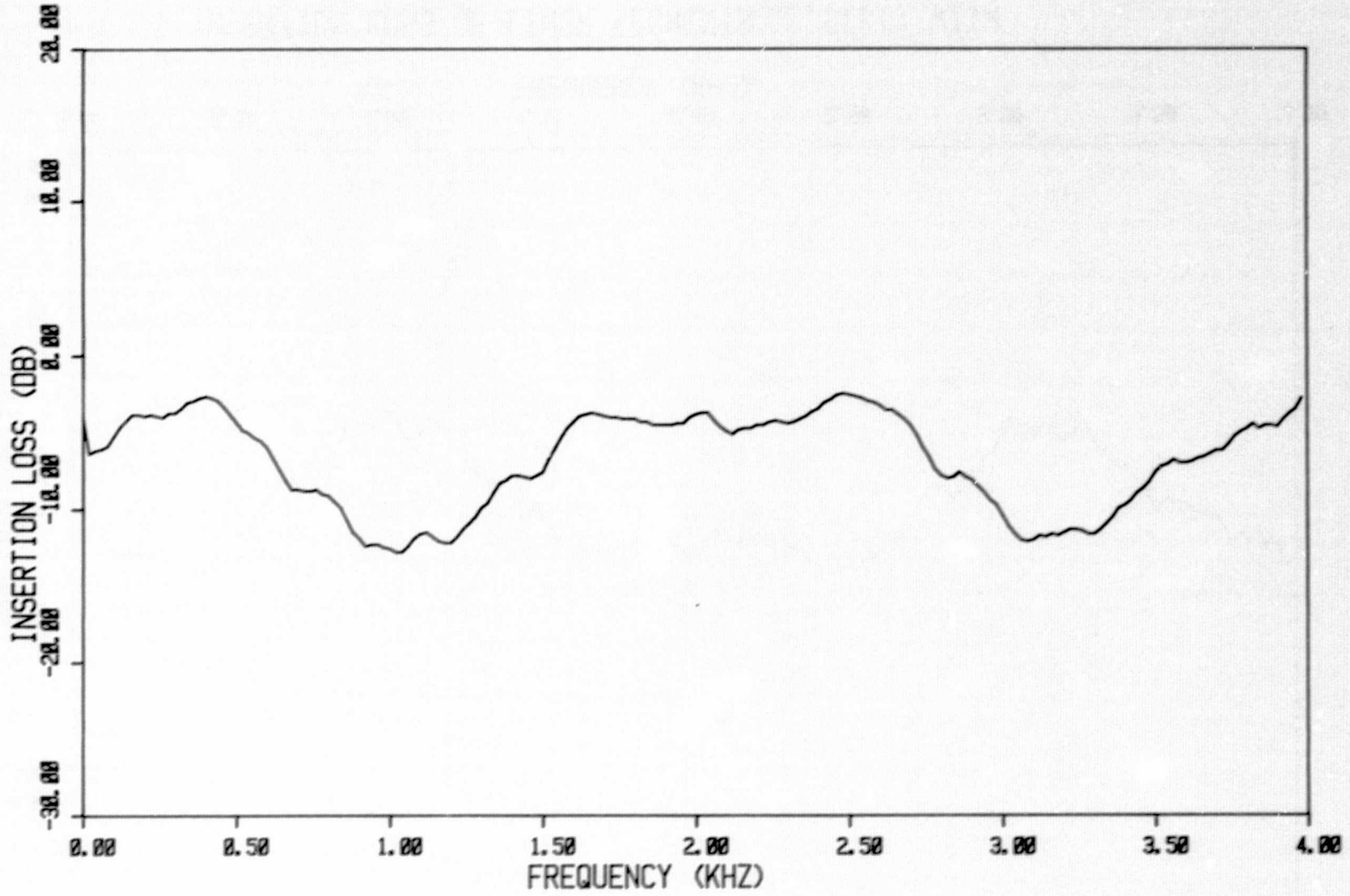


FIG. 24 INSERTION LOSS OF LINER SEGMENTS C1, C1, C1 WITH BIAS FLOWS OF 0 %, 0 %, 0 % RESPECTIVELY.

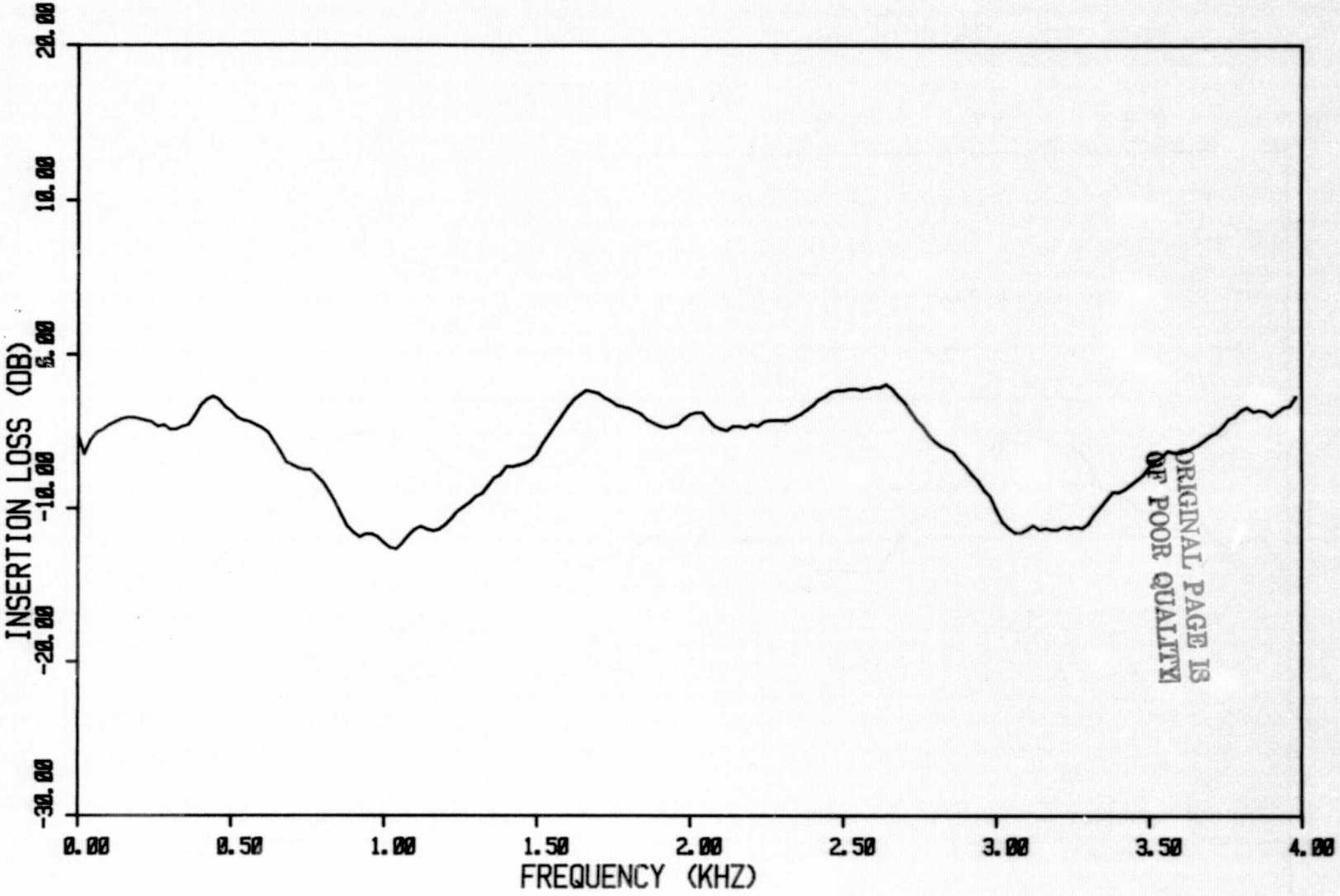




FIG. 25 INSERTION LOSS OF LINER SEGMENTS C1, C1, C1 WITH BIAS FLOWS OF 25 %, 25 %, 25 % RESPECTIVELY.

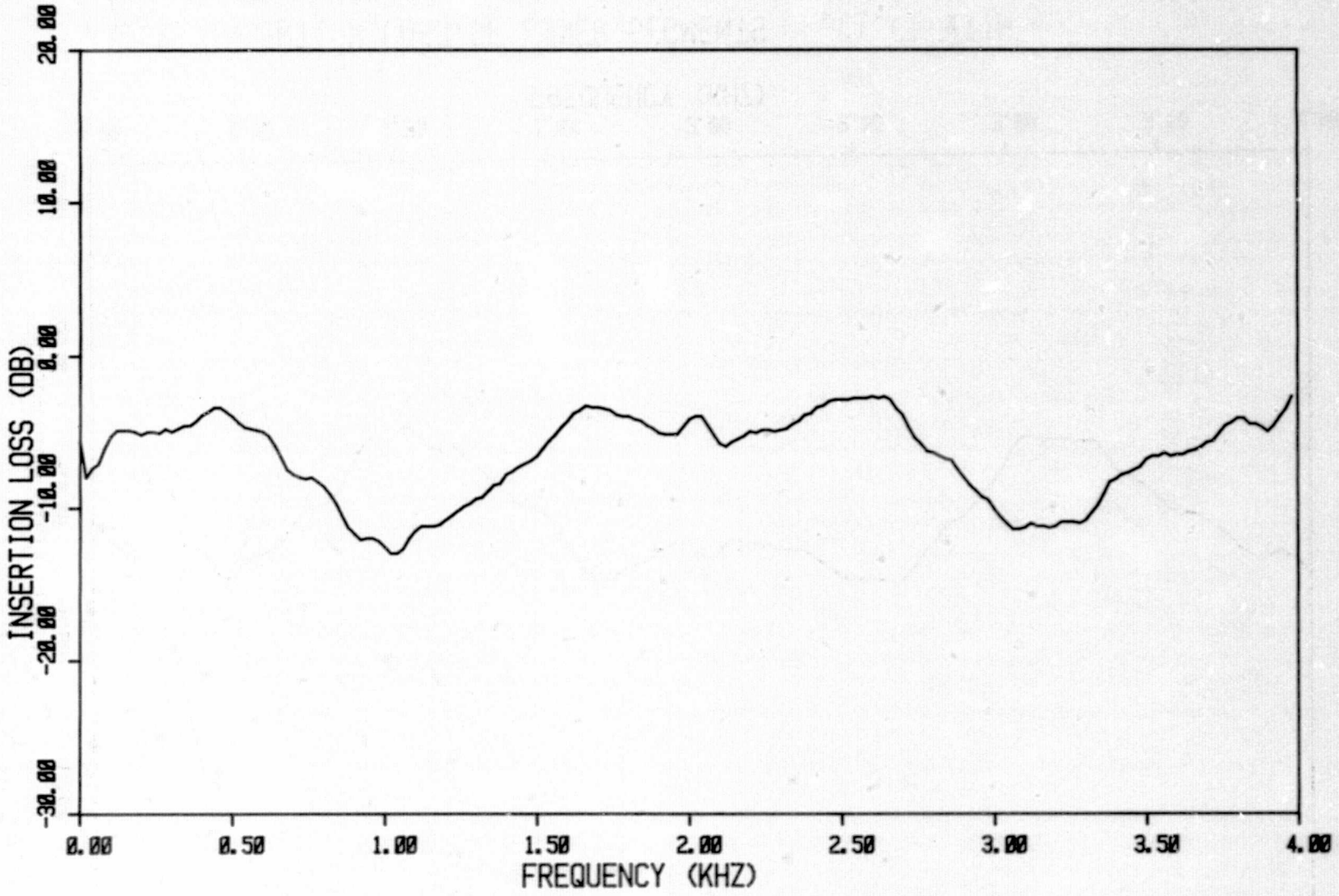


FIG. 26 INSERTION LOSS OF LINER SEGMENTS C1, C1, C1 WITH BIAS FLOWS OF 50 %, 50 %, 50 % RESPECTIVELY.

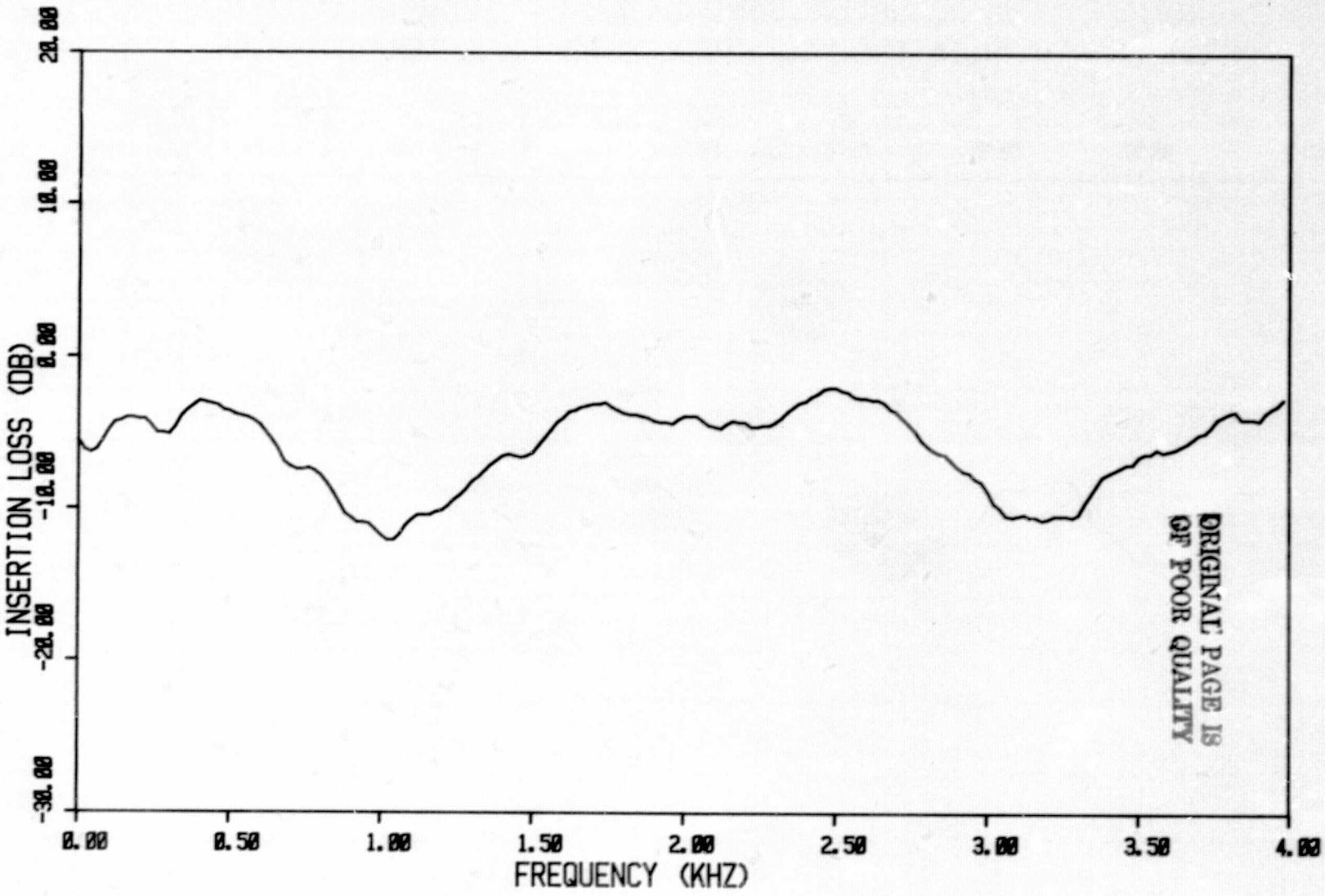




FIG. 27 INSERTION LOSS OF LINER SEGMENTS C1, C1, C1 WITH BIAS FLOWS OF 75 %, 75 %, 75 % RESPECTIVELY.

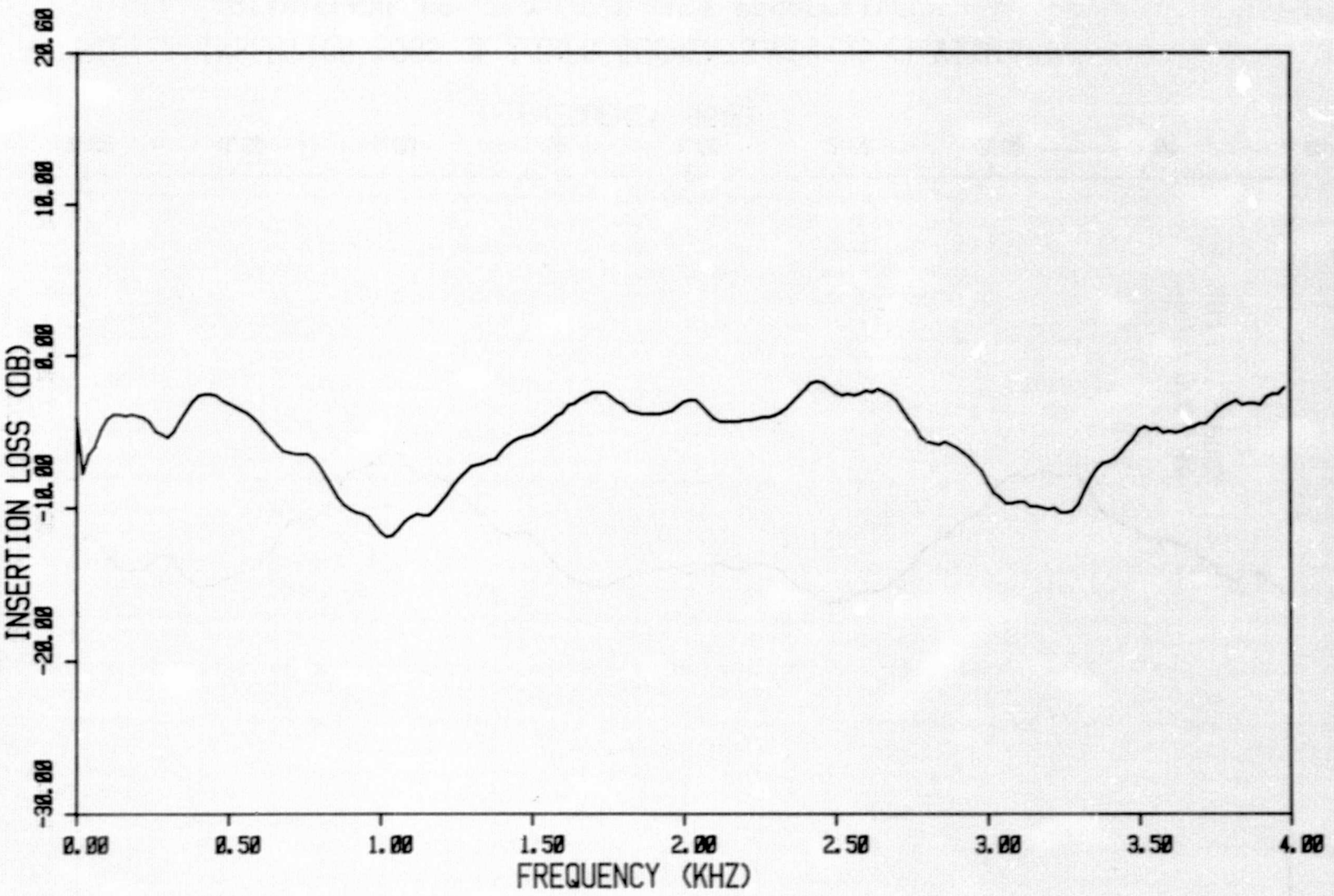


FIG. 28 INSERTION LOSS OF LINER SEGMENTS C1, C1, C1 WITH BIAS FLOWS OF 100 %, 100 %, 100 % RESPECTIVELY.

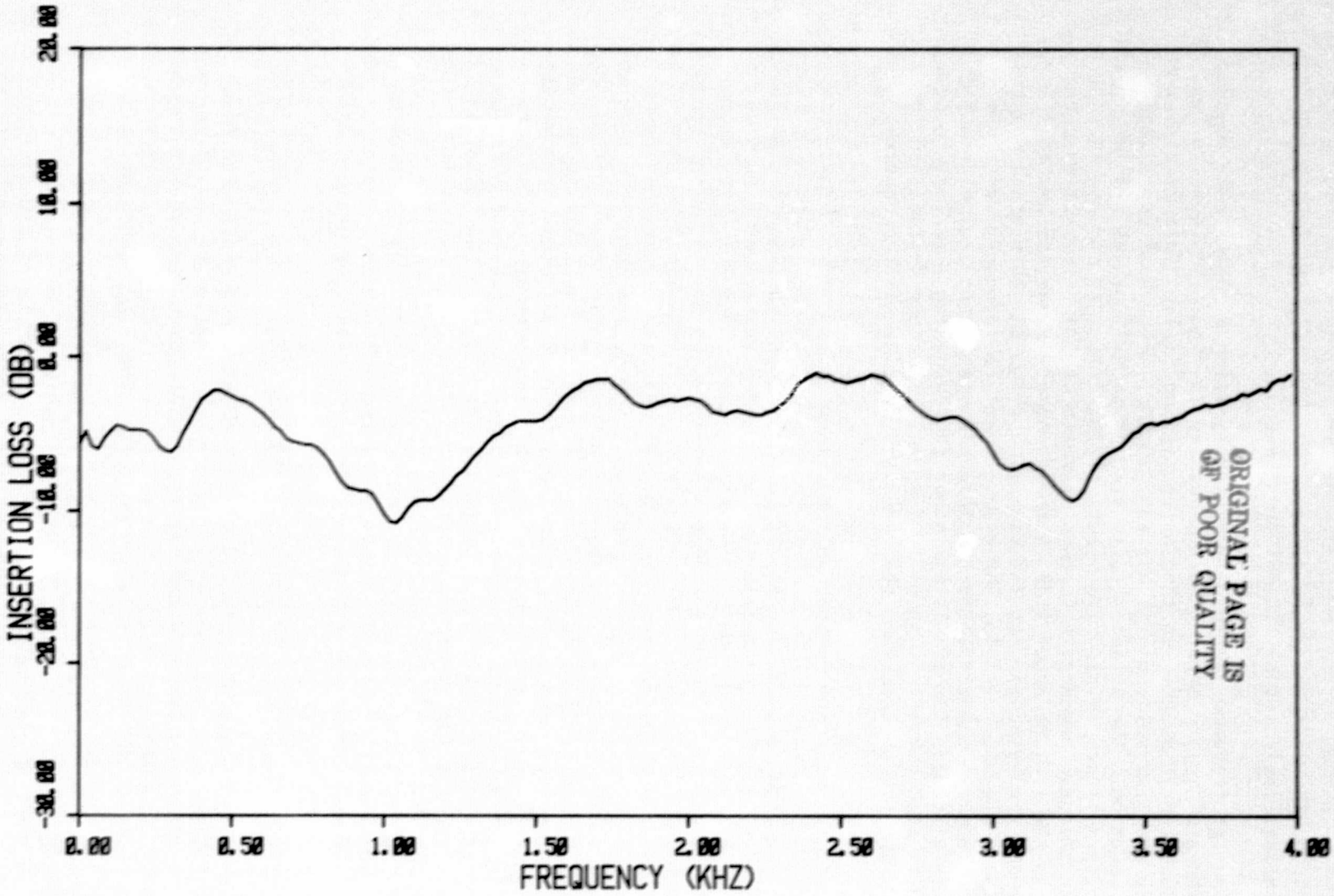


FIG. 29 INSERTION LOSS OF LINER SEGMENTS C1, C1, C1 WITH BIAS FLOWS OF 100%, 100%, 100% RESPECTIVELY @ 276 KPa (40 PSI) SUPPLY PRESSURE.

### 4.2.2 Characteristics of $\eta = 1.0$ Uniform Liner

The design frequency of this liner (designation B1) is 2 kHz, however, the existence of only a small 5 dB I.L. valley in figure 30 seems to imply a far from optimum impedance for the incident sound field. This is with comparison to the I.L. valleys at 1 kHz and 3.5 kHz, which have approximately 12 dB attenuation. The effect of bias flow on this liner was similar to the $\eta = 1.6$ uniform liner. A bias flow level of 25% (fig. 31) did not include any measurable change. However, a further increase of 50% (fig. 32) produced an increase in the I.L. of about 1 dB in the frequency range 1.5 kHz to 2.6 kHz (i.e. between the valleys). At 75% bias flow (fig. 33) this trend reversed and a general decrease of 1 to 2 dB over the entire frequency range was observed. Thus, in comparison to the zero bias case, the region from 1.5 to 2.6 kHz was virtually identical, all other regions being 1 dB less in attenuation. With 100% bias flow, shown in figure 34, further degradation occurred, the I.L. being 2-3 dB less than the zero bias case at all frequencies.

### 4.2.3 Characteristics of $\eta = 0.25$ Uniform Liner

The insertion loss characteristics of this liner (designation A1) at zero bias flow (fig. 35) is essentially flat with three valleys of 8 to 9 dB, one at the design frequency of 500 Hz, the others at 1.6 and 2.7 kHz. With a bias flow of 25% (fig. 36), the only change appears in the 300 to 500 Hz range as an improvement in I.L. of about 1 dB. This improves further to 2 dB with an increase of bias flow to 50% (shown in fig. 37) over the frequency range 250 Hz to 600 Hz, while a 1 dB increase in attenuation over the zero bias flow case is observed in the 2.0 to 2.6 kHz region. At a bias flow level of 75%, again further improvement to 3 dB is observed in figure 38, over the 250 to 600 Hz range with a general 1 to 2 dB increase in I.L. over all other frequencies. However, in figure 39, at 100% bias flow, this improvement is dissipated with the I.L. reverting to the 2 dB improvement levels near the design frequency and a general characteristic shape virtually identical to the 50% bias flow plot. This degradation trend was further confirmed by an I.L. test at 100% bias flow but with double the supply pressure (i.e. 276 KPa). In this test (shown in fig. 40), the 250 to 500 Hz region showed a 1-2 dB improvement over the zero bias flow I.L. levels, however, the remaining higher frequency region showed 1-2 dB I.L. reduction compared to the zero bias flow measurements.

### 4.2.4 Characteristics of $\eta = 0.25$ Two-Segment Liner

The insertion loss was measured with liner segments designated A1 and A2 with A1 being the upstream segment. A matrix combination of bias flows was measured according to Table IV and the results are presented in the respective figure number designations on that table. Figure 41 shows the reference case, that of zero bias flow on both liner segments. The I.L. characteristic is essentially flat over the whole frequency range at 6 to 8 dB attenuation level, with no noteworthy I.L. peaks or valleys. If the bias flow on segment A2 is now increased to 50% (fig. 42), the only change that can be seen is a 1 dB increase in the I.L. in the 300 to 500 Hz range (just below the design frequency). Otherwise, the I.L. remains the same over the rest of the frequency range of interest. A further increase in bias flow of segment A2 to

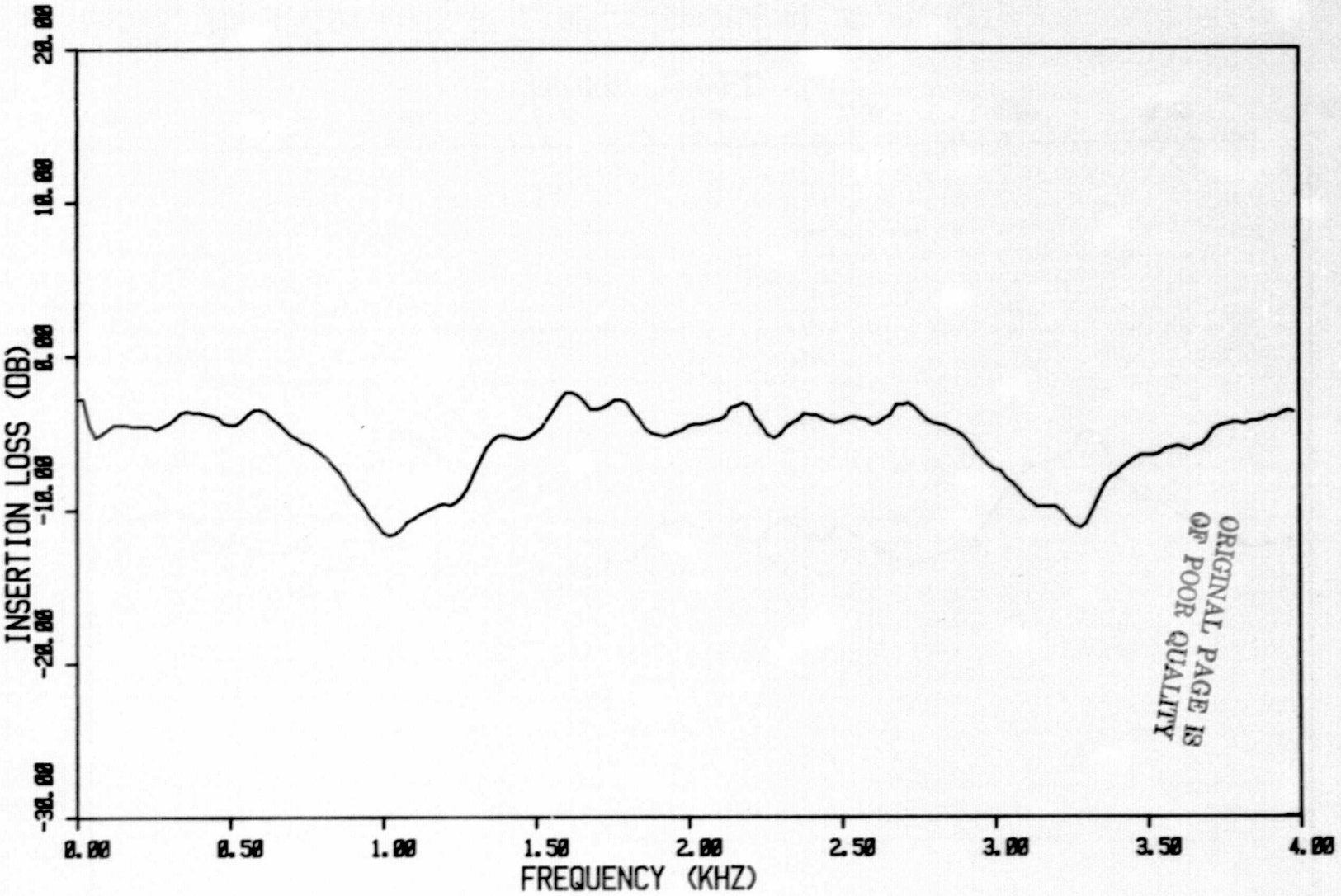


FIG. 30 INSERTION LOSS OF LINER SEGMENTS B1, B1, B1 WITH BIAS FLOWS OF 0 %, 0 %, 0 % RESPECTIVELY.

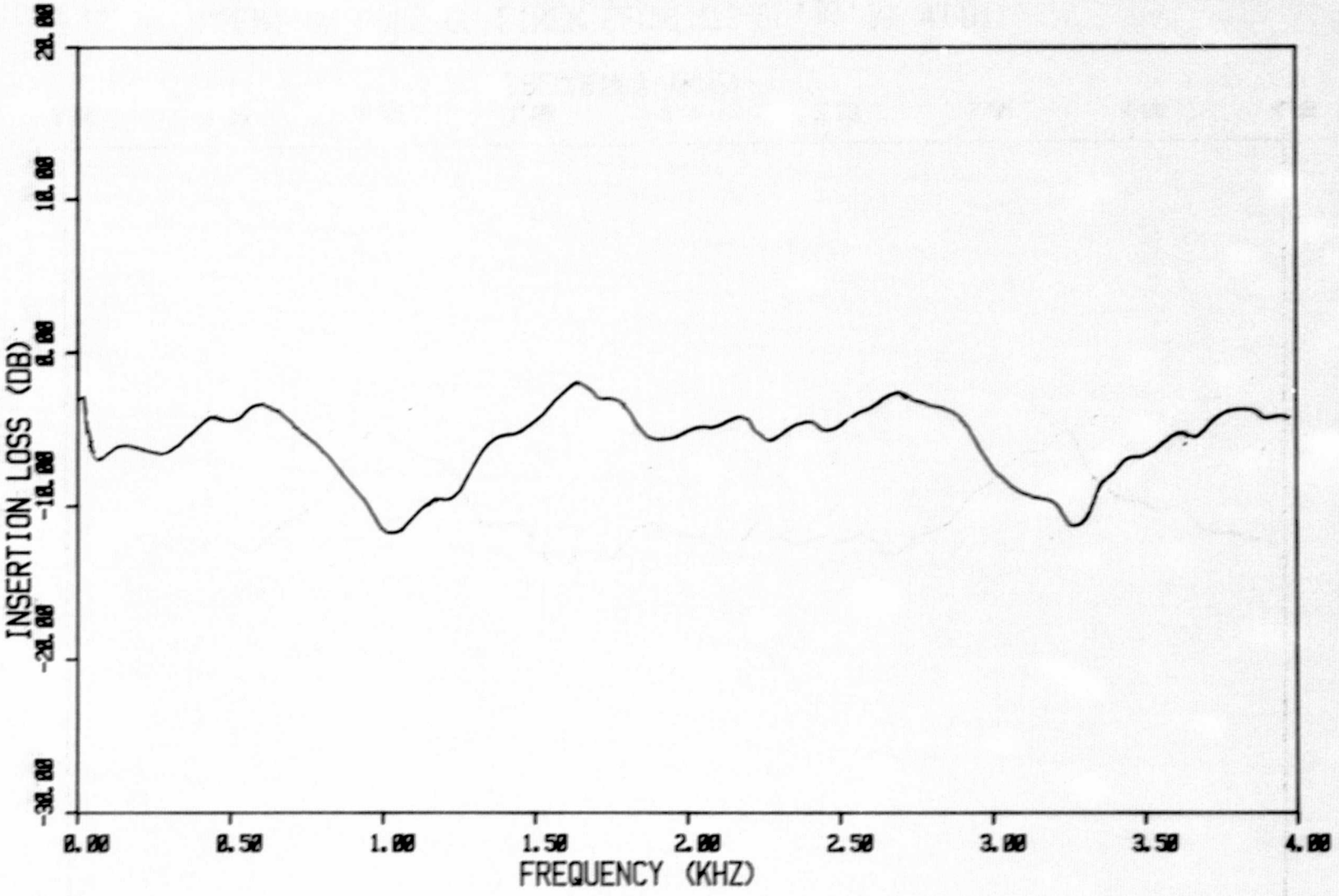


FIG. 31 INSERTION LOSS OF LINER SEGMENTS B1, B1, B1 WITH BIAS FLOWS OF 25 %, 25 %, 25 % RESPECTIVELY.

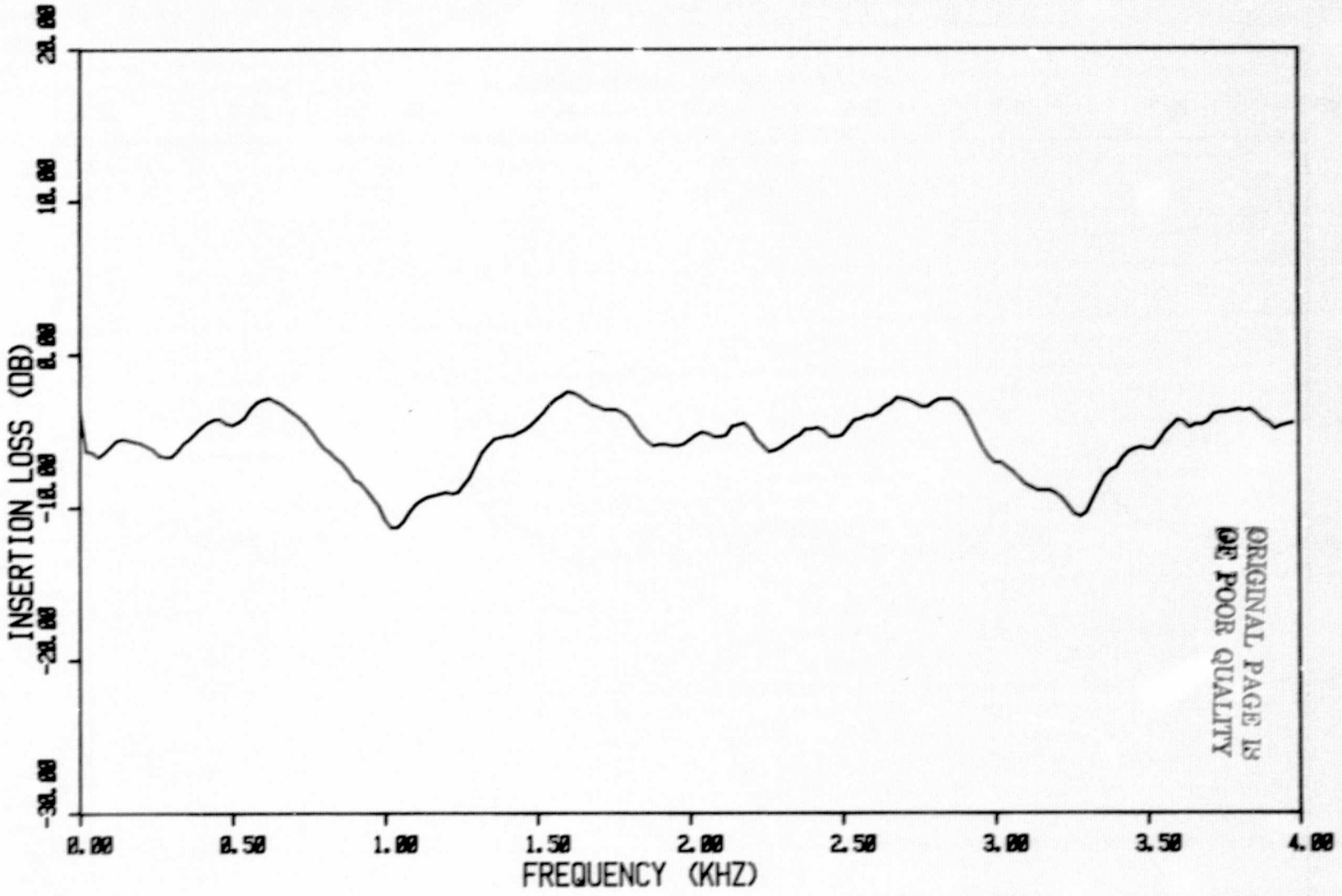


FIG. 32 INSERTION LOSS OF LINER SEGMENTS B1, B1, B1 WITH BIAS FLOWS OF 50 %, 50 %, 50 % RESPECTIVELY.

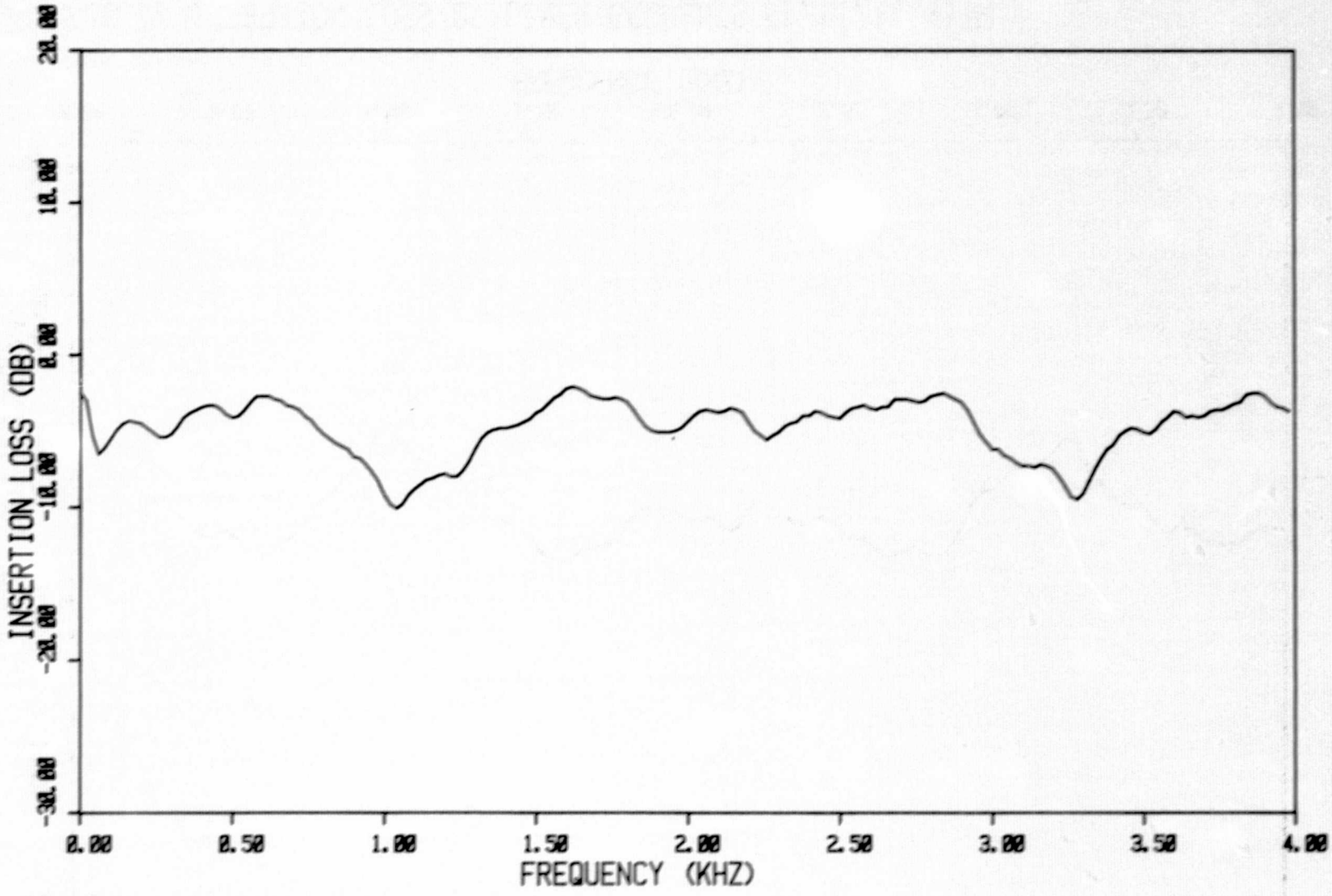


FIG. 33 INSERTION LOSS OF LINER SEGMENTS B1, B1, B1 WITH BIAS FLOWS OF 75 %, 75 %, 75 % RESPECTIVELY.

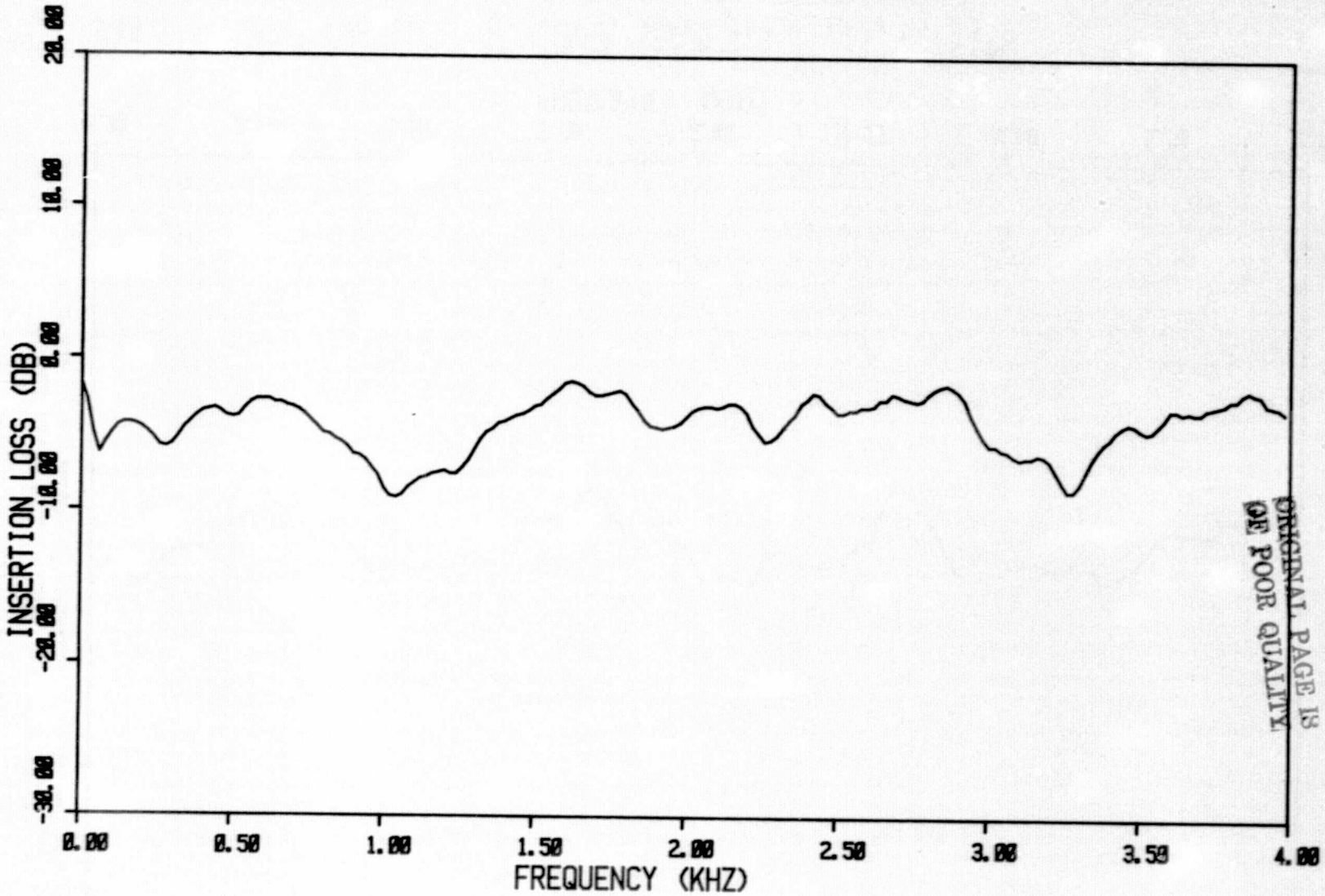




FIG. 34 INSERTION LOSS OF LINER SEGMENTS B1, B1, B1 WITH BIAS FLOWS OF 100%, 100%, 100% RESPECTIVELY.

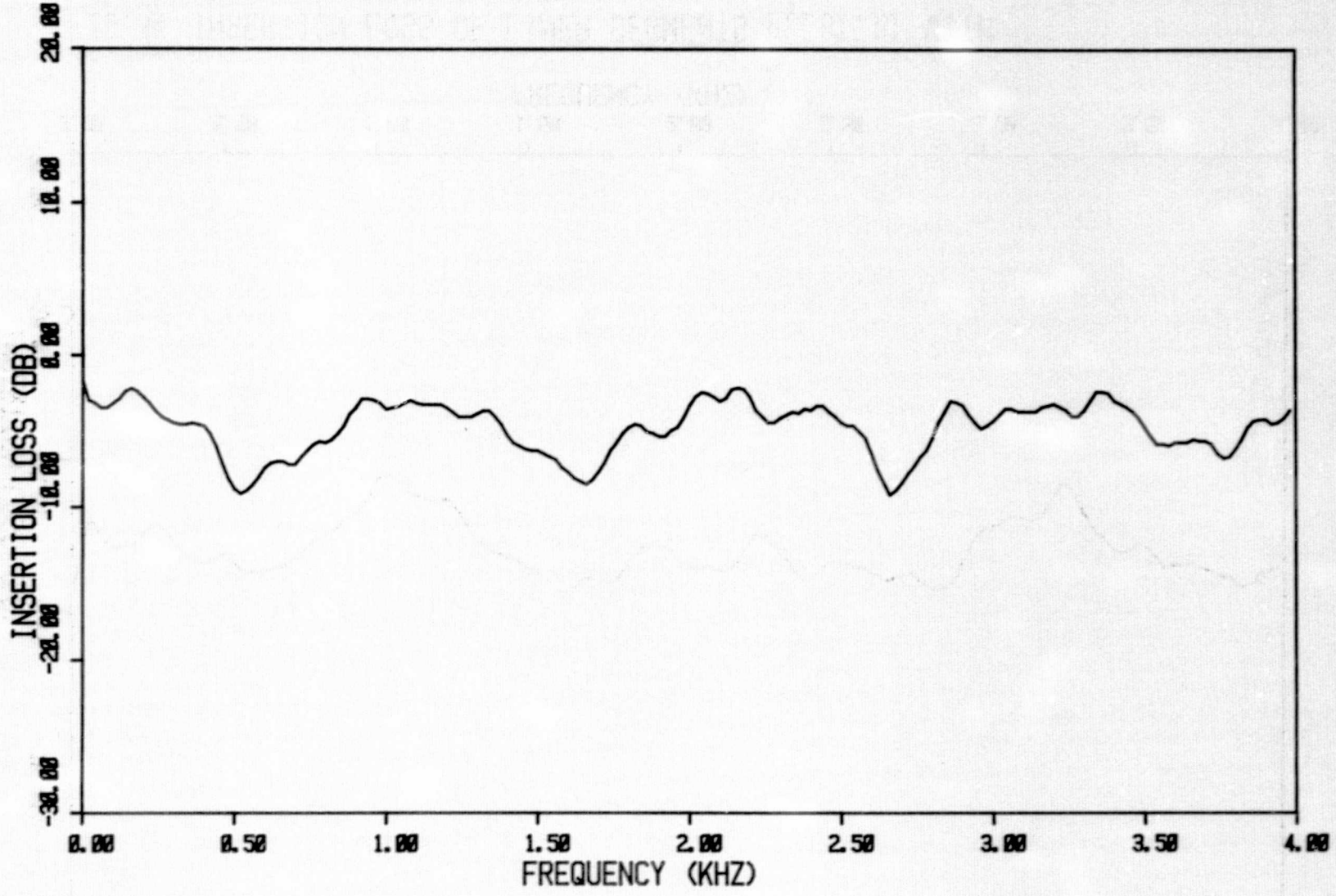


FIG.35 INSERTION LOSS OF LINER SEGMENTS A1, A1, A1 WITH BIAS FLOWS OF 0 %, 0 %, 0 % RESPECTIVELY.

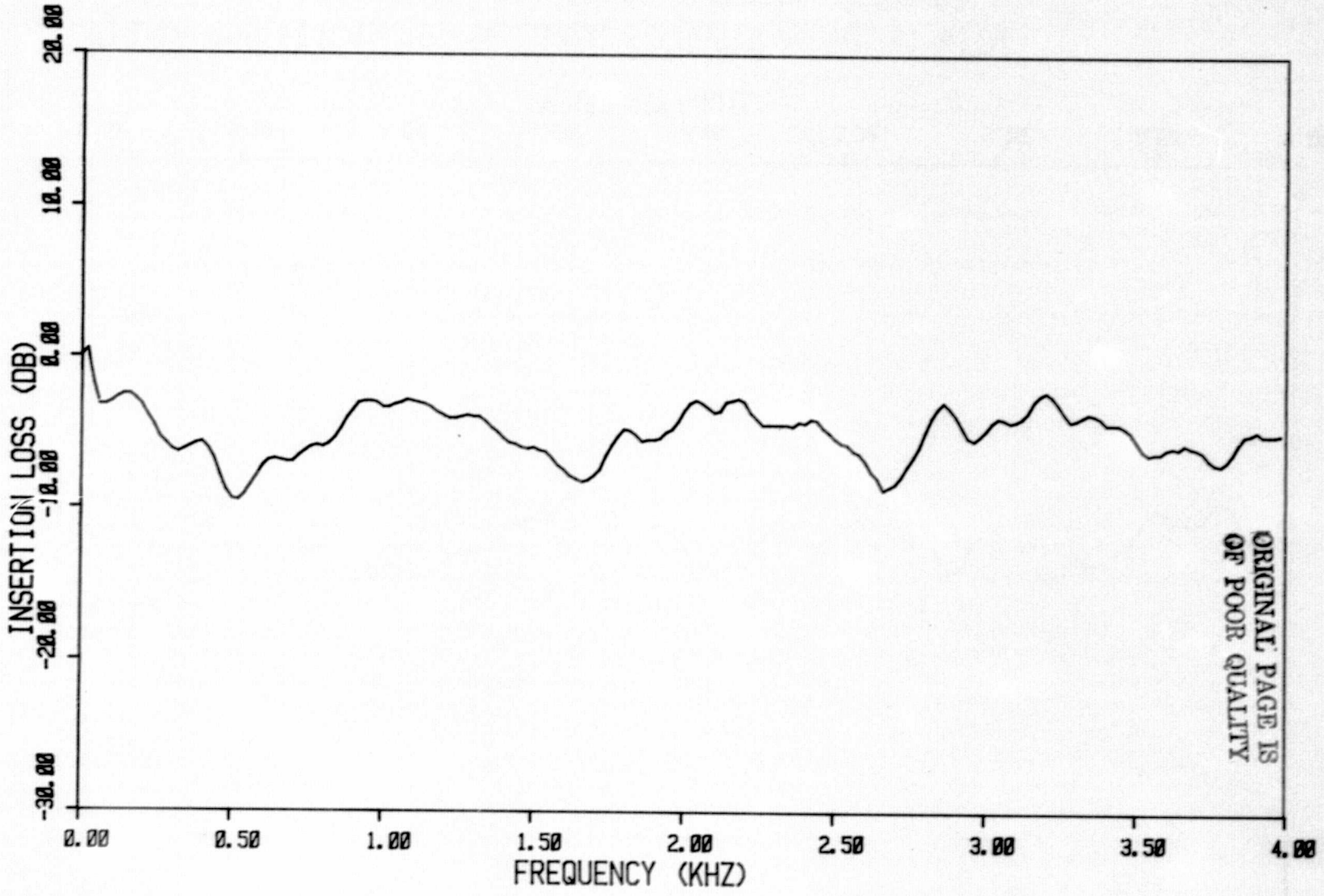


FIG.36 INSERTION LOSS OF LINER SEGMENTS A1, A1, A1 WITH BIAS FLOWS OF 25 %, 25 %, 25 % RESPECTIVELY.

FIG. 37 INSERTION LOSS OF LINER SEGMENTS A1, A1, A1 WITH BIAS FLOWS OF 50 %, 50 %, 50 % RESPECTIVELY.

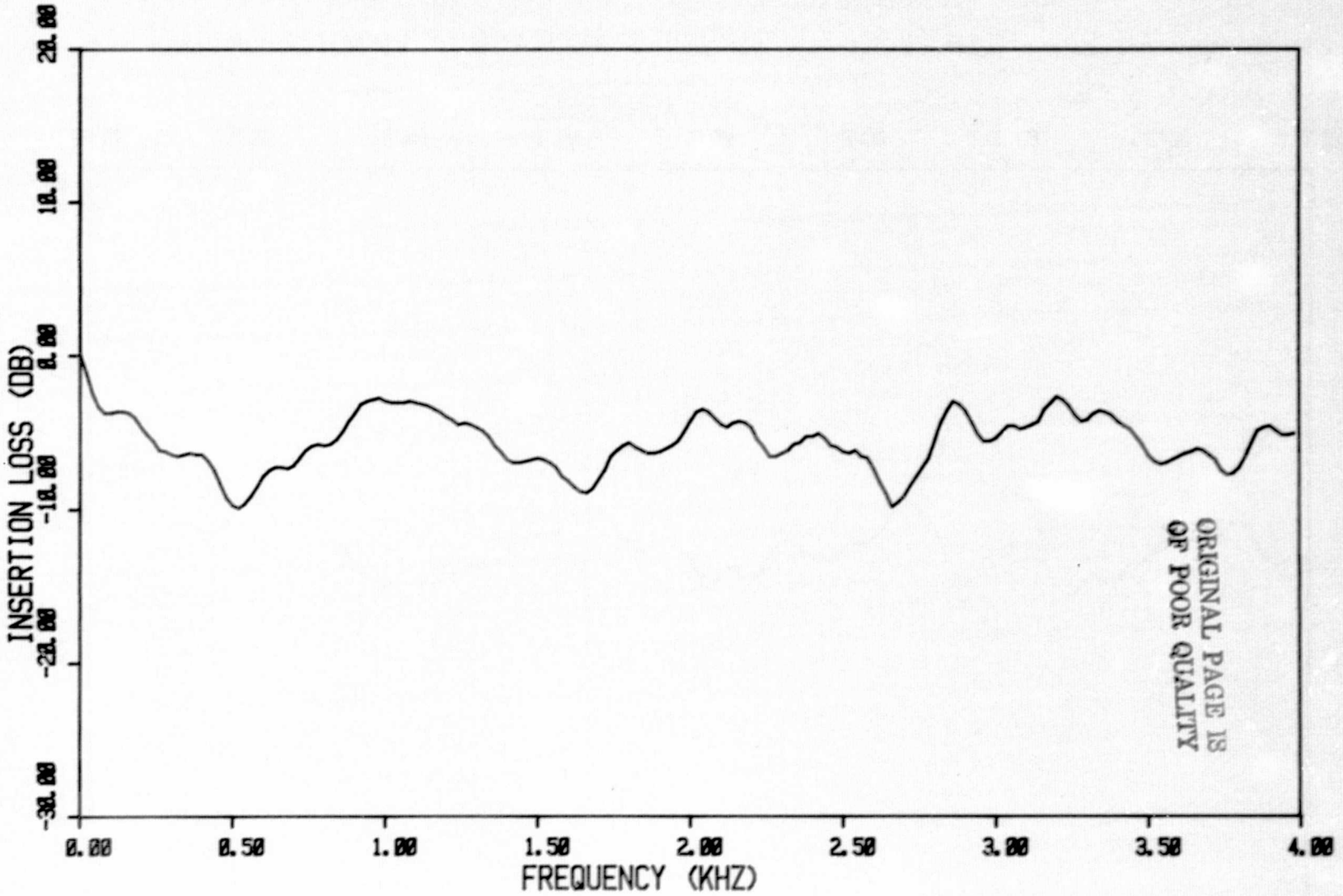


FIG. 38 INSERTION LOSS OF LINER SEGMENTS A1, A1, A1 WITH BIAS FLOWS OF 75%, 75%, 75% RESPECTIVELY.

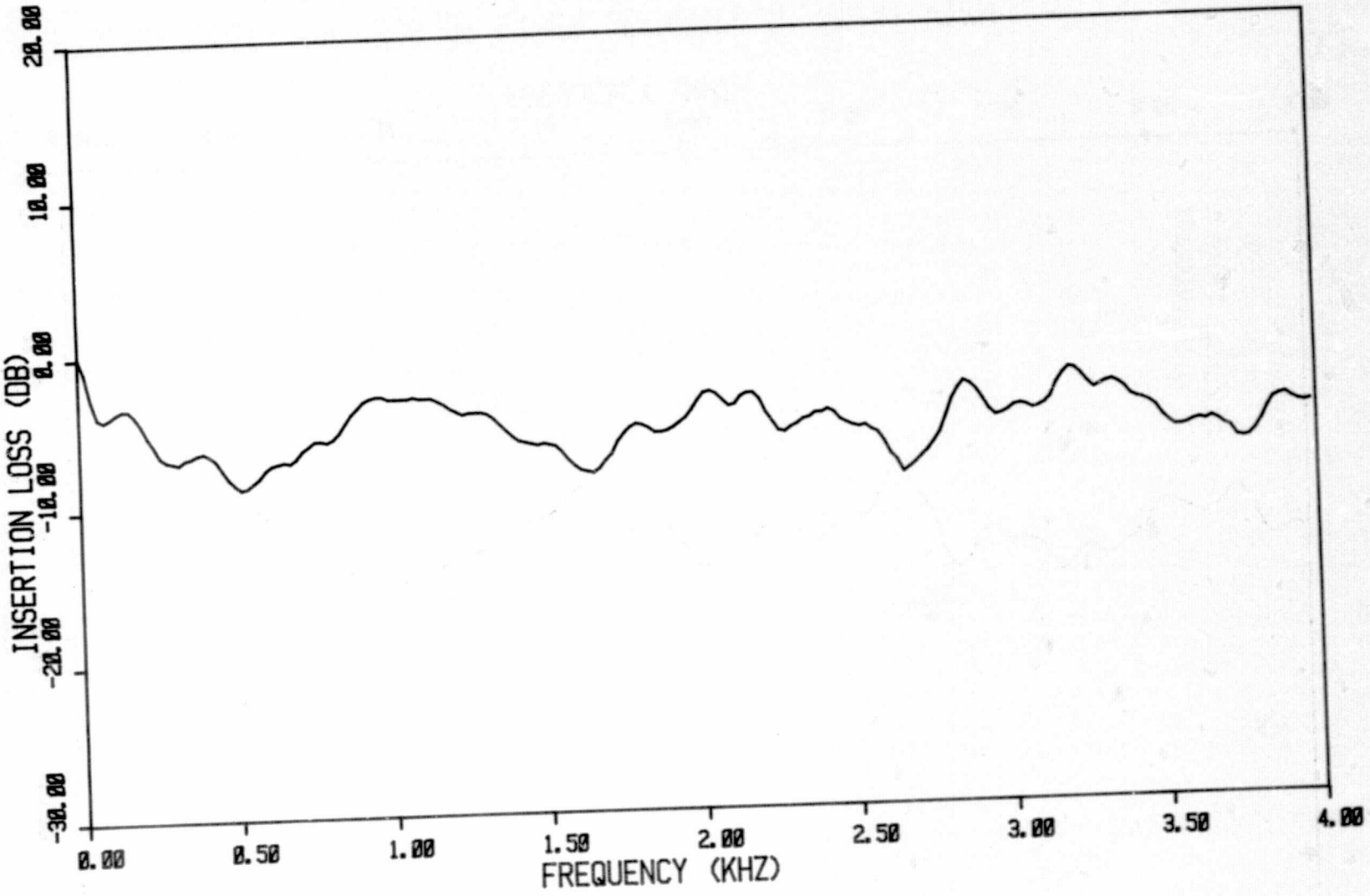


FIG. 39 INSERTION LOSS OF LINER SEGMENTS A1, A1, A1 WITH BIAS FLOWS OF 100 %, 100 %, 100% RESPECTIVELY.

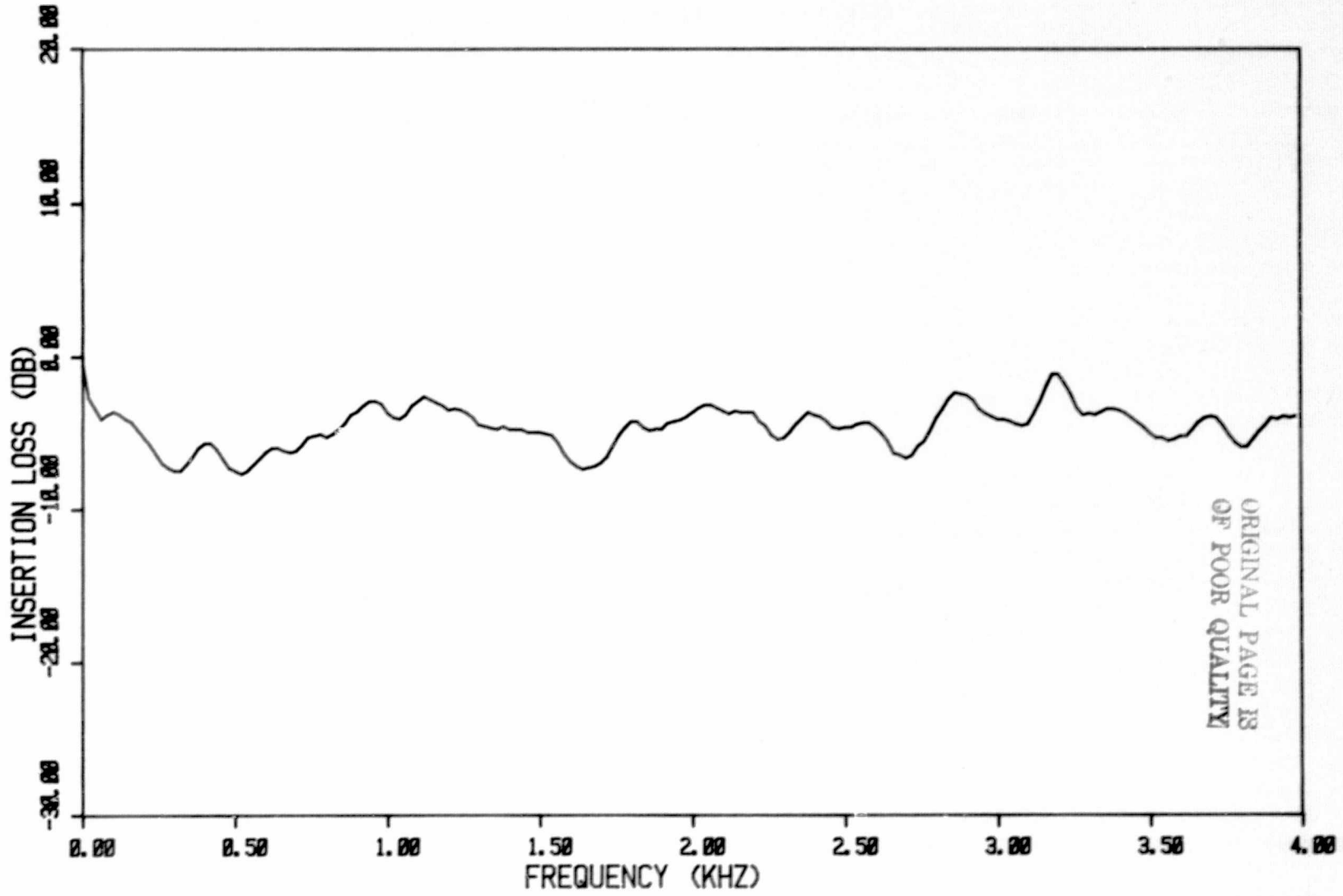


FIG. 40 INSERTION LOSS OF LINER SEGMENTS A1, A1, A1 WITH BIAS FLOWS OF 100%, 100%, 100% RESPECTIVELY @ 276 $KP_a$ (40 PSI) SUPPLY PRESSURE.

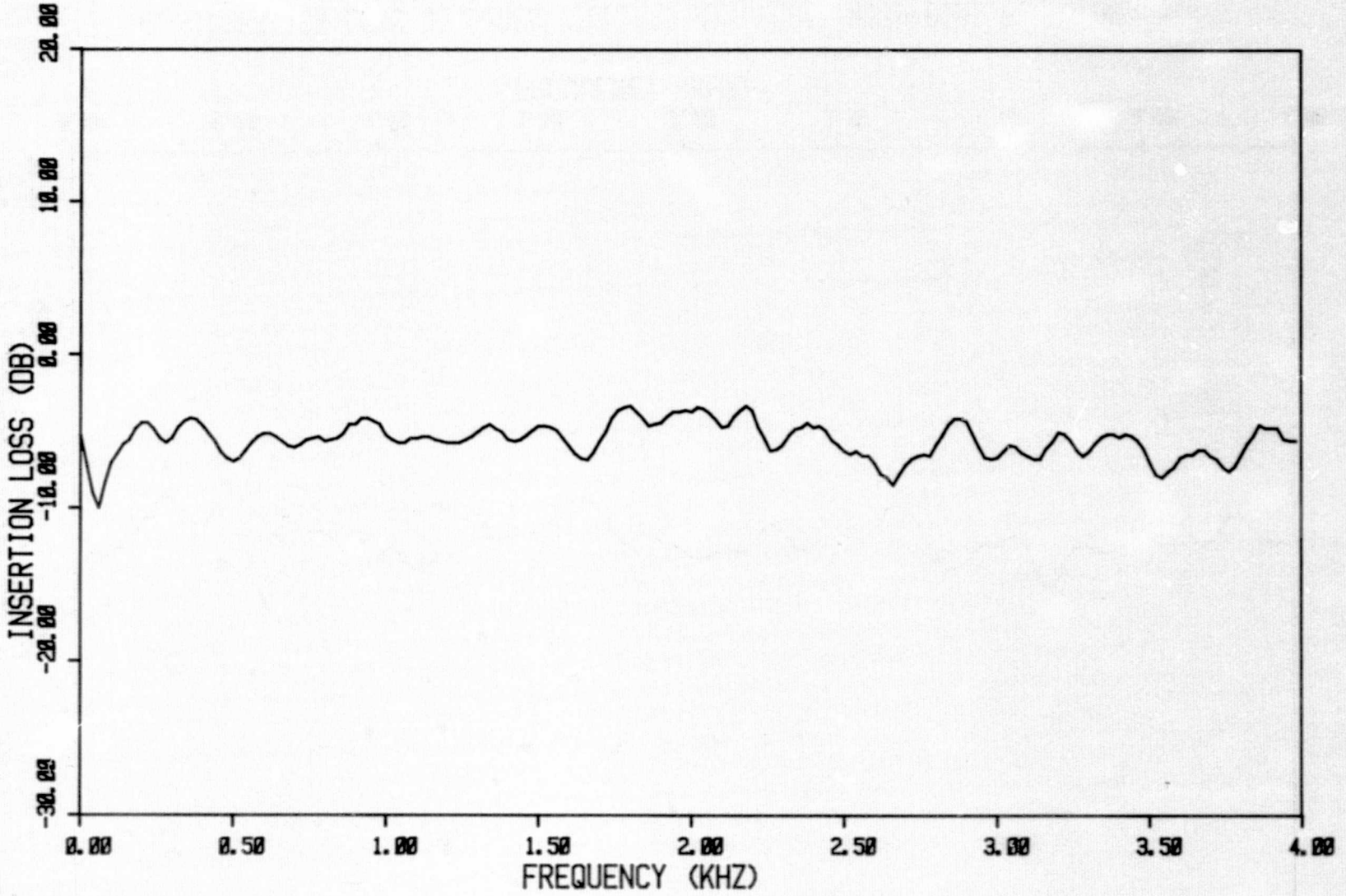


FIG. 41 INSERTION LOSS OF LINER SEGMENTS A1, A2 WITH BIAS FLOWS OF 0 %, 0 % RESPECTIVELY.

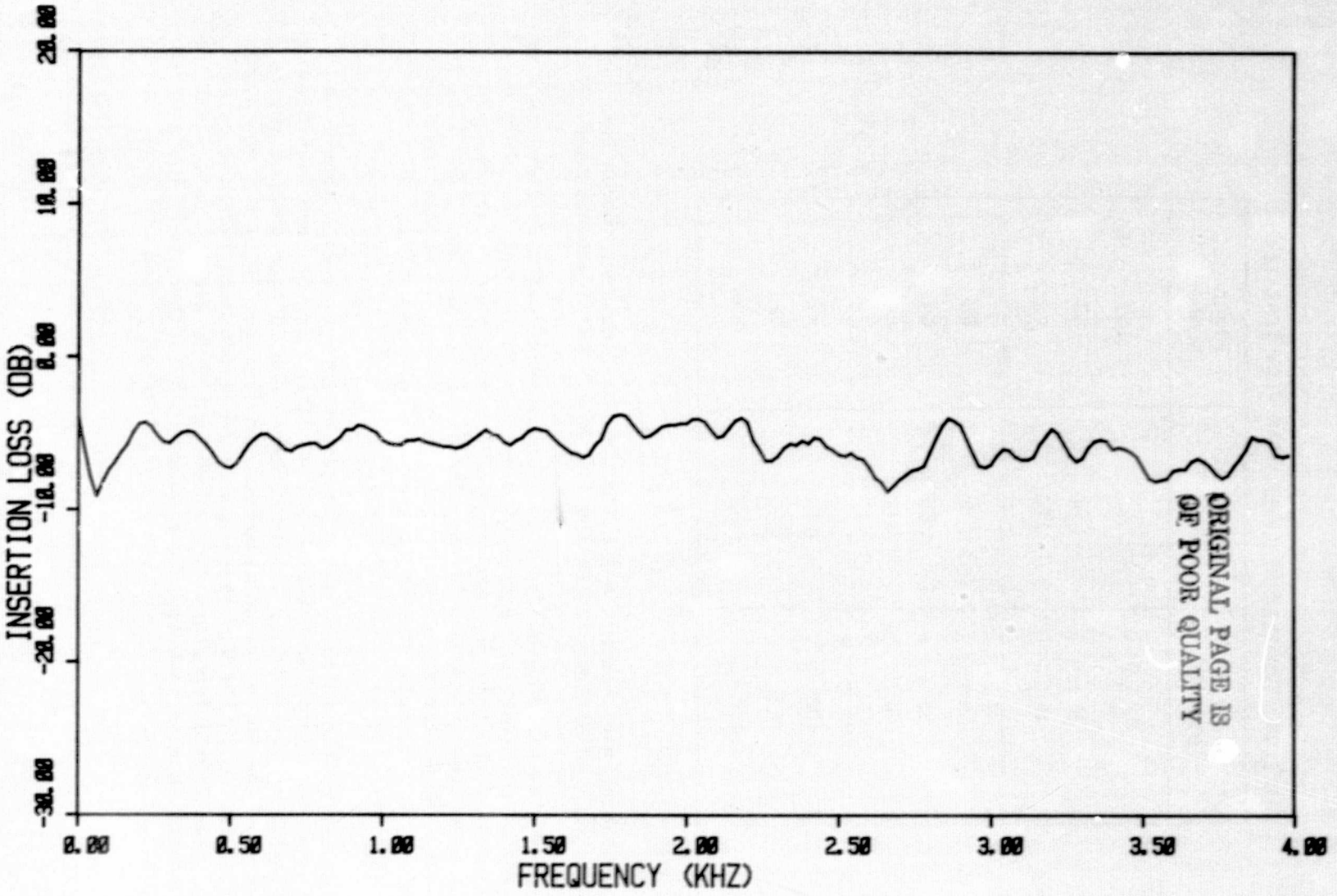




FIG. 42 INSERTION LOSS OF LINER SEGMENTS A1, A2 WITH BIAS FLOWS OF 0%, 50% RESPECTIVELY.

TABLE IV. TWO-SEGMENT LINER BIAS FLOW TEST LEVELS

| Liner A1 Bias % | Liner A2 Bias % | Figure Number |
|---|---|---|
| 0 | 0 | 41 |
| 0 | 50 | 42 |
| 0 | 100 | 43 |
| 50 | 0 | 44 |
| 50 | 50 | 45 |
| 50 | 100 | 46 |
| 100 | 0 | 47 |
| 100 | 50 | 48 |
| 100 | 100 | 49 |

100% (fig. 43) does not change the I.L. in the low-frequency region but induces an extra 1 dB attenuation in the 1.8 to 2.7 kHz frequency band.

Figures 44, 45 and 46 show the I.L. of a constant 50% bias flow level on liner segment A1 with varying degrees of bias flow on segment A2. Zero bias flow on segment A2 shows no improvement over the reference case. However, an increase of bias flow to segment A2 has the effect of increasing the I.L. to 1 to 2 dB over the entire frequency range. An additional increase to 100% reduces this back to levels similar to that of figure 43, viz. 1 dB in the 200 to 600 Hz range and 1.8 to 2.5 kHz range.

The results of the third series of tests at 100% bias flow levels on segment A1 are shown in figures 47, 48 and 49. The case of zero bias flow on segment A2 exhibits reduced I.L. levels of zero to 1 dB from that of the reference case over the whole frequency range. An increase in bias flow to 50% on segment A2 increases the I.L. such that 1 dB improvement over the reference case can be seen in the frequency ranges 200 to 600 Hz and 1.7 to 2.7 kHz. A further increase in bias flow to 100% results in a further small increase in I.L. to levels of 1 to 1.5 dB over the entire frequency range.

It is apparent from the above results that the optimum bias flow for this two-segment configuration lies somewhere in the region of equal bias flows to each segment of about 50%.

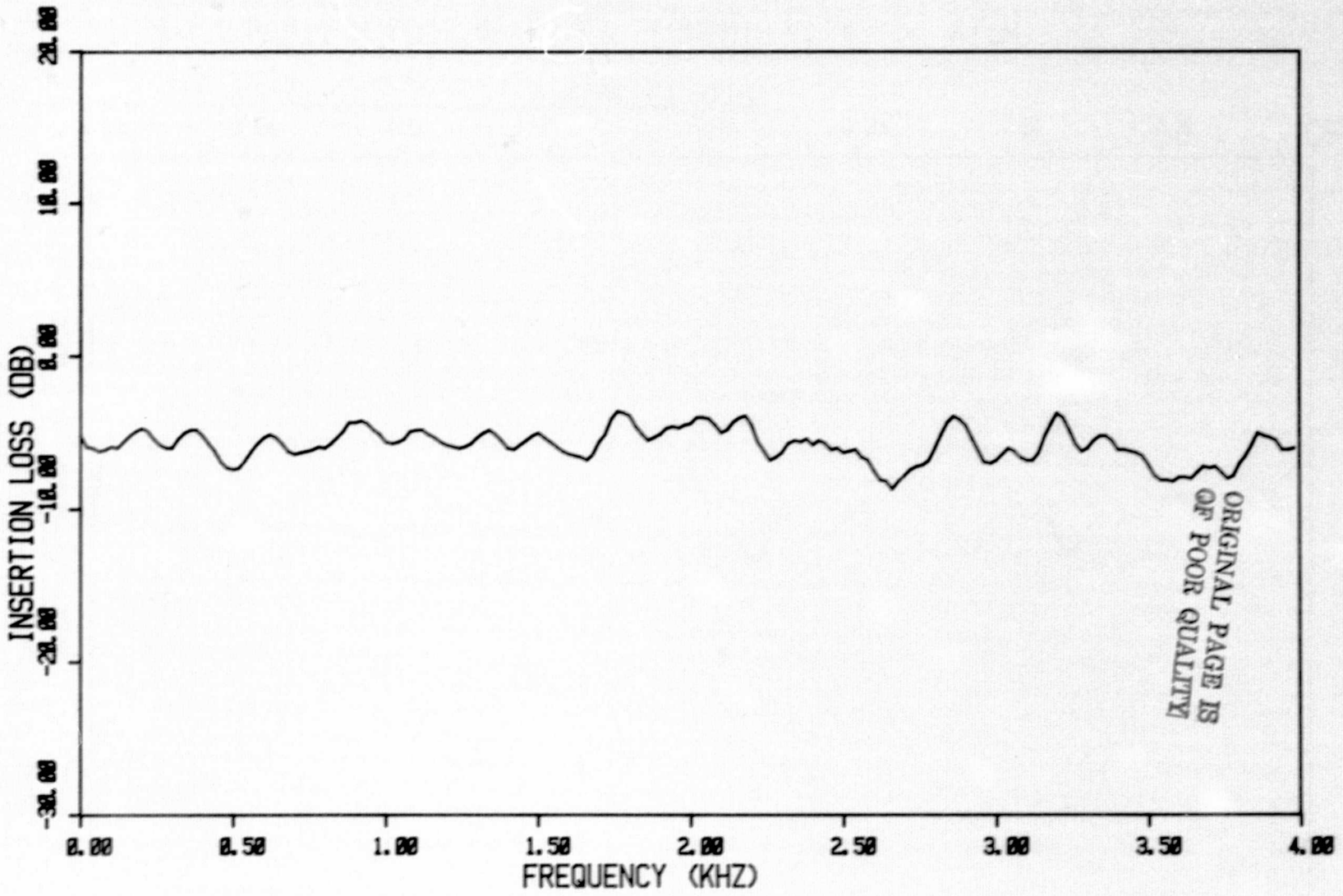


FIG. 43 INSERTION LOSS OF LINER SEGMENTS A1 , A2 WITH BIAS FLOWS OF 0 %, 100% RESPECTIVELY.

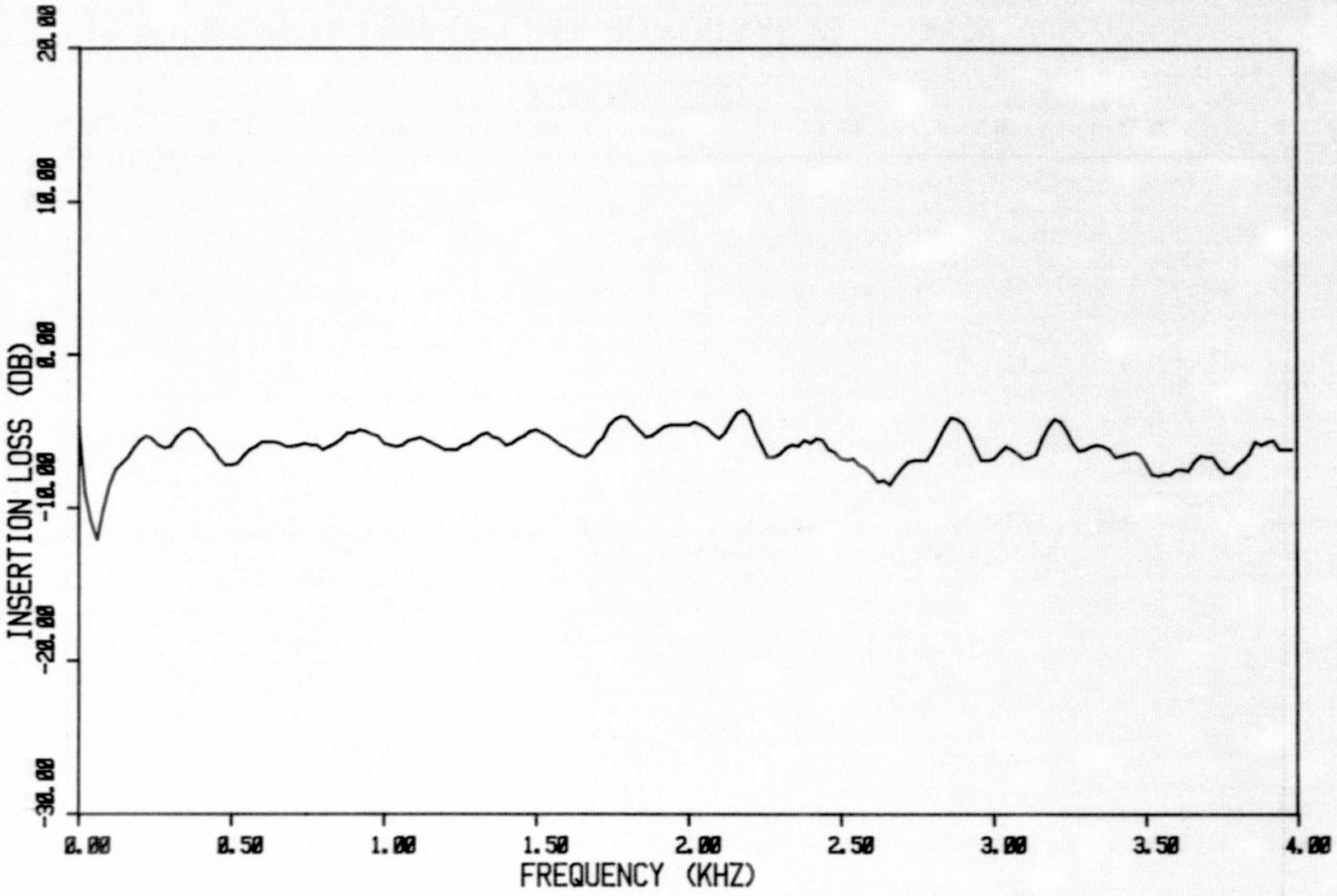


FIG. 44 INSERTION LOSS OF LINER SEGMENTS A1, A2 WITH BIAS FLOWS OF 50 %, 0 % RESPECTIVELY.

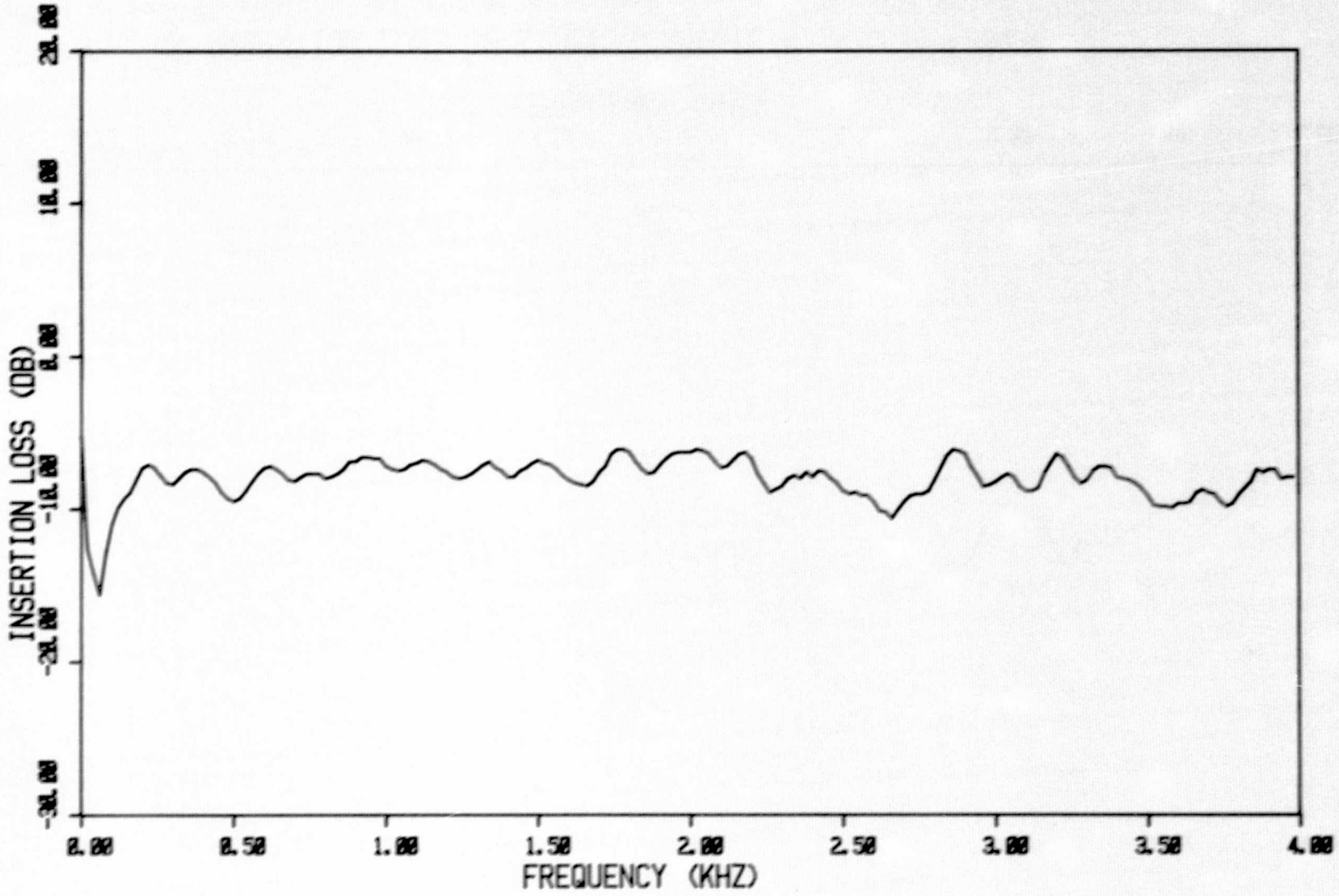


FIG. 45 INSERTION LOSS OF LINER SEGMENTS A1 , A2 WITH BIAS FLOWS OF 50 %, 50 % RESPECTIVELY.

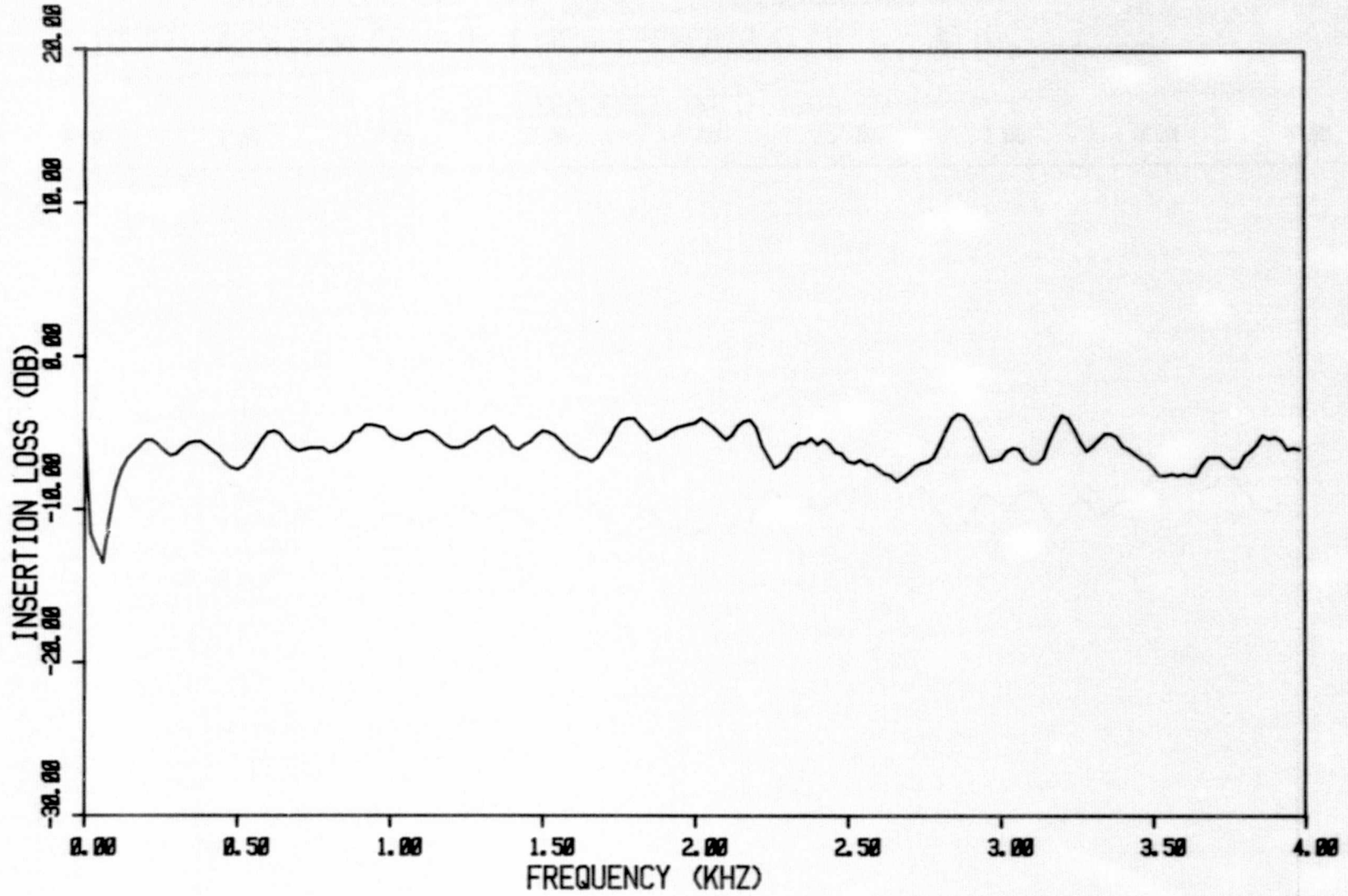


FIG. 46 INSERTION LOSS OF LINER SEGMENTS A1 , A2 WITH BIAS FLOWS OF 50 %, 100 % RESPECTIVELY.

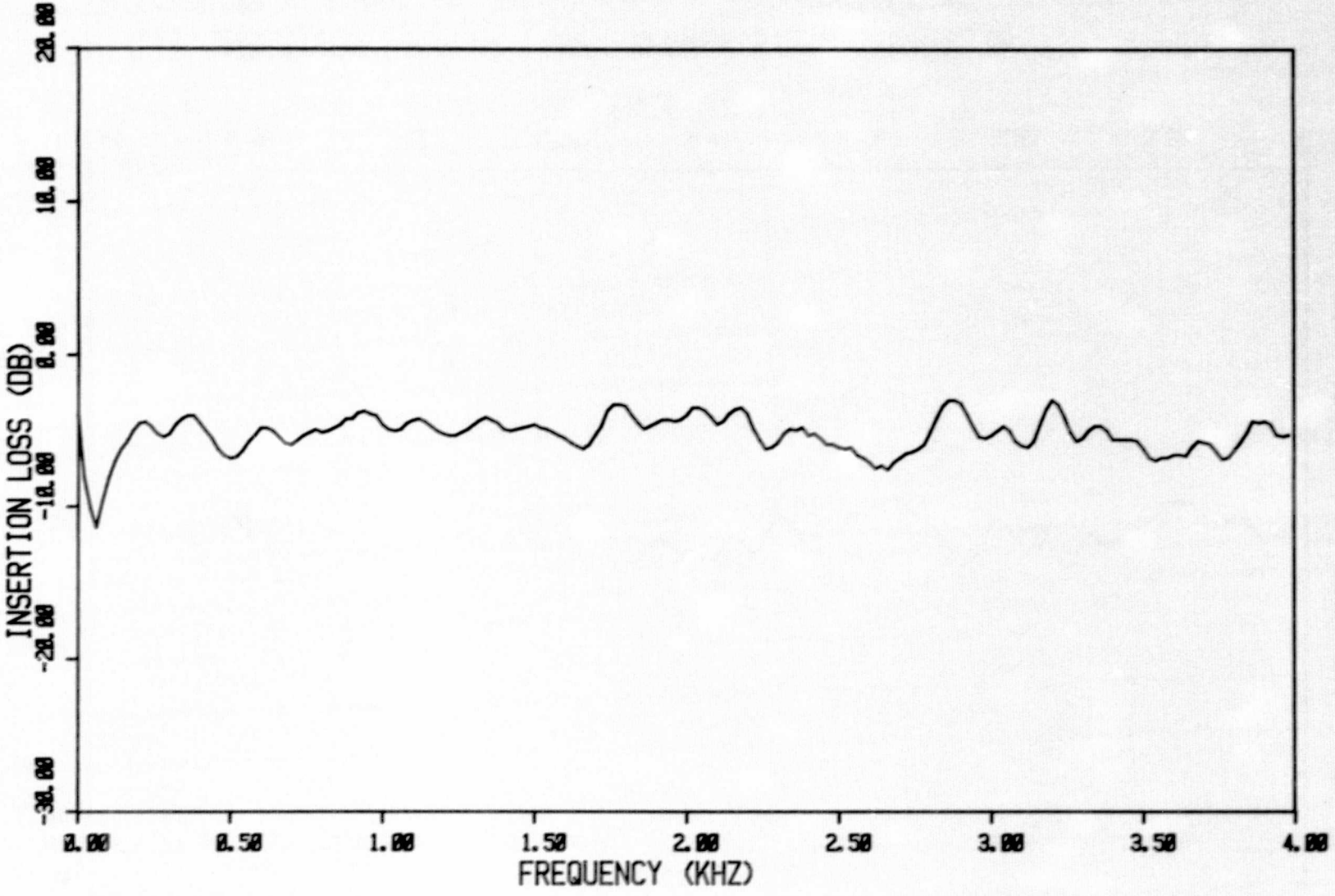


FIG. 47 INSERTION LOSS OF LINER SEGMENTS A1 , A2 WITH BIAS FLOWS OF 100 %, 0 % RESPECTIVELY.

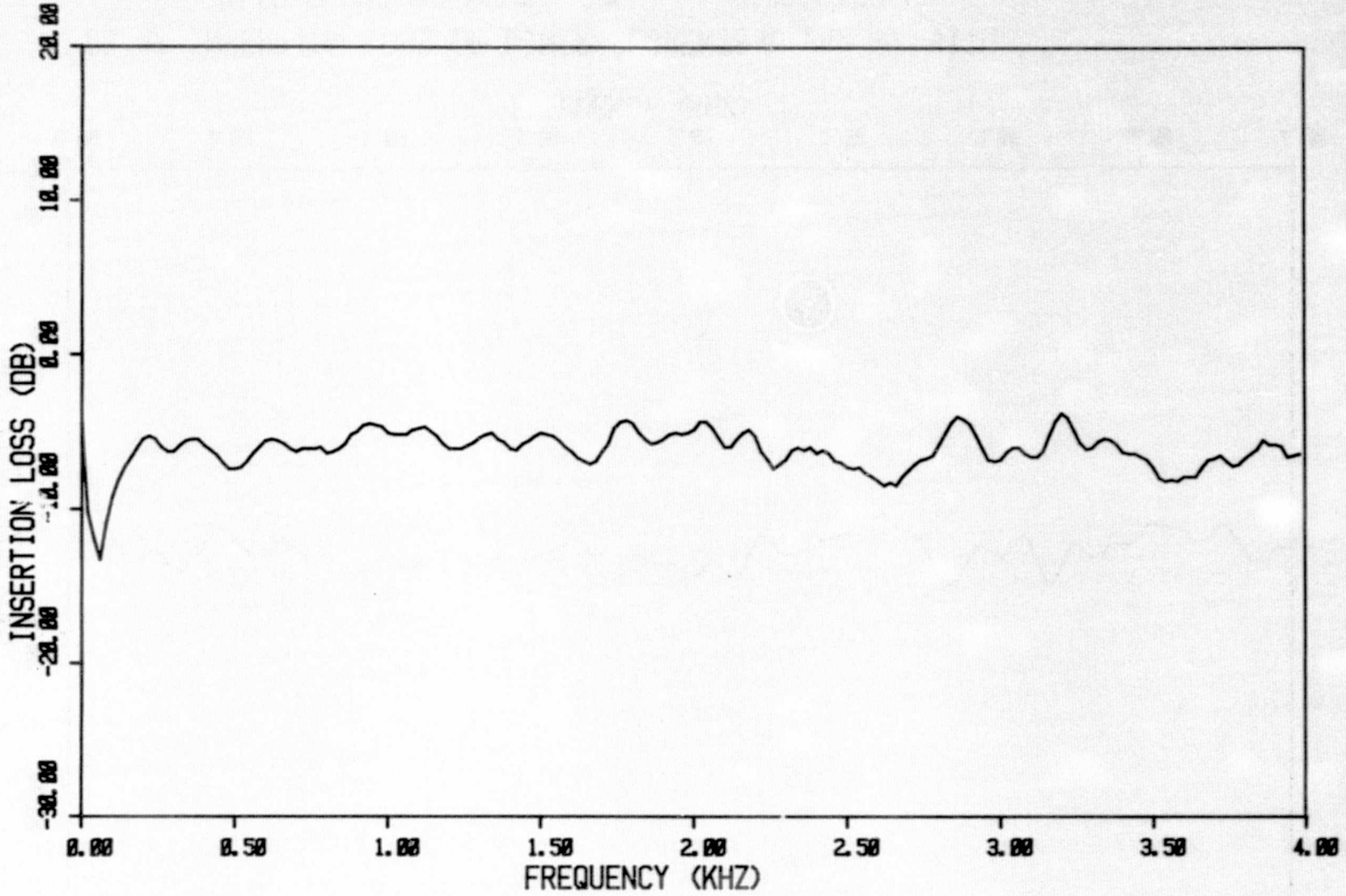


FIG. 48 INSERTION LOSS OF LINER SEGMENTS A1 , A2 WITH BIAS FLOWS OF 100 %, 50 % RESPECTIVELY.

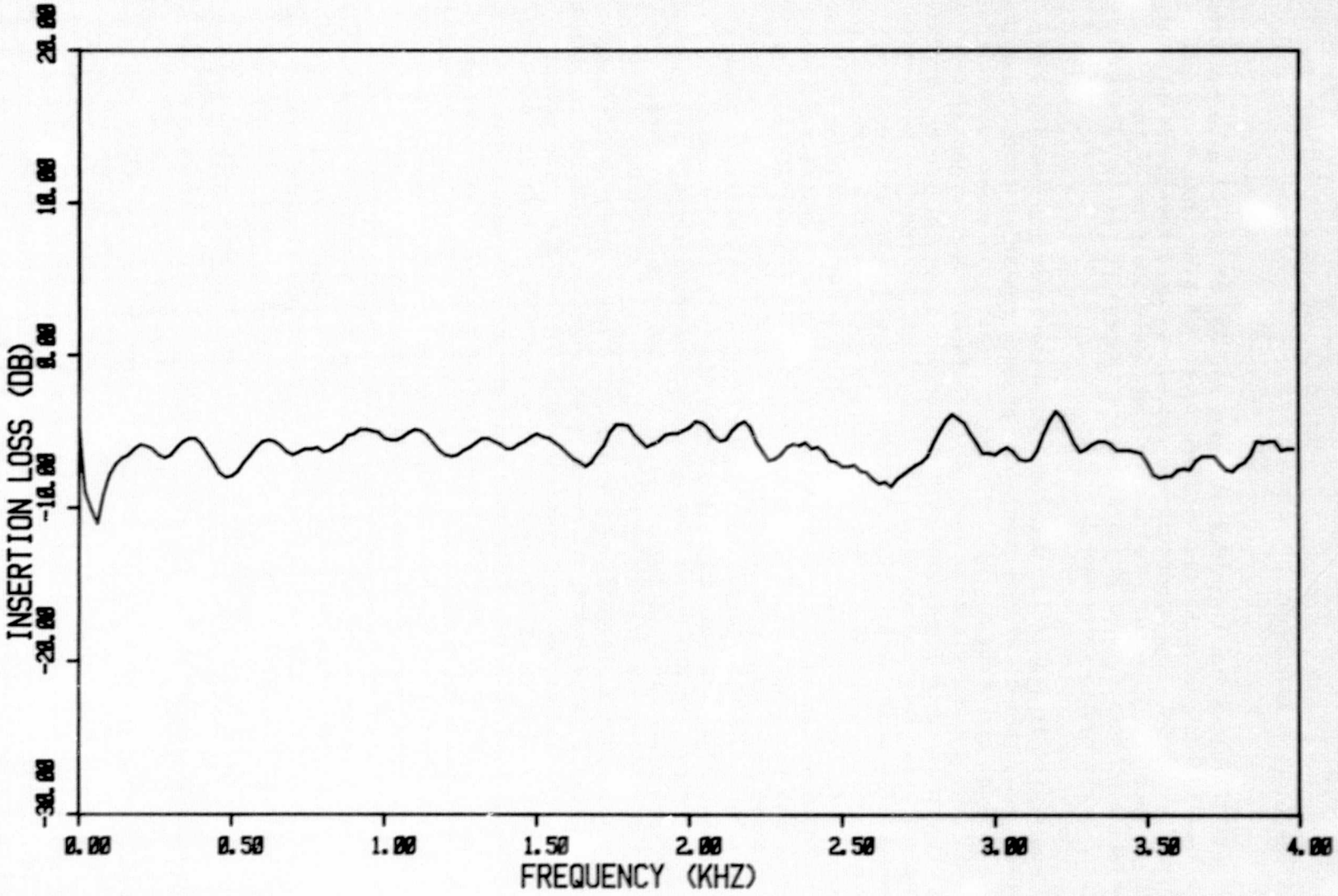


FIG. 49 INSERTION LOSS OF LINER SEGMENTS A1 , A2 WITH BIAS FLOWS OF 100 %, 100 % RESPECTIVELY.

## 4.3 WALL IMPEDANCE MEASUREMENTS

The wall impedance for liner designations A1, A2, B1 and C1 were measured using the four microphone technique at five levels of bias flow, viz. zero, 25%, 50%, 75% and 100%. The apparatus and procedures used have been fully described in section 2, however, for a more complete discussion of the characteristics of this type of measurement and the analytical formulation, the reader is referred to reference 3.

The most critical aspect for accurate measurements is the necessity for SPL and phase measurements at the front face of each resistive layer. Due to the finite size of the probe microphone sensing holes, this point, acoustically, is in fact a small distance away from the face. Thus, a pressure traverse of each liner configuration must be performed and this point located, by definition, as a "knee" point where departure from the standing wave shape within each cavity occurs just prior to probe passage through the resistive layer. In addition, a pressure traverse supplies confirmation of the standing wave structure in the respective cavities, any leakage or significant nonlocal reactivity being evidenced as gross anomalies or "glitches" in the standing wave. Traverses for liners A1, B1, and C1 are shown in figures 50, 51, and 52, respectively for frequencies of 500, 1 K, 2 K and 3 kHz. It can be seen that except for the lowest plotted frequency of 500 Hz, the resistive layers are easily identified, the only anomaly of note, being a a relatively slow decay of pressure as the probe sensing holes are traversed through and covered by the rear hard wall. This is indicative of excessive hole clearance.

The acoustic source of sound for the impedance measurements was broadband random noise, thus a large number of averages was necessary in order to obtain a good estimate of the narrow band spectral components of the probe versus wall reference transfer function. However, the inevitable small variance of SPL from band to band, did introduce some scatter, with the occasional "wild" point, in the calculated impedance as shown in figure 53(a). Thus, some spectral smoothing was desirable [as shown in fig. 53(b)] in order to more clearly delineate trends and was implemented using a Simpson's rule running average technique in the subsequent plots for all wall impedance tests (figs. 53(b) through 57). It should be noted that the reactance values in these plots near the second resonant point and all other subsequent anti-resonant points are, in fact, not correct in the sense that extremely rapid changes are occurring (from $+\infty$ to $-\infty$ theoretically) thus finite bandwidth analysis coupled with spectral smoothing will round off and considerably degrade the plotted magnitudes in this narrow frequncy region.

### 4.3.1 Characteristics of $\eta = 1.6$ Liner

The first point of note in the plots of figures 54 through 57 is the classic single resonant cavity absorber characteristic of the liner. That is, the reactance moves from $-\infty$ at low frequencies through the first resonance at about 1.4 kHz to the second resonance point at 2.8 kHz, following the classic cot kd curve. Again, the classical resistance peak is markedly evident in the second resonance region. The design frequency for this configuration (C1) is around 3 kHz, thus the desired negative reactances in the design frequency

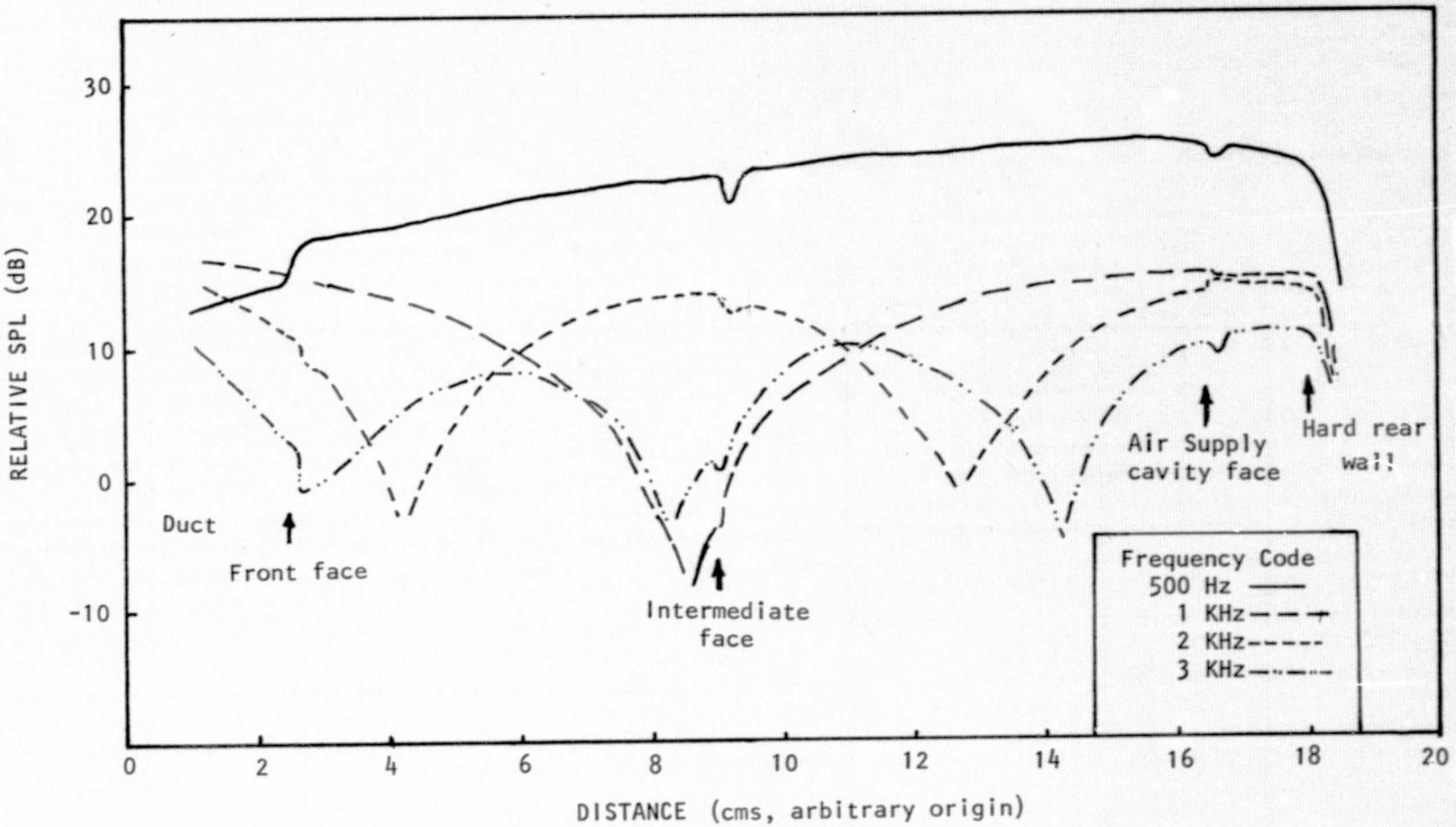


Figure 50. SPL TRAVERSE THROUGH LINER A1 ($\eta$ = 0.25)

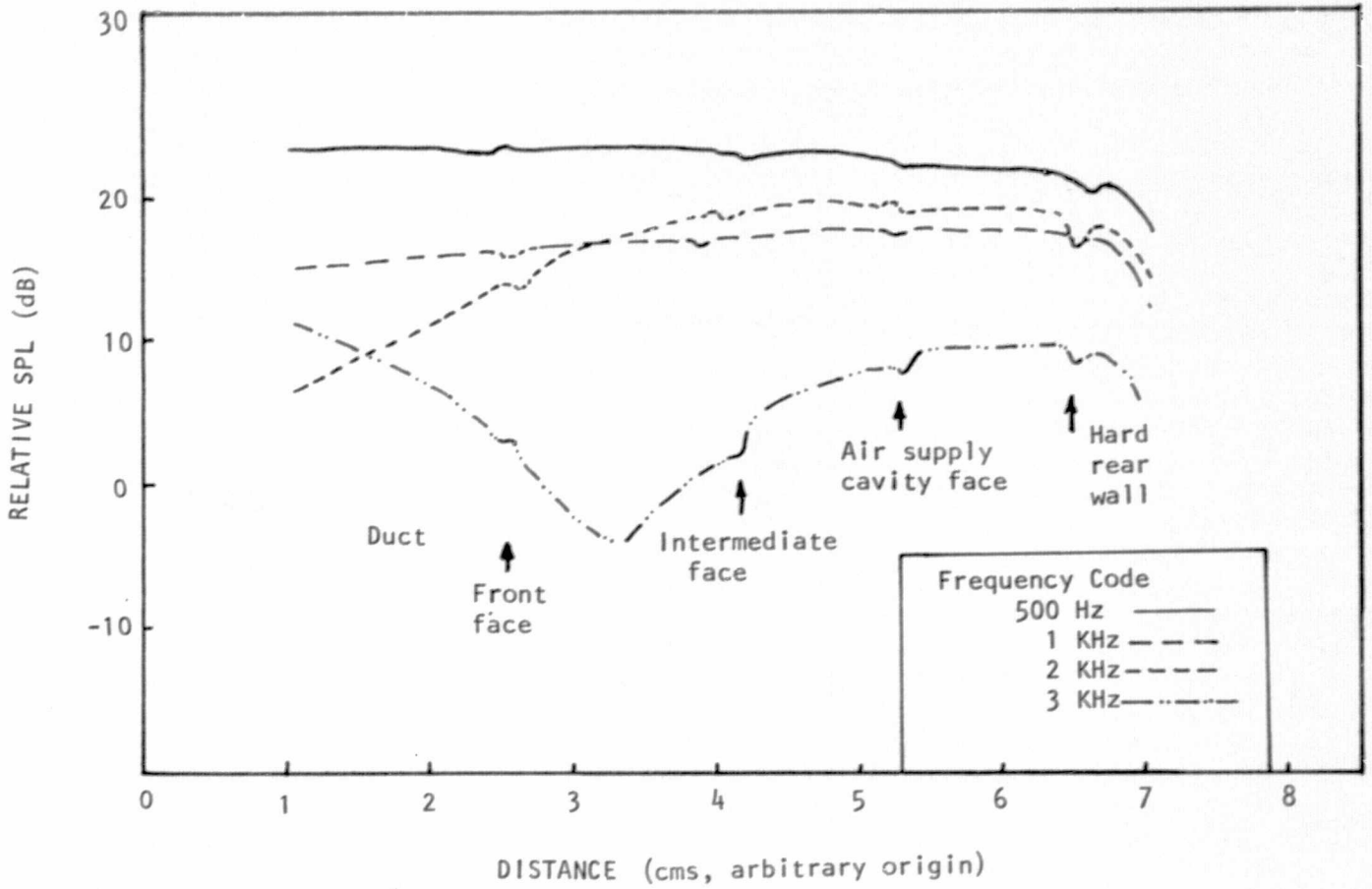


Figure 51. SPL TRAVERSE THROUGH LINER B1 ($\eta$ = 1.0)

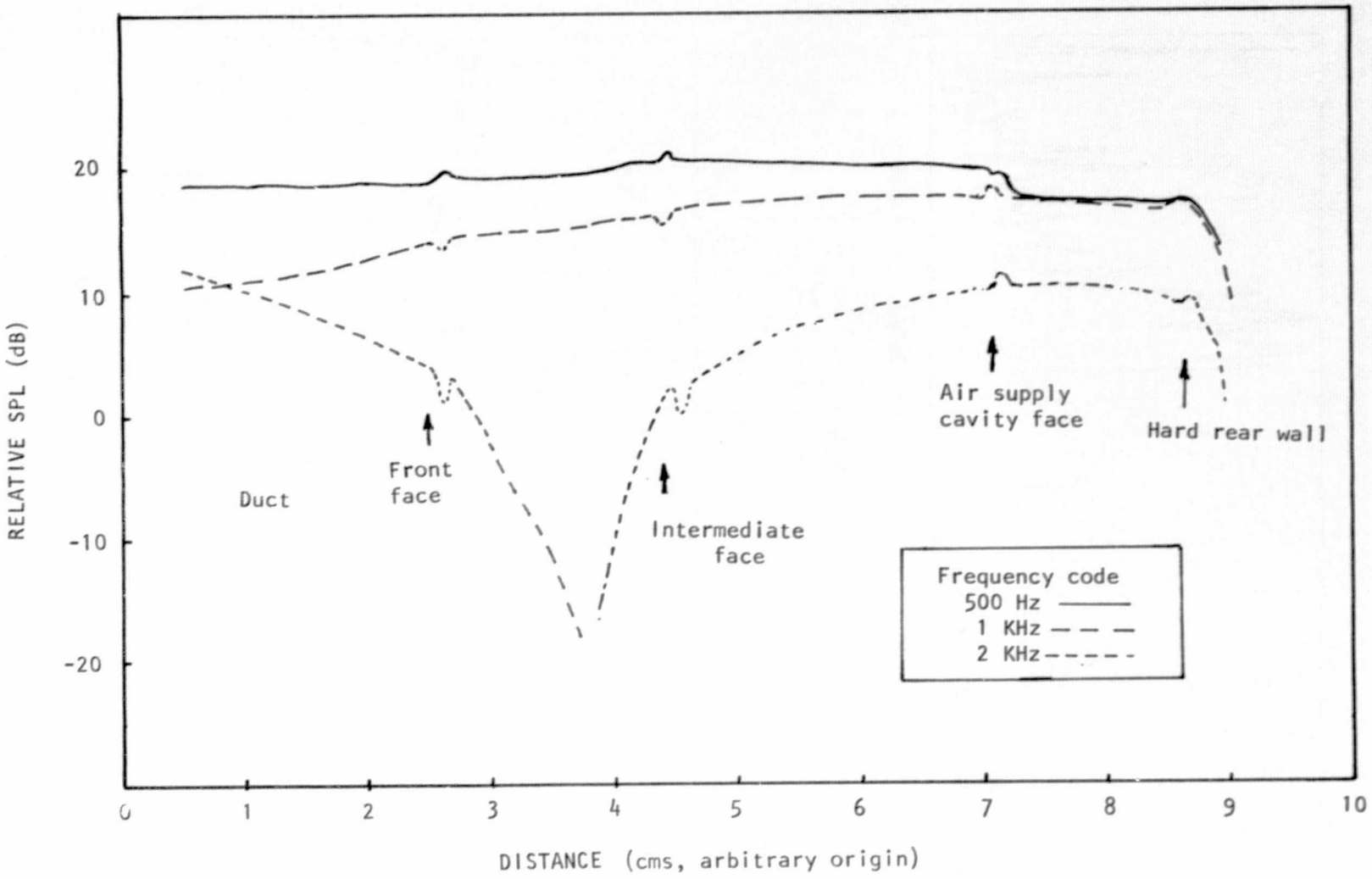


Figure 52. SPL TRAVERSE THROUGH LINER C1 ($\eta$ = 1.6)

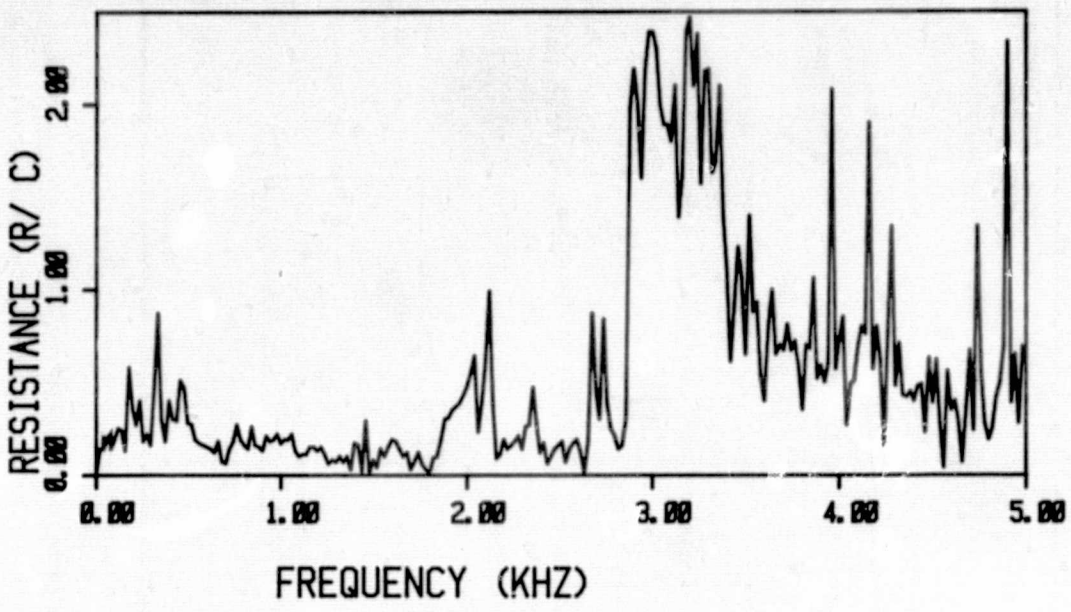


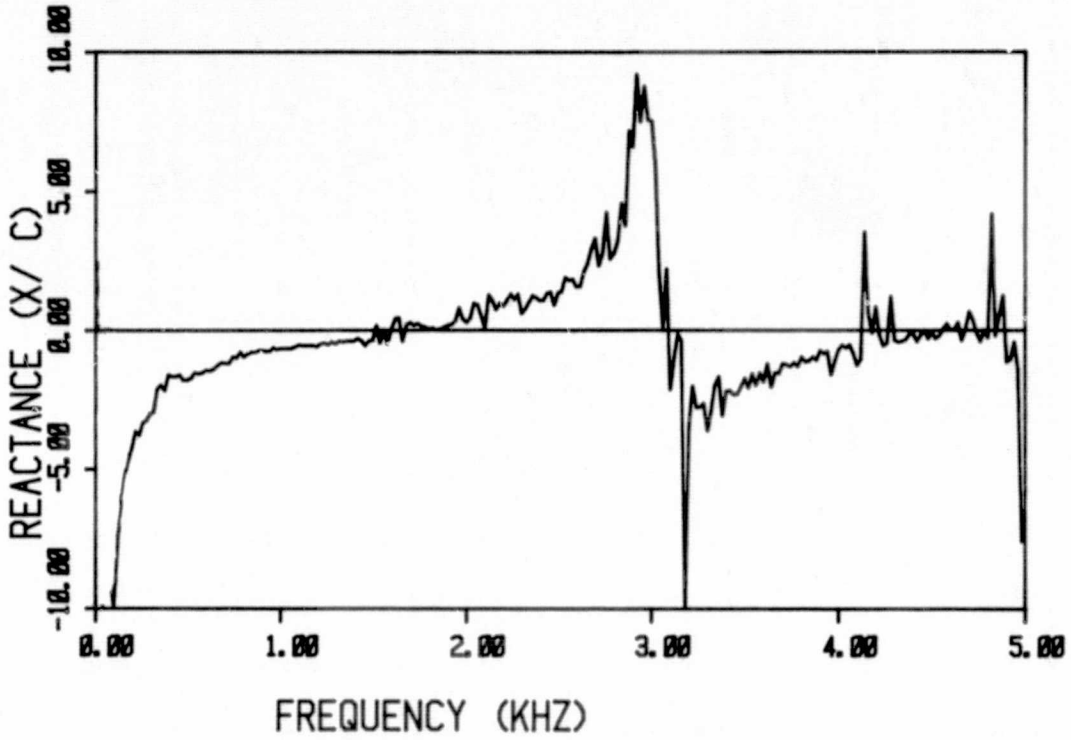


FIG.53(a) WALL IMPEDANCE FOR LINER C1 AT BIAS FLOW LEVEL OF 0 %.

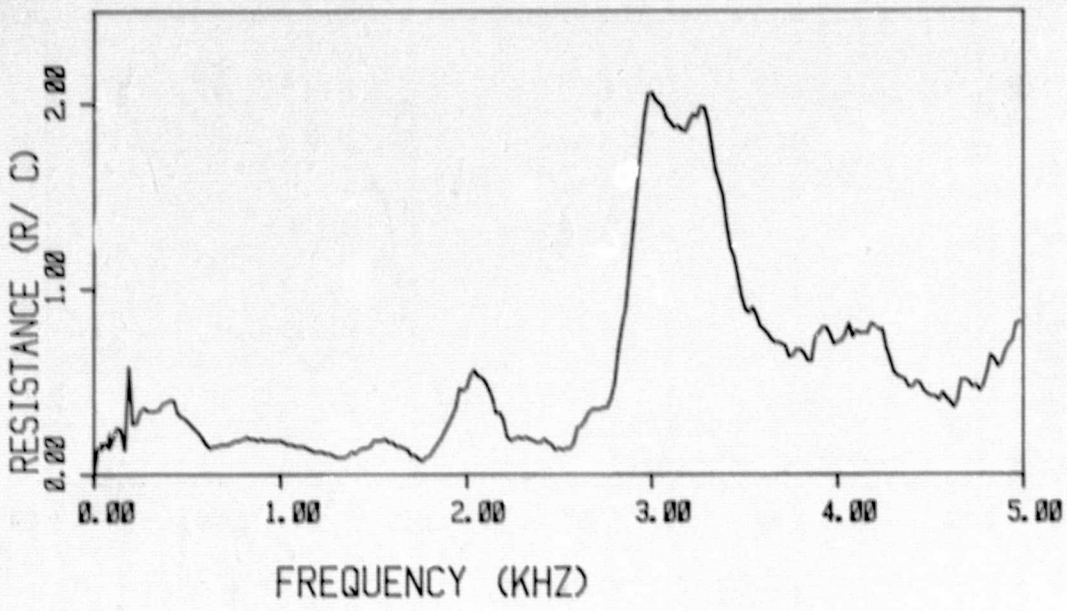


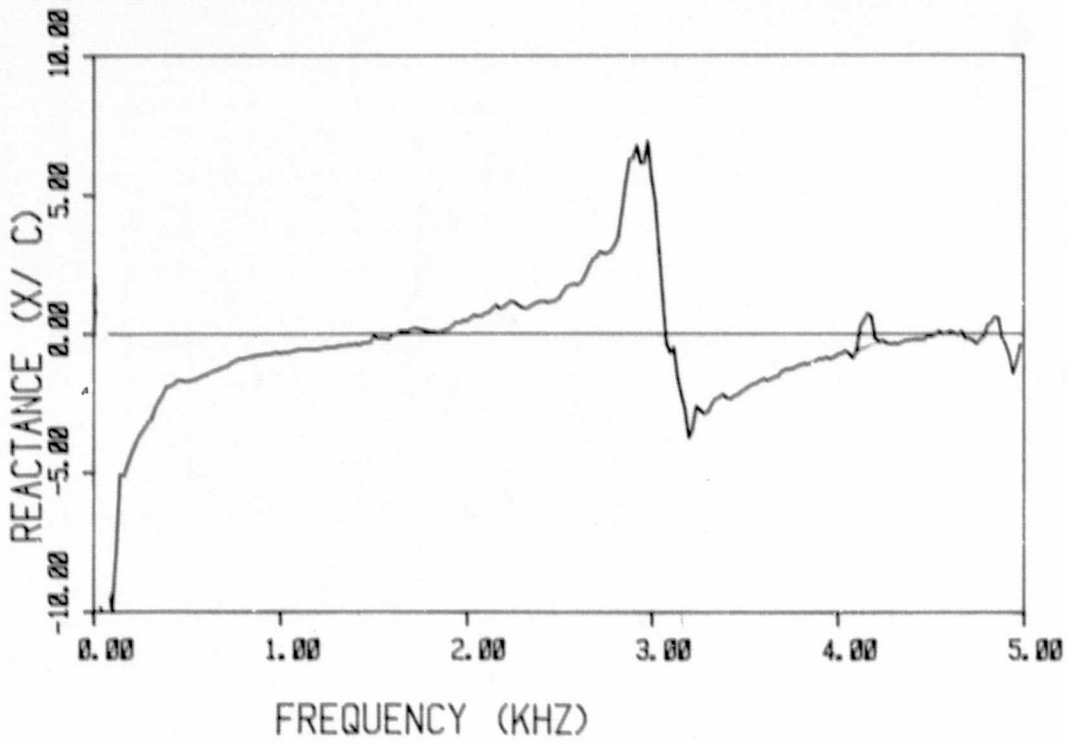


FIG.53(b)WALL IMPEDANCE FOR LINER C1 AT
BIAS FLOW LEVEL OF 0 %.

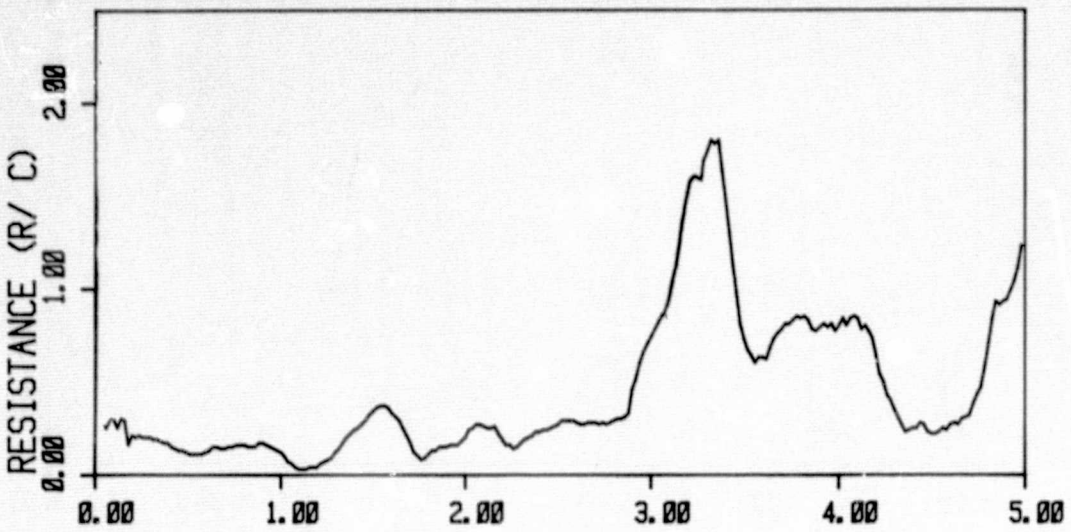


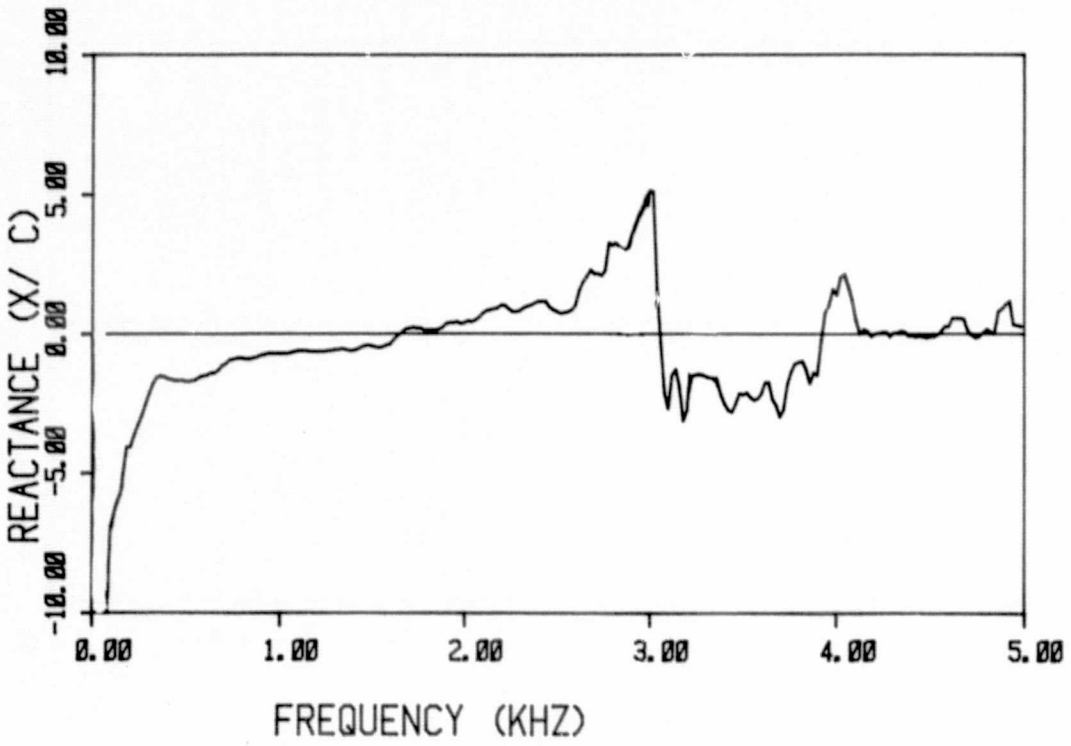


FIG. 54 WALL IMPEDANCE FOR LINER C1 AT BIAS FLOW LEVEL OF 25 %.

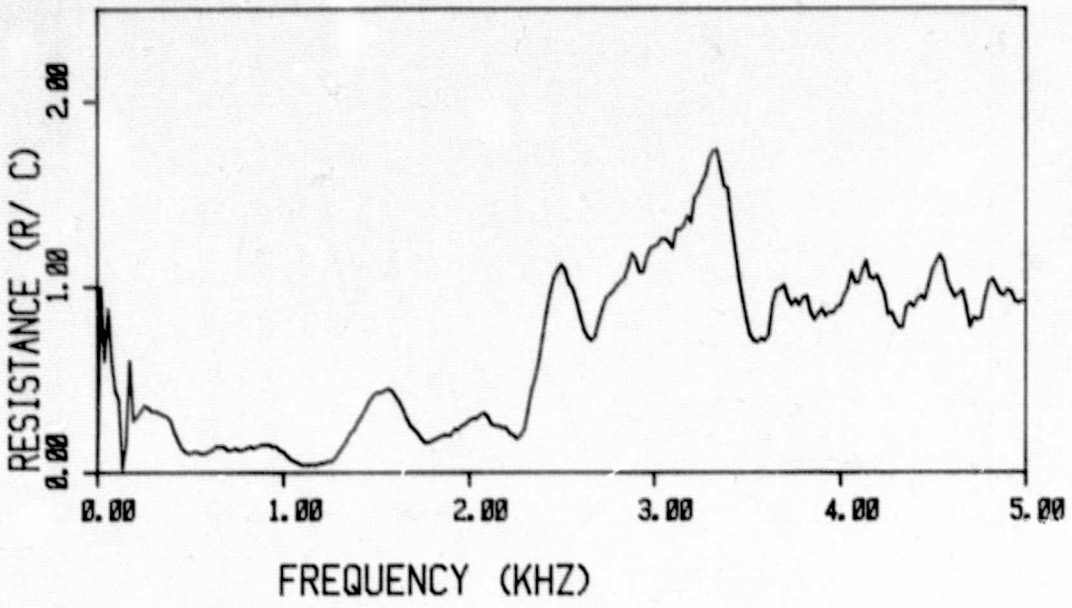


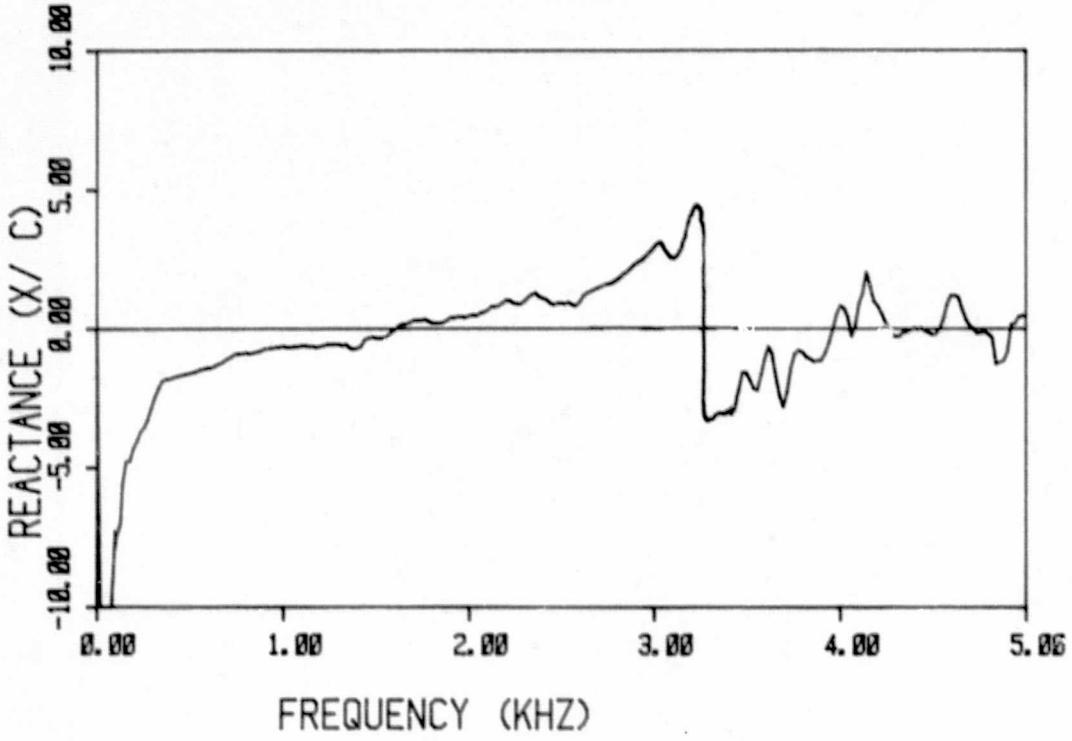


FIG. 55 WALL IMPEDANCE FOR LINER C1 AT BIAS FLOW LEVEL OF 50 %.

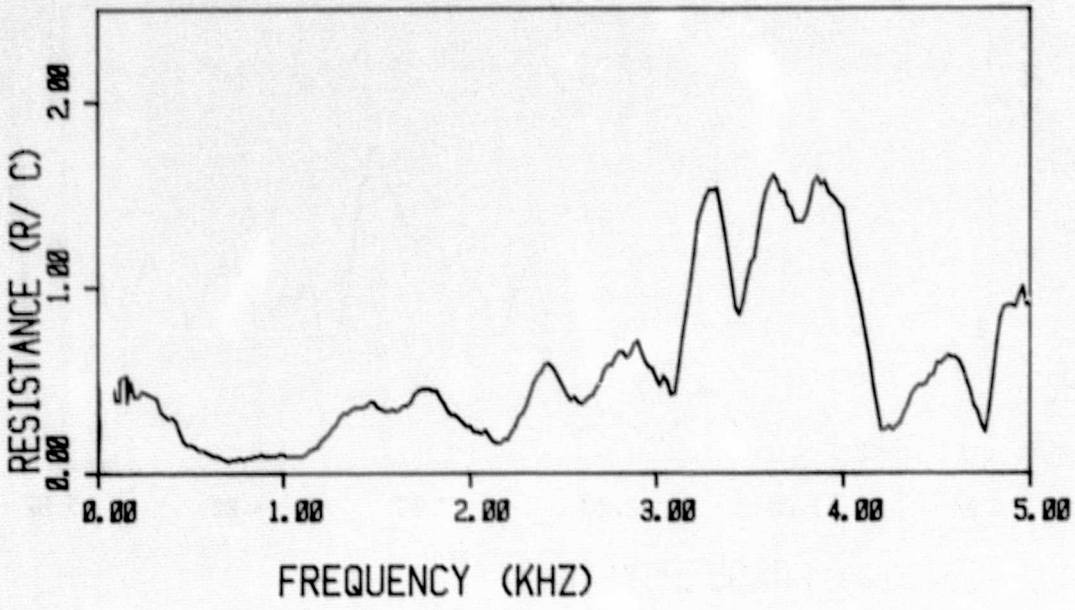


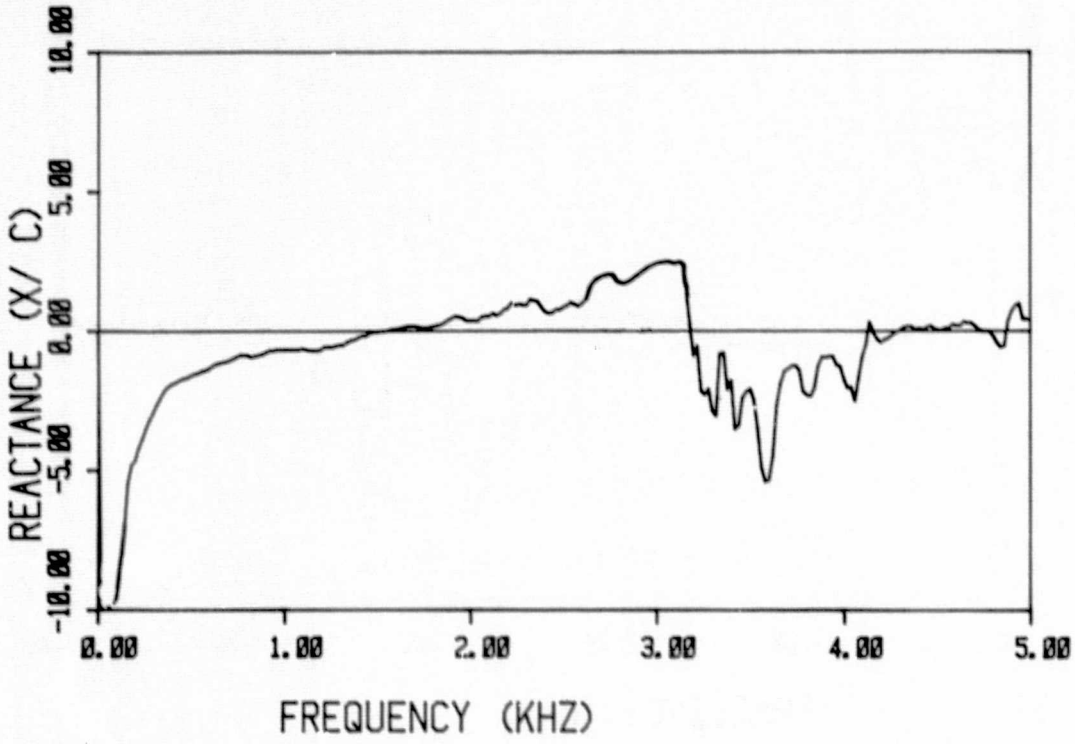


FIG. 56 WALL IMPEDANCE FOR LINER C1 AT BIAS FLOW LEVEL OF 75 %.

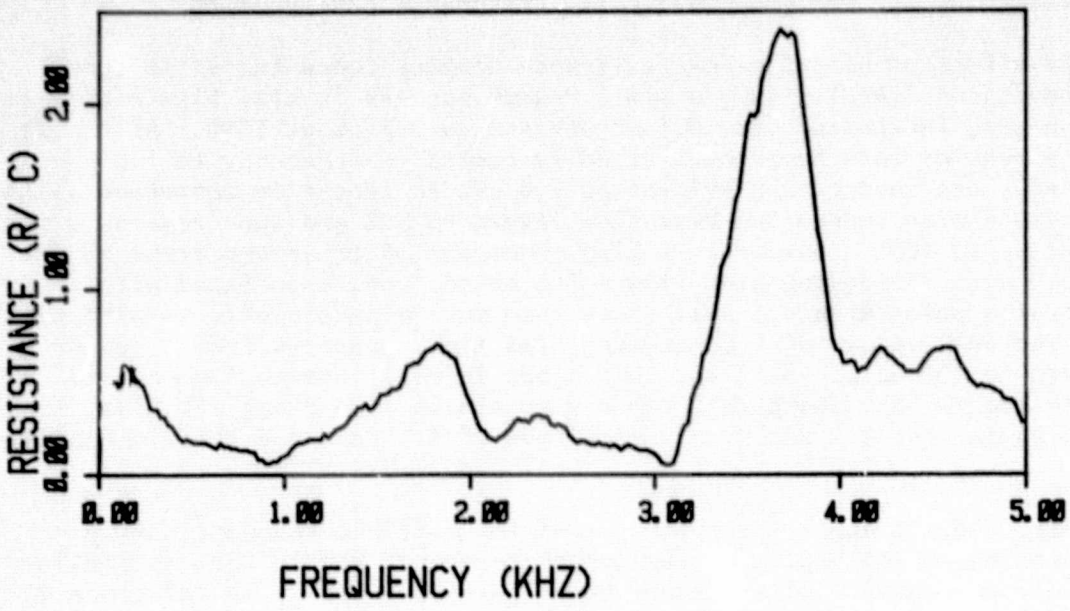


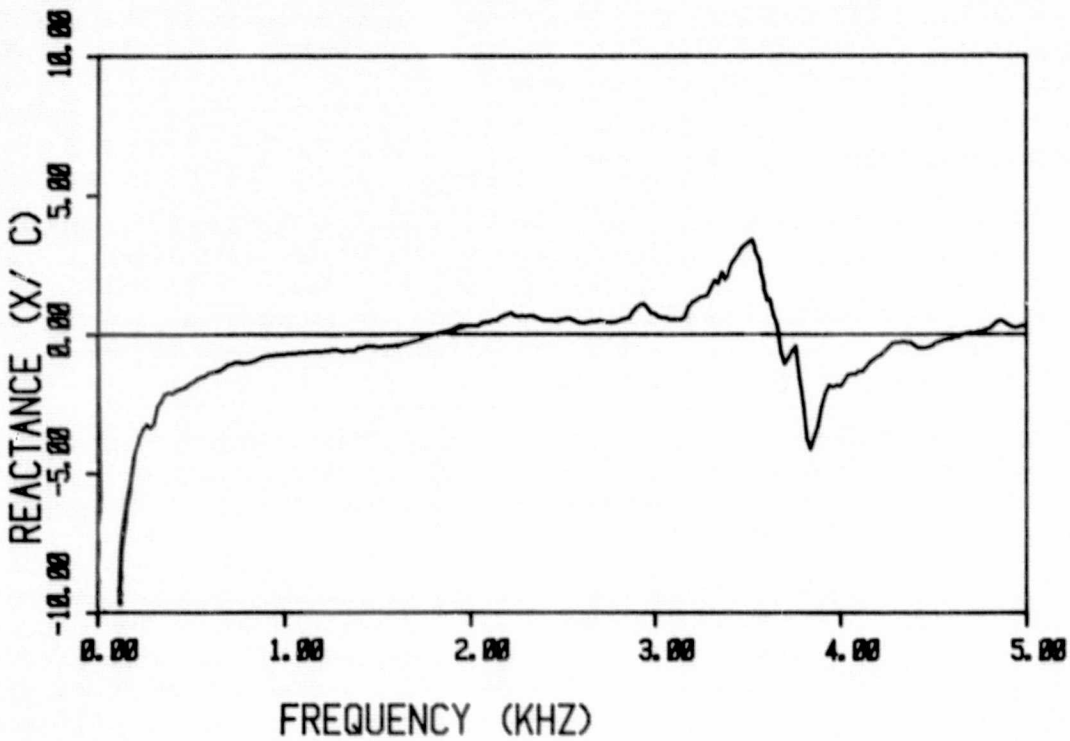


FIG. 57 WALL IMPEDANCE FOR LINER C1 AT BIAS FLOW LEVEL OF 100 %.

region result with associated high resistances. This region of operation, although undesirable from the point of view of frequency lattitude,was necessitated by the need for physically reasonable cavity depths.

The effect of bias flow on resistance appears concentrated in three frequency bands. At 1.3 kHz, a small "hump" appears in bias flow increases, its magnitude increasing from 0.1 ρc at zero to 0.7 ρc at 100%. At the same time the peak of this hump moves steadily upward in frequency to 1.6 kHz. Conversely, the second hump evident at 1.8 kHz to zero flow decreases slightly in amplitude with increasing bias flow levels to 50% and then remains almost constant up to 100%. However, it also shows a similar upward trend of peak frequency with increasing bias flow. The third hump, associated with the liner design point around 3 kHz, shows much more dramatic effects with bias flow. The peak values of 2 ρc at zero bias flow, narrows from a 400 Hz bandwidth to 100 Hz at 25% bias, then drops in amplitude to 1.3 ρc, and increases bandwidth upward in frequency to almost 1000 Hz at 75% bias, finally peaking again near 3.5 kHz with a magnitude of 2.1 ρc and a bandwidth of 150 Hz.

This behavior appears symptomatic of the multiple resonant cavity configuration in the region of the second resonance and in fact is similar to the predicted behavior of the liner model (discussed fully in reference 2).

The reactance changes with bias flow completely support the upward trend in frequency of the peak resistance values, as evidenced by the cross-over or resonance points (i.e. where $x = 0$). The first crossover point at 1.4 kHz increases to 1.7 kHz at 100% bias flow, while the second increases from 2.8 kHz through 3.1 kHz to 3.5 kHz at 100% bias flow.

### 4.3.2 Characteristics of $\eta = 1.0$ Liner

In contrast to the previous liner where the design frequency was above the first resonant point, the design frequency (2 kHz) for this liner (designated B1) was below the first resonant point. Thus, the impedance sensitivities to frequency and bias flow near the design point should be very much less than the $\eta = 1.6$ liner. This prediction was confirmed by the measurements shown in figures 58 through 62.

The expected increases in the first resonant cross-over point with bias flow occurred (e.g. from 2.4 kHz at zero to 3 kHz at 75%), thus confirming the design characteristic of increasing negative reactance with small increases in resistance at the design frequency.

However, this liner exhibited some most unexpected and unusual behavior above about 2.5 kHz with increasing bias flow. At anti-resonance (or second resonance point) at 3.9 kHz, the peak of resistance and the reactance cross-over appear reasonably well behaved but as bias flow increases the resistance peak broadens and reduces in magnitude. This broadening is shown as a trend of increasing resistances extending down to 2.5 kHz with marked secondary peaks around an almost linear mean line. The reactance shows considerable scatter in this region remaining essentially within ±1ρc of zero up to 4 kHz with occasional zero crossing occurring up to 75% bias. However, these zero

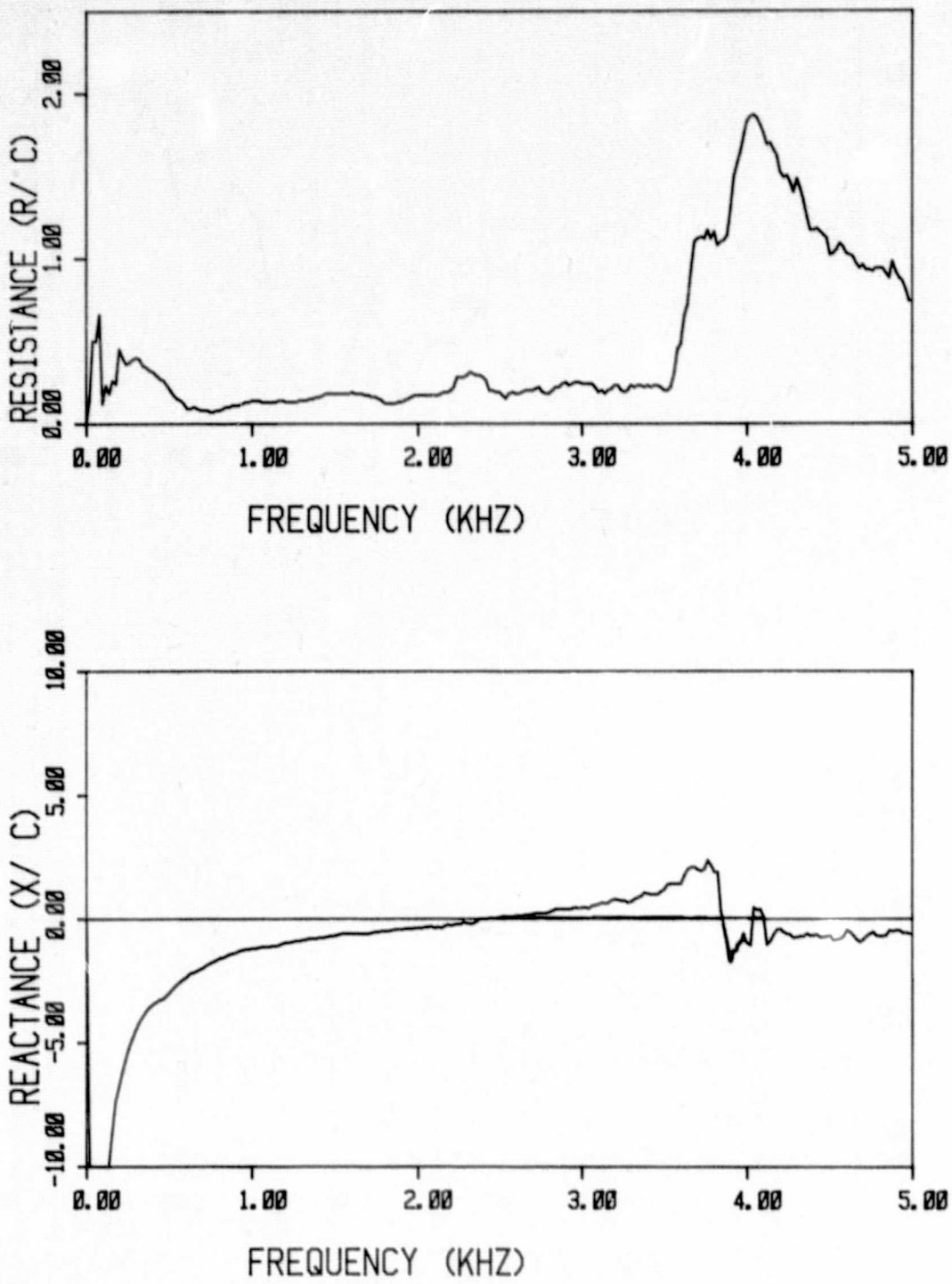


FIG. 58 WALL IMPEDANCE FOR LINER B1 AT BIAS FLOW LEVEL OF 0 %.

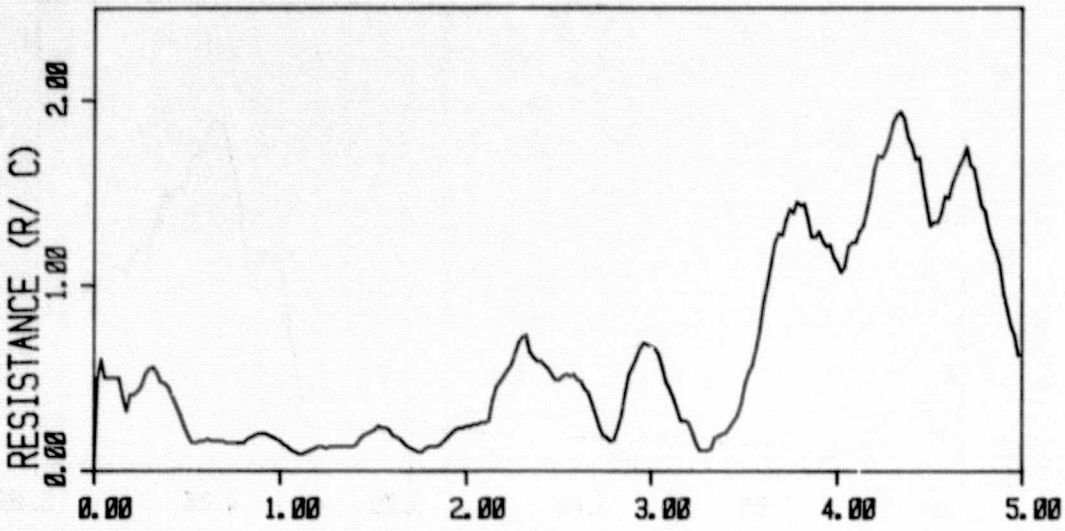


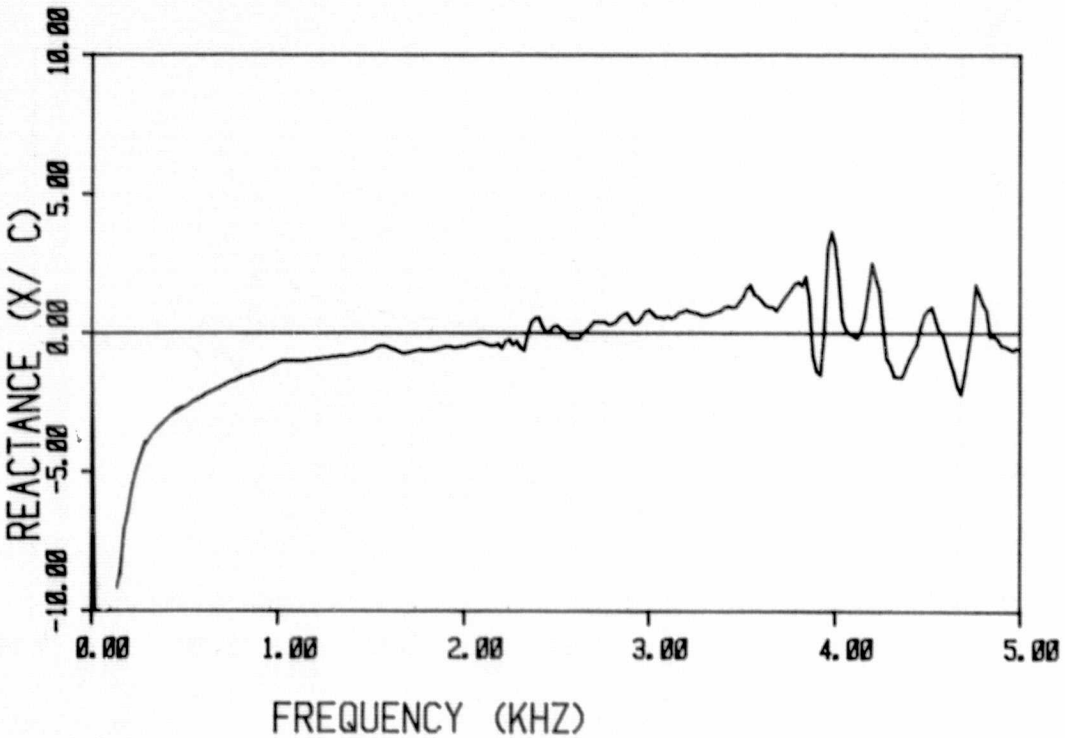


FIG. 59 WALL IMPEDANCE FOR LINER B1 AT BIAS FLOW LEVEL OF 25 %.

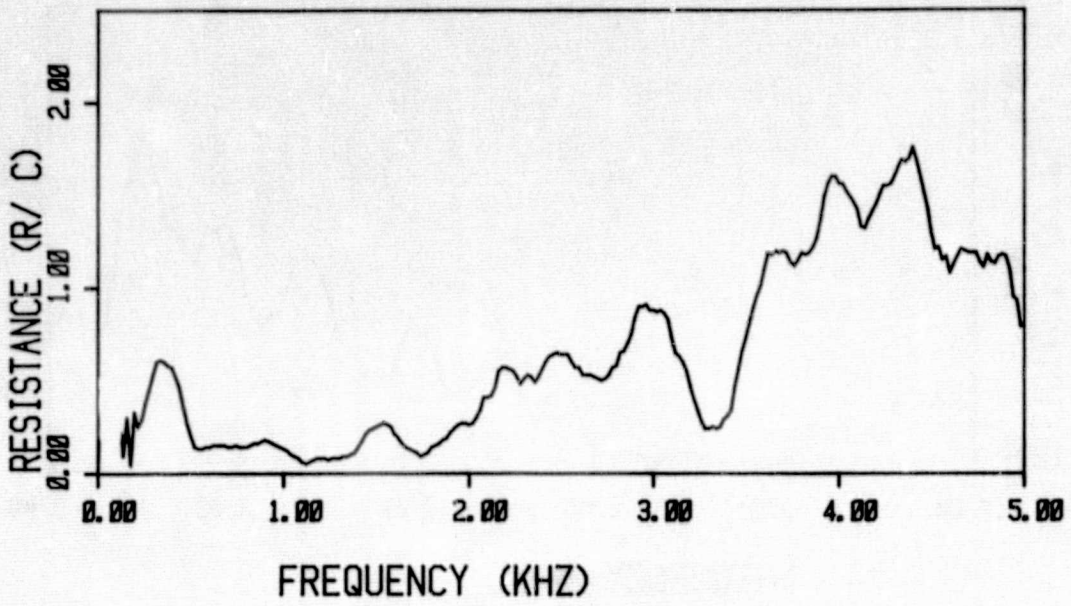


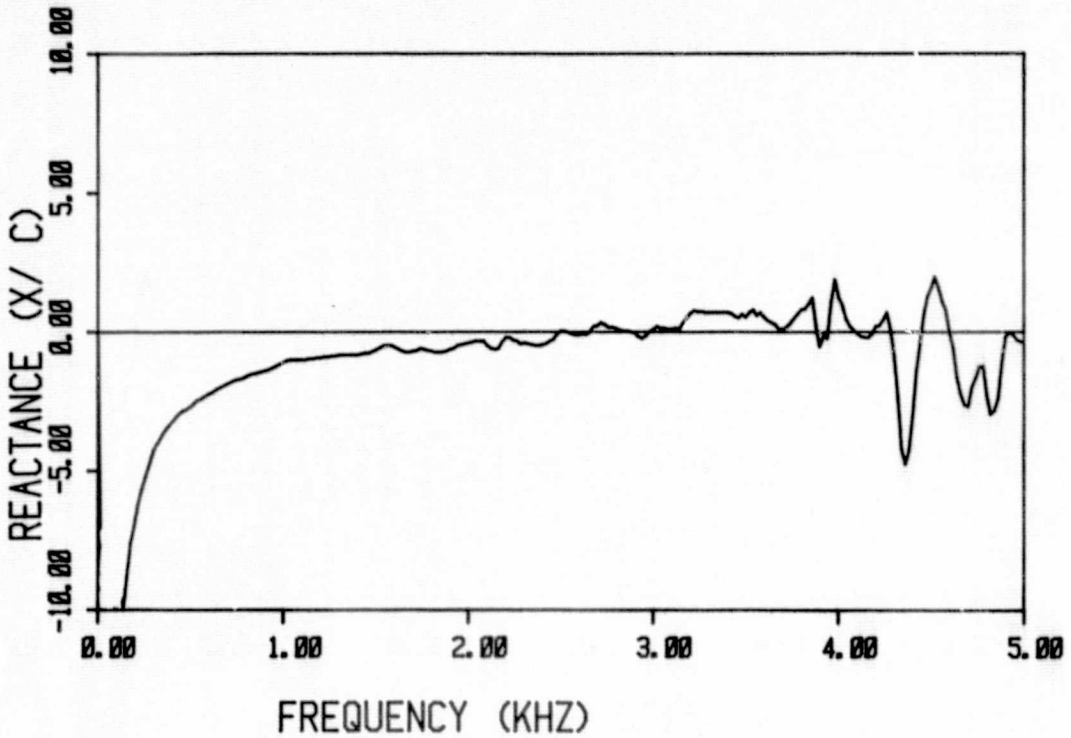


FIG. 60 WALL IMPEDANCE FOR LINER B1 AT BIAS FLOW LEVEL OF 50 %.

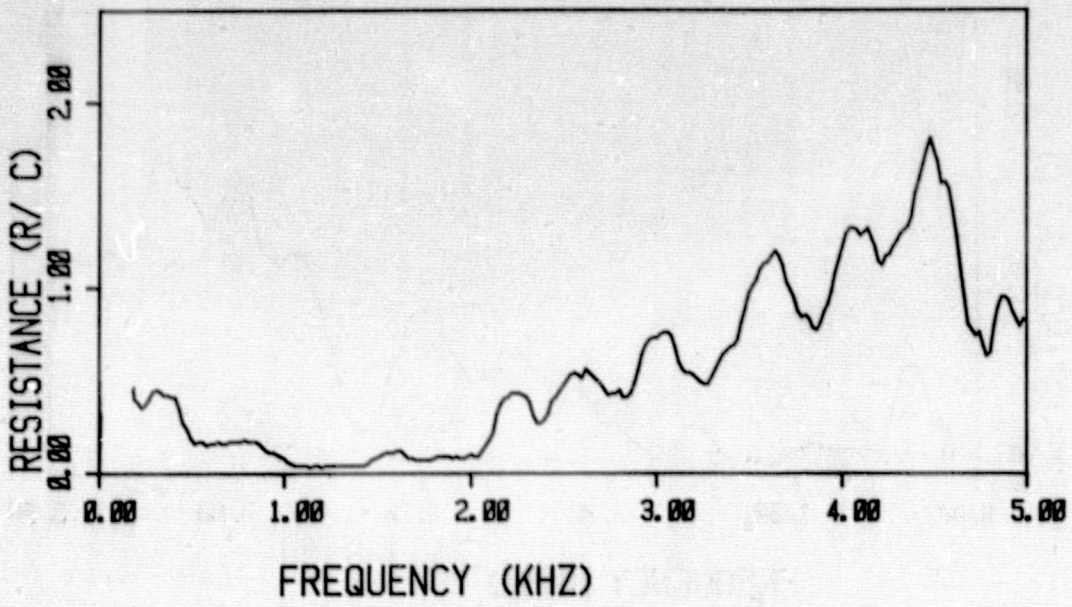


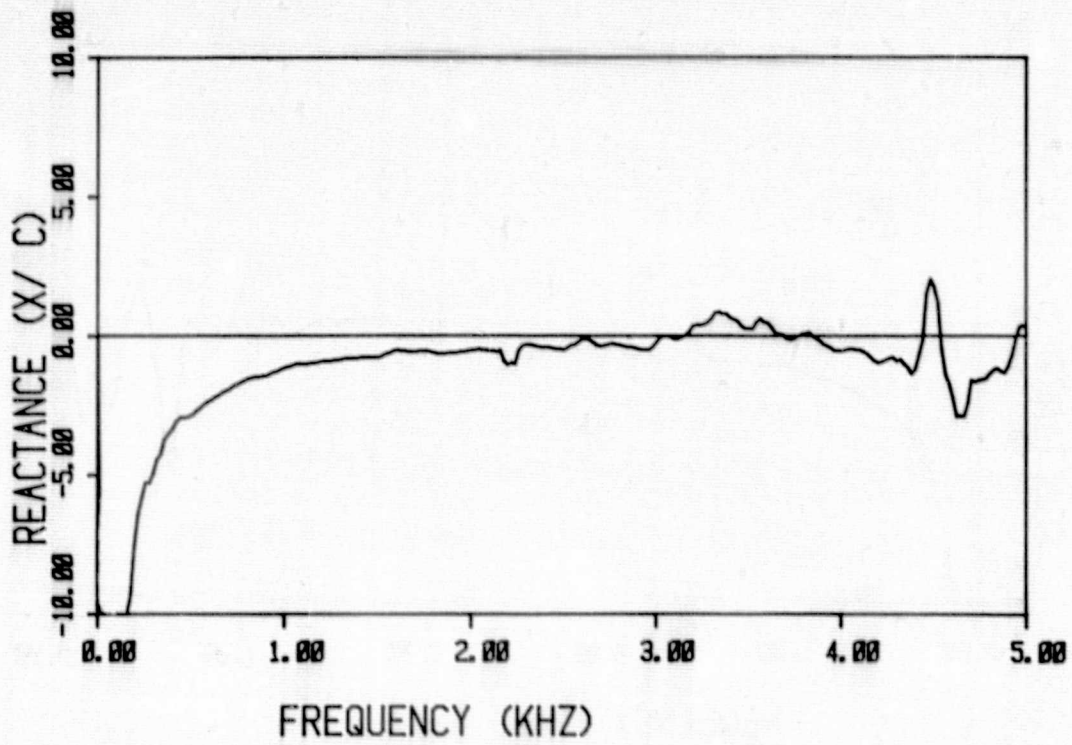


FIG. 61 WALL IMPEDANCE FOR LINER B1 AT BIAS FLOW LEVEL OF 75 %.

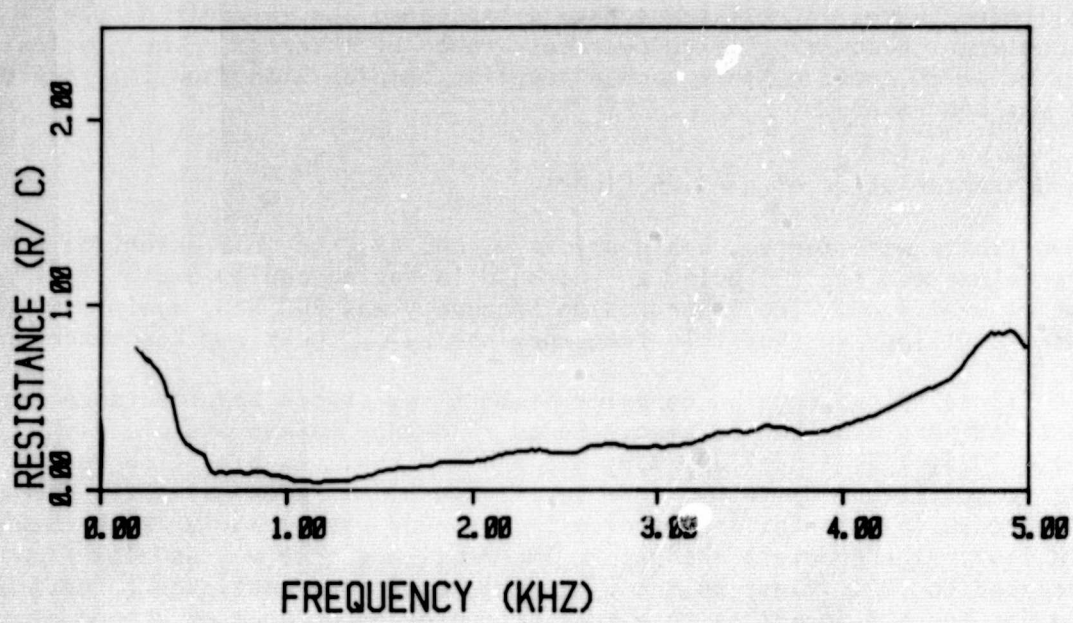


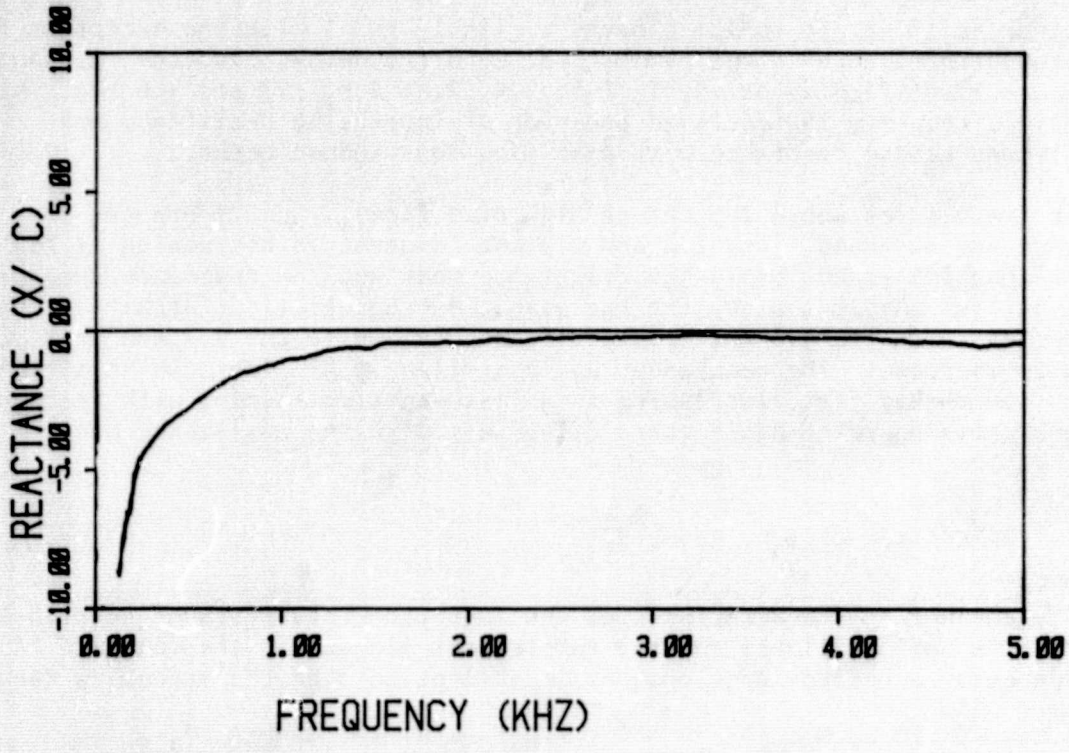


FIG.62 WALL IMPEDANCE FOR LINER B1 AT BIAS FLOW LEVEL OF 100 %.

crossings correspond well to the resistance humps which is indicative of a real effect and not just random scatter. The 100% bias flow is notable in that all minor humps in resistance have disappeared and in addition the reactance *never* becomes positive over test range of interest. The physical mechanisms which could exhibit such a peculiar complex bias flow interaction is not yet understood.

### 4.3.3 Characteristics of $\eta = 0.25$ Liners

Two liners were tested, designations A1 and A2, the only essential difference between the two being an increase in facing cavity depth of A2 over that of A1 by 1.3 cm. The liner design frequency was 500 Hz , again similar to the $\eta = 1.0$ liner in that this frequency was below the first resonance point.

In figure 63 the regular behavior of both resistance and reactance with frequency at zero bias can be seen. Seven resonance points are clearly defined at 0.6, 1.2, 1.8, 2.25, 2.9, 3.5 and 4.2 kHz. As bias flow is increased to 50% (figs. 63 to 65), the resistance peaks reduce slightly and a small increase in resonant frequencies is observed particularly at the higher frequencies*. The greatest changes in impedance are observed as bias flow is increased to 100% (figs. 66 and 67). The resistance continues to decline and the reactance degenerates to a weak frequency dependence of around $\pm 1\rho c$, again such that, in a similar manner to the $\eta = 1.0$ liner, the anti-resonance zero crossing of reactance, are associated with resistive peaks.

Liner A2 (figs. 68 to 72) behaves similarly to A1 with the exception that the resonant structure is not symmetrical with frequency, viz. the resonance points are identified as at .5, 1, 1.6, 2.4, 2.8, 2.9, 3.7 and 4.6 kHz. At the design frequency the designed behavior of increasing resistance and slightly decreasing reactance with bias flow does indeed occur.

At frequencies above 2.5 kHz at high bias flows, radical changes in impedance are observed. The 2.8 and 2.9 kHz resonant points vanish at 75% bias, with a 50% reduction in the resistance peak and the reactance remaining well negative. At 100% bias, the resistance decreases still further at these frequencies (also the 4.6 kHz resonant frequency) while the 3.7 kHz peak begins to increase. The reactance, again similar to A1 liner, in this region becomes remarkably flat, increasing in a less negative fashion with frequency, the zero crossing point again correlating well with the resistance peak.

## 4.4 INTERPRETATION OF I.L. RESULTS

The dominating characteristic of the insertion loss tests of section 4.2, both for the uniform liners and the two-segment liners was the complete lack of evidence of expected large changes in absorption over the extensive range

---

*In general, all frequencies above 4 kHz should be treated with caution and in particular above 4.5 kHz as the anti-aliasing filter roll-off of the FFT analyzer influences this region.*

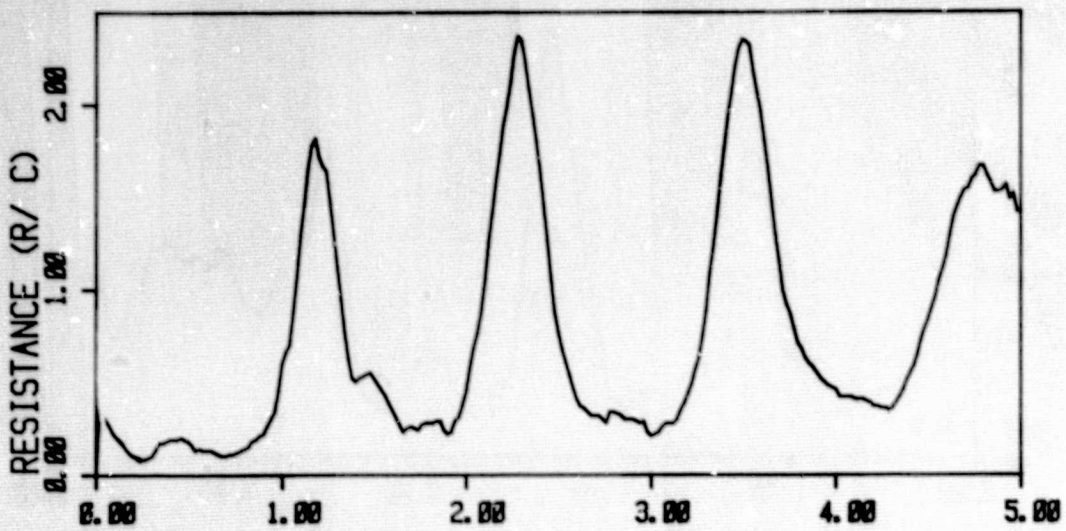


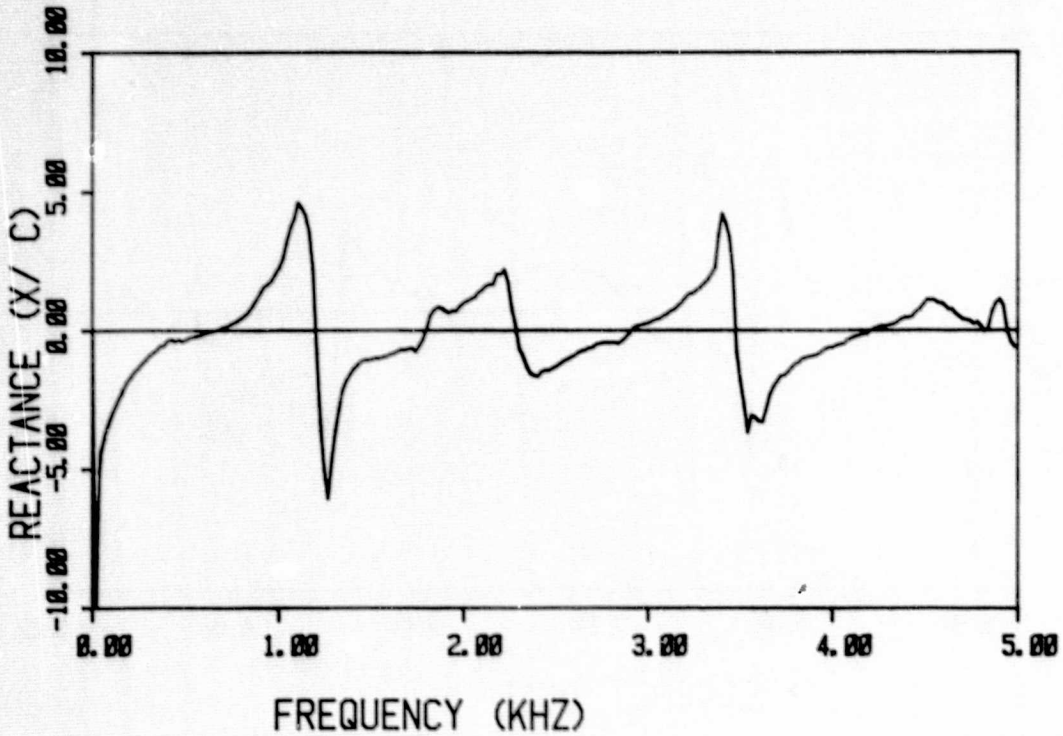


FIG. 63 WALL IMPEDANCE FOR LINER A1 AT BIAS FLOW LEVEL OF 0 %.

C-2

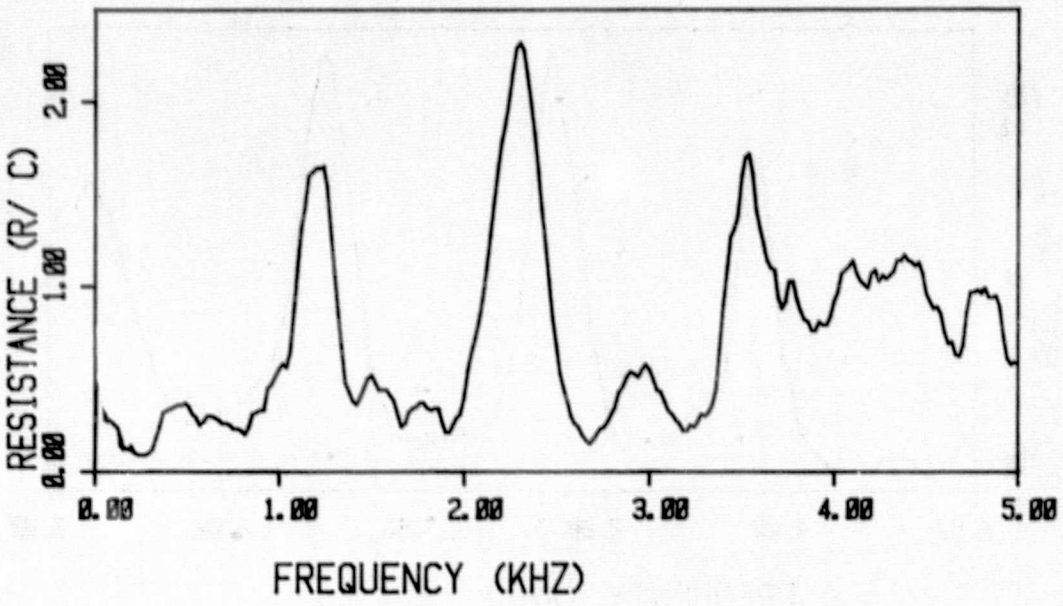


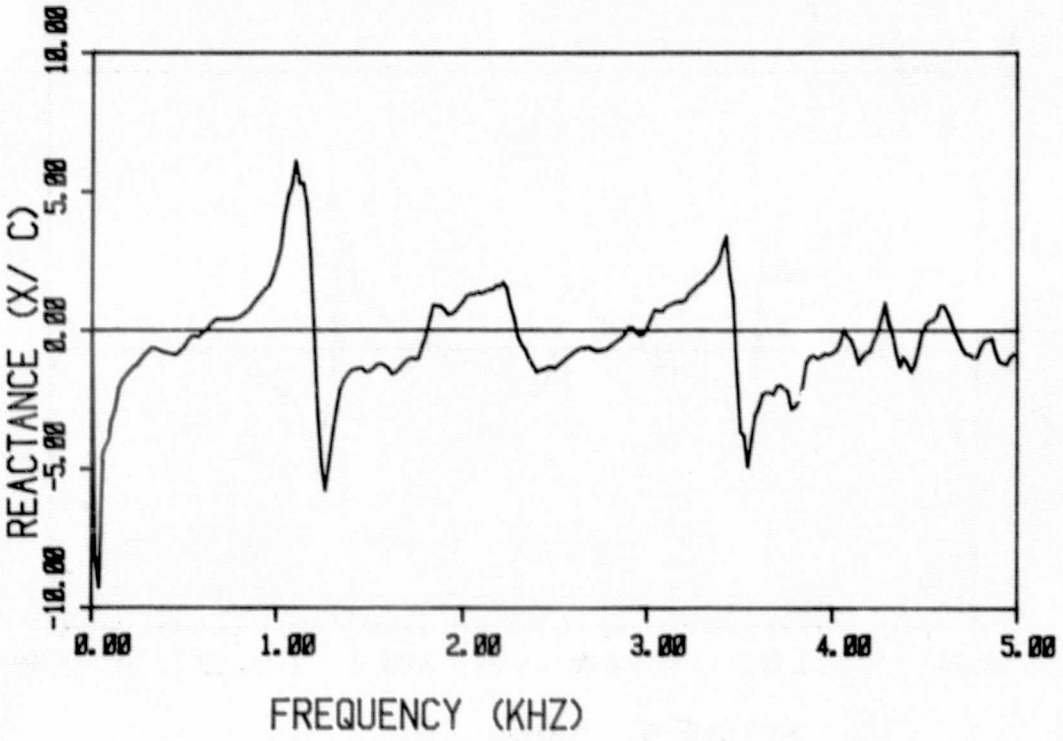


FIG. 64 WALL IMPEDANCE FOR LINER A1 AT BIAS FLOW LEVEL OF 25 %.

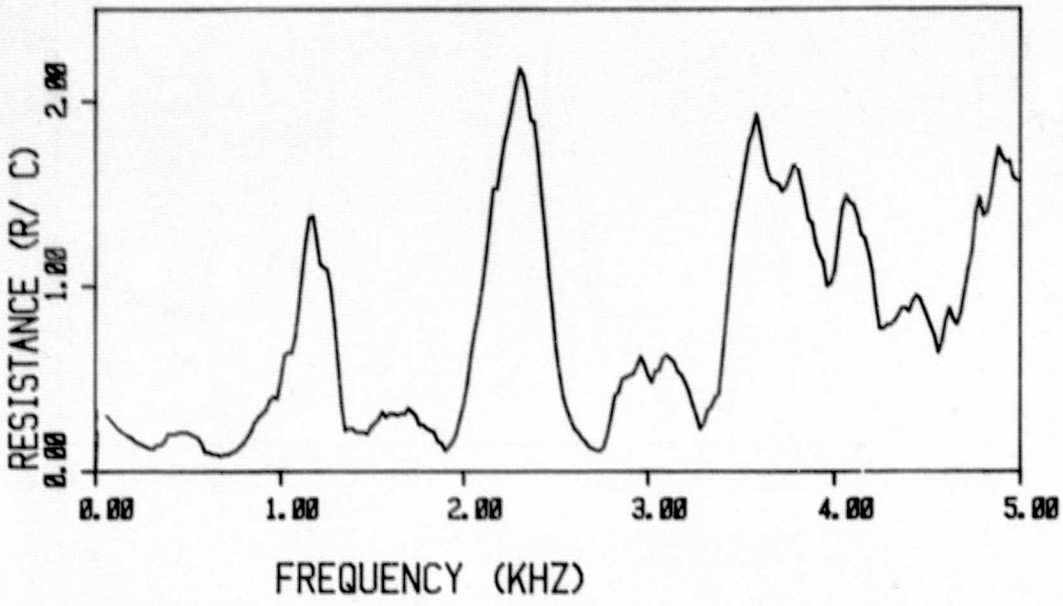


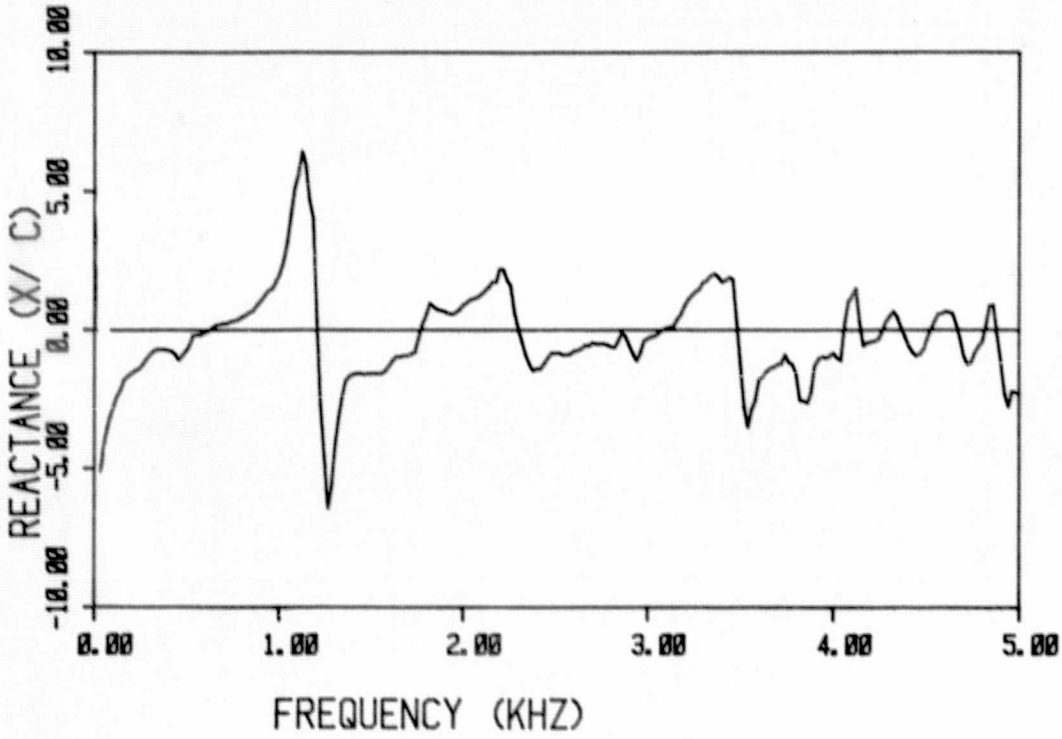


FIG. 65 WALL IMPEDANCE FOR LINER A1 AT BIAS FLOW LEVEL OF 50 %.

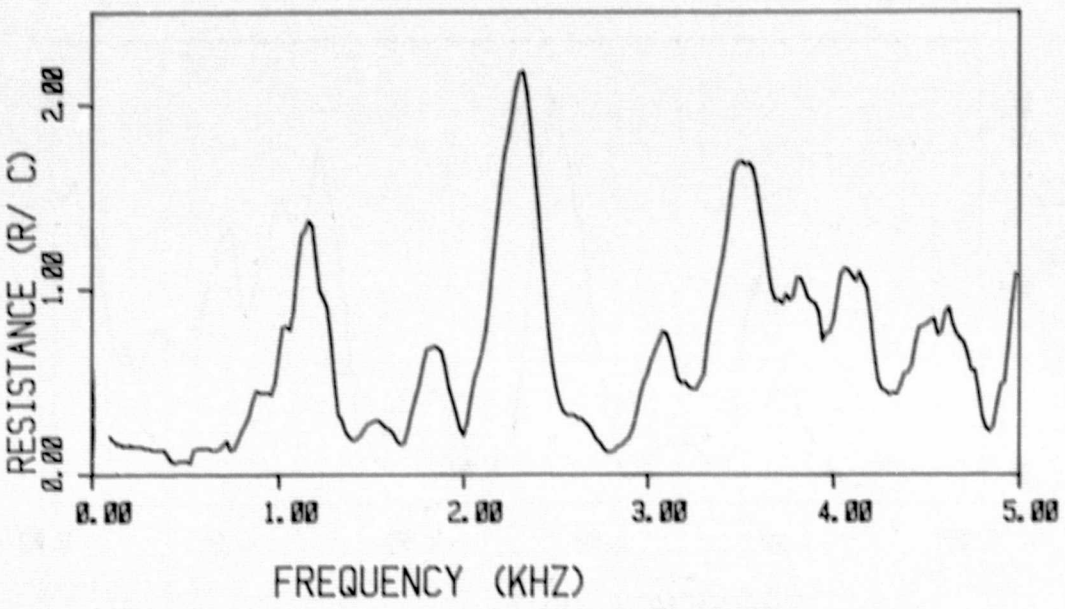


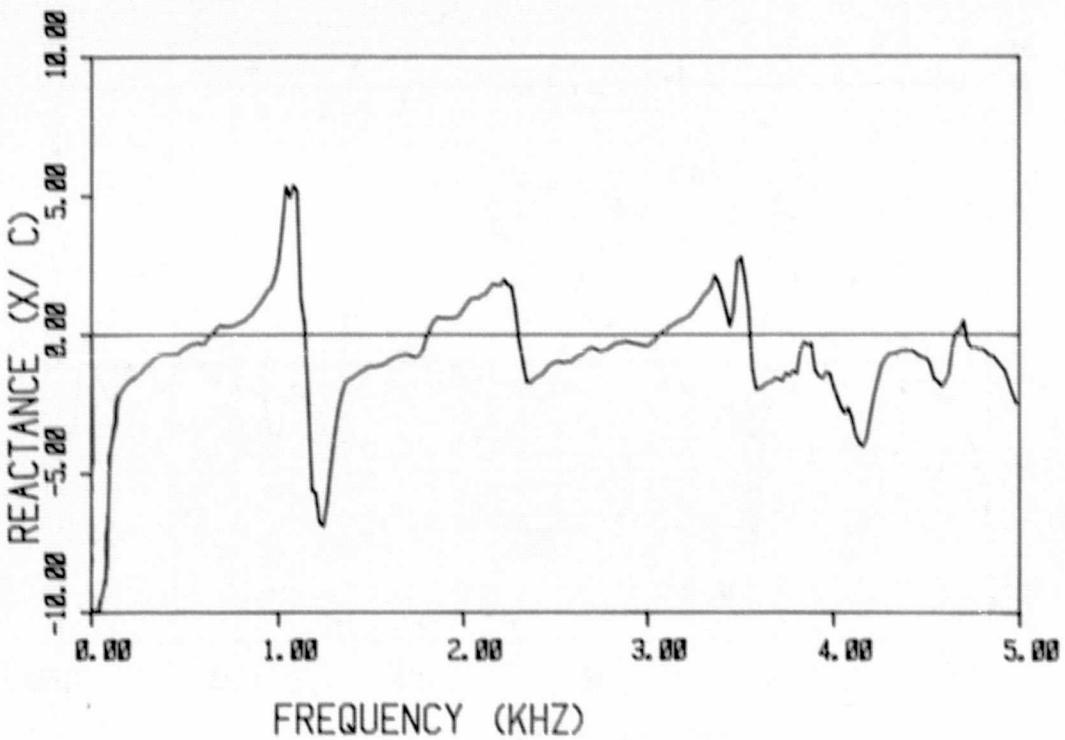


FIG. 66 WALL IMPEDANCE FOR LINER A1 AT BIAS FLOW LEVEL OF 75 %.

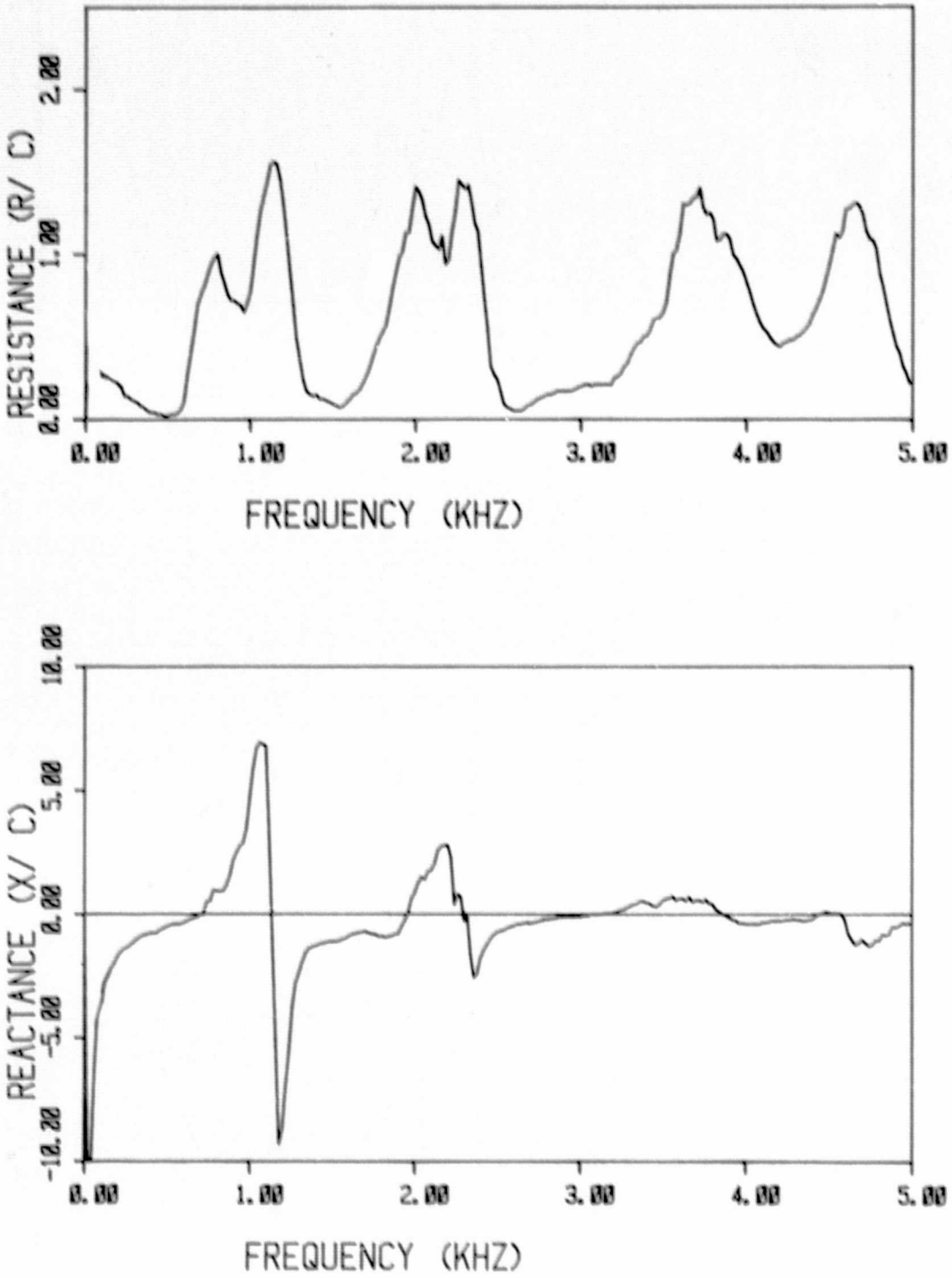


FIG. 67 WALL IMPEDANCE FOR LINER A1 AT BIAS FLOW LEVEL OF 100 %.

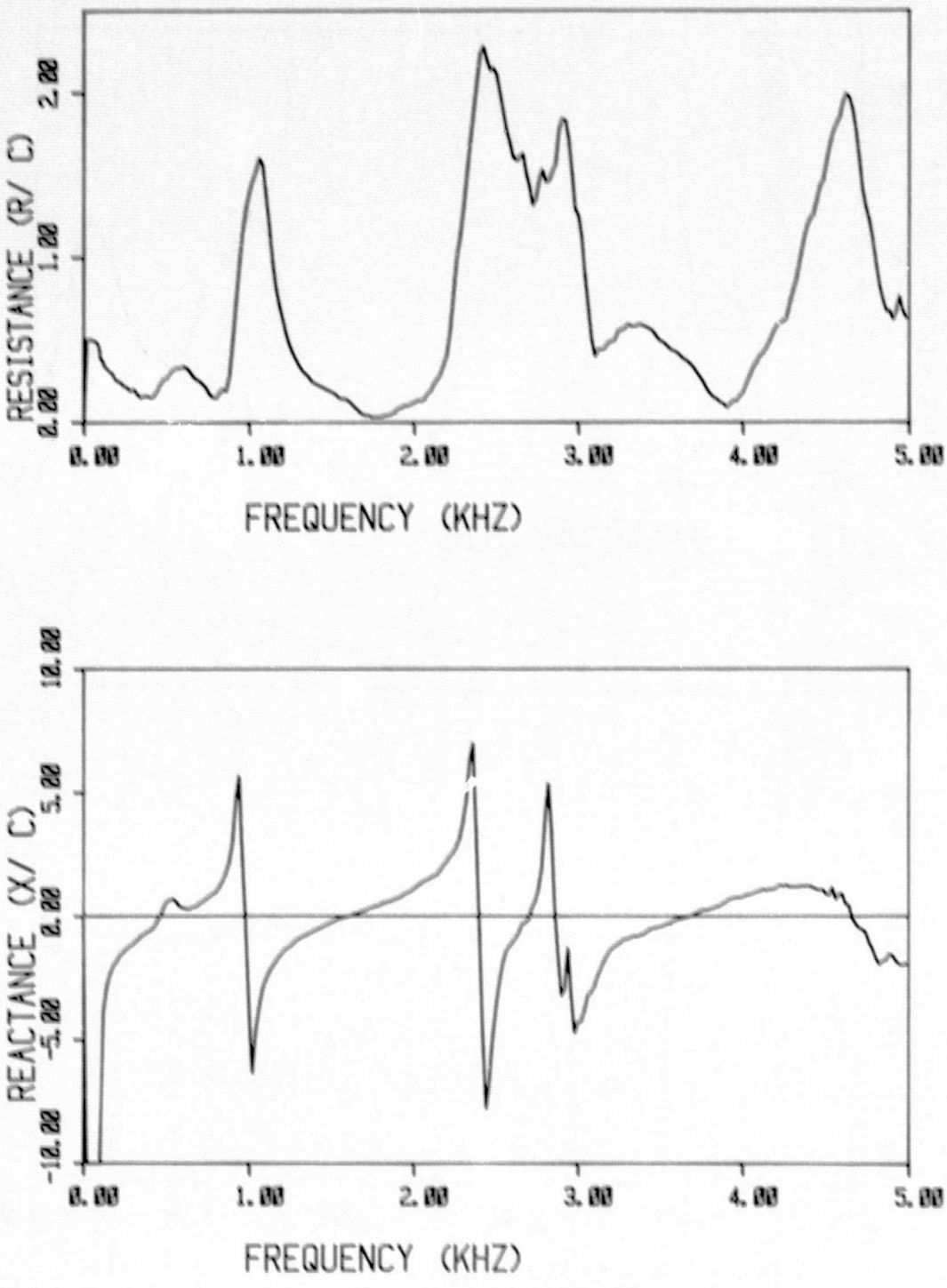


FIG. 68 WALL IMPEDANCE FOR LINER A2 AT BIAS FLOW LEVEL OF 0 %.

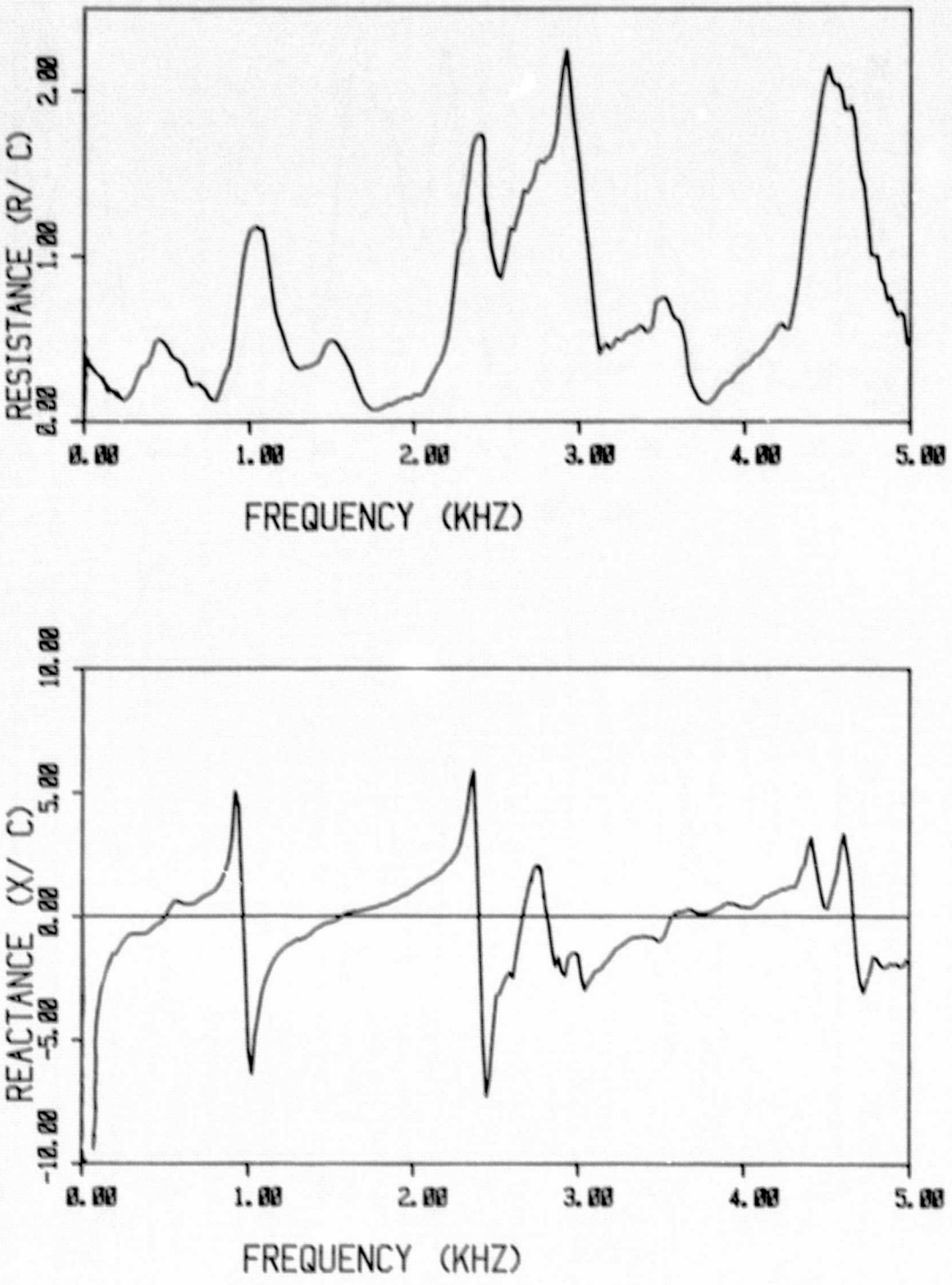


FIG. 69 WALL IMPEDANCE FOR LINER A2 AT BIAS FLOW LEVEL OF 25 %.

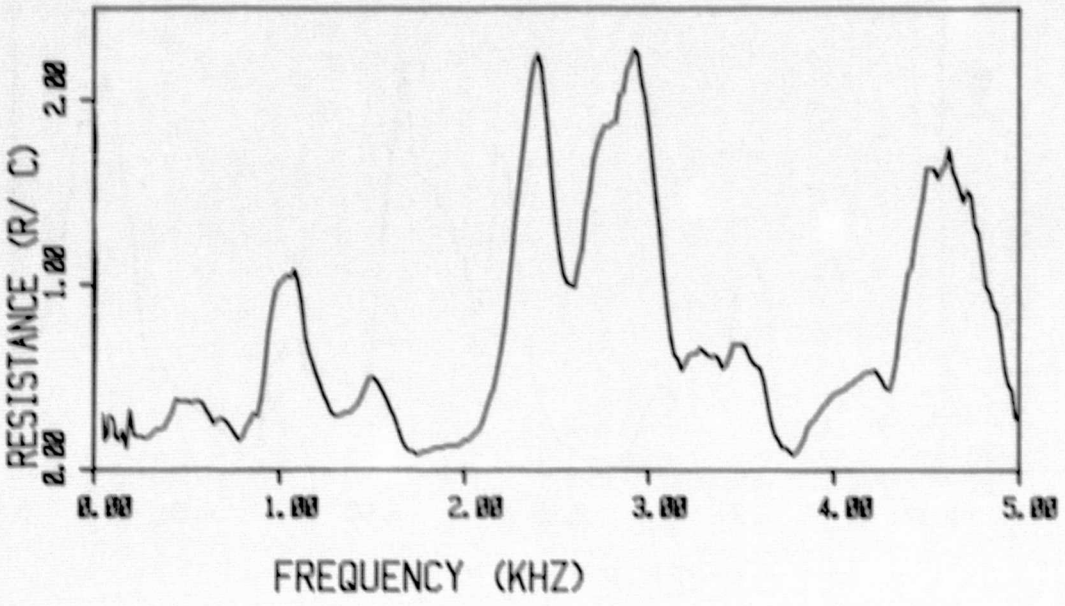


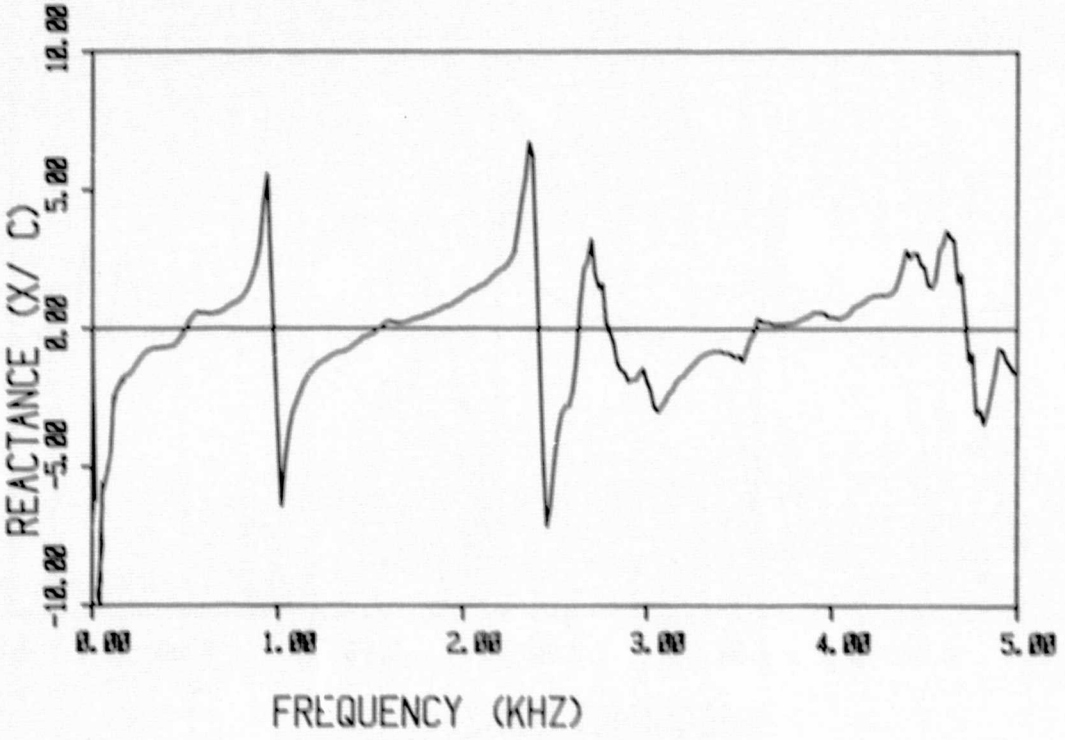


FIG. 70 WALL IMPEDANCE FOR LINER A2 AT BIAS FLOW LEVEL OF 50 %.

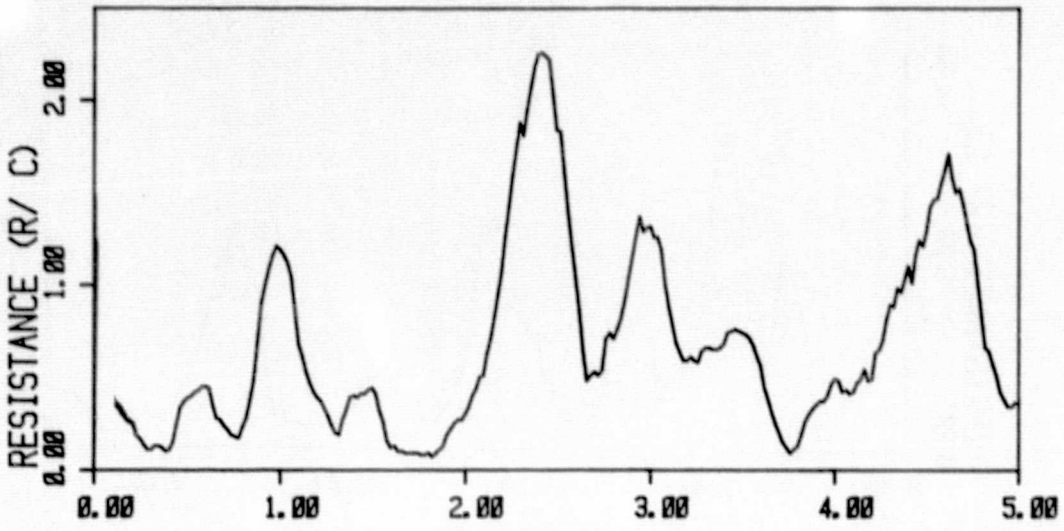


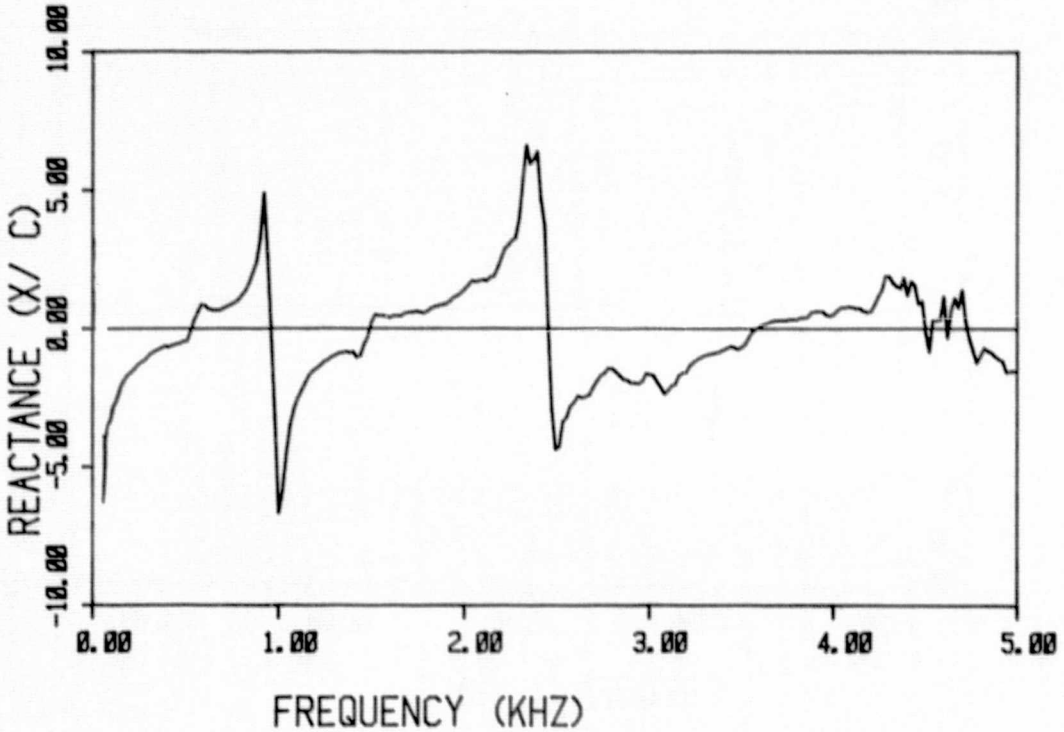


FIG. 71 WALL IMPEDANCE FOR LINER A2 AT BIAS FLOW LEVEL OF 75 %.

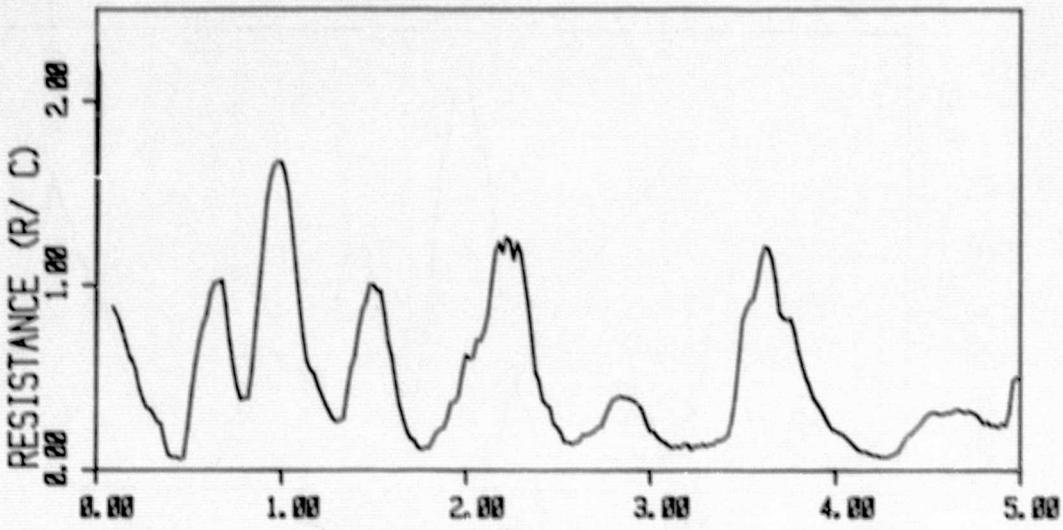


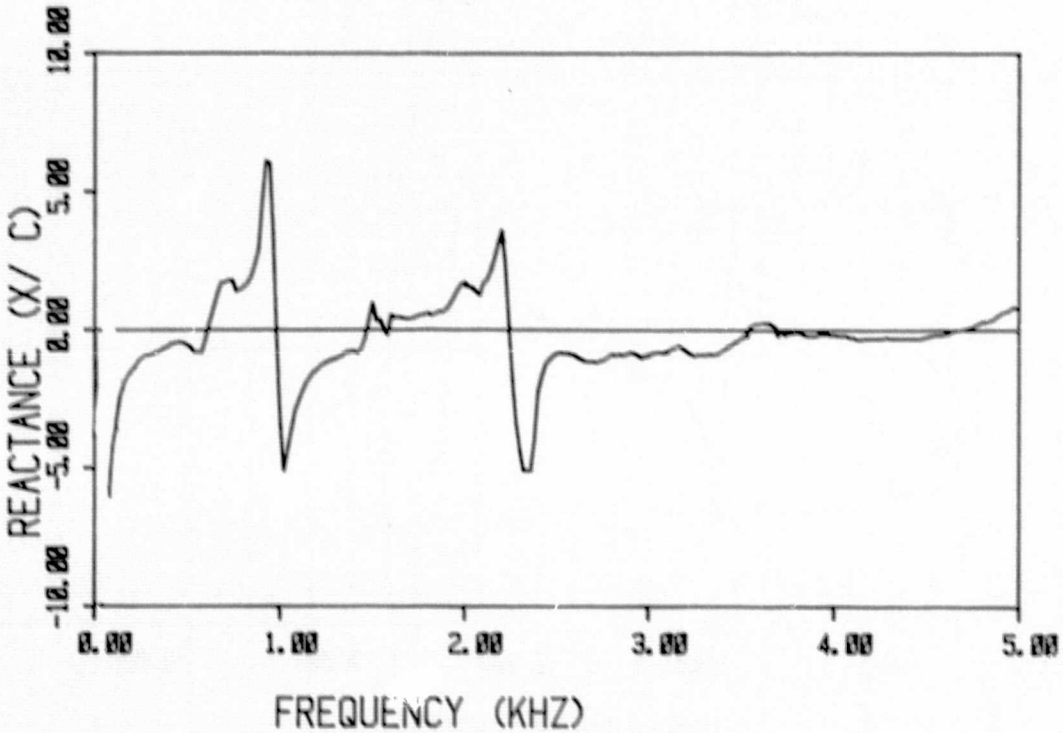


FIG. 72 WALL IMPEDANCE FOR LINER A2 AT BIAS FLOW LEVEL OF 100 %.

of bias flows tested. For the $\eta = 1.6$ liner, the maximum improvement in I.L. observed was 1 dB, with a maximum degradation of 3-4 dB. Similarly, the $\eta = 1.0$ and 0.25 uniform liners showed improvements in I.L. of 1 and 2 dB, with maximum reductions of 3 and 2 dB, respectively. The two-segment liner performed marginally better showing 2 dB increase in I.L. over a broader bandwidth, and maximum reductions of 2 dB in the worst case. Thus, it is not surprising that the bias flow optimization procedure could not converge with such weak changes in I.L. when considered on a 1/3-octave basis. Three hypotheses for this behavior can be identified and are discussed below.

### 4.4.1 Hypothesis I: Non-optimum Design Wall Impedance

A possible cause for this I.L. behavior is that the wall impedance was not the "optimum" value for the incident modal mix at the design frequency. If the assumption is made that only the plane wave or perhaps the next two lowest mode orders exist, then a clue to the validity of this argument can be obtained from the I.L. spectra. For example, the $\eta = 1.6$ liner shows a marked I.L. valley of 10 dB at the design frequency which is analogous to the I.L. expected from a single layer resonant cavity liner in a single low-order incident mode situation. However, the $\eta = 1.0$ shows no such valley at the design frequency, but instead has I.L. valleys on either side. This would seems to indicate that the design wall impedance was indeed not optimum. The $\eta = 0.25$ liner does exhibit a small I.L. valley at the design frequency, however, its deviation (of about 3 dB) about the I.L. mean value is similar in magnitude to the deviations observed over the rest of the frequency range and thus cannot be considered as evidence of nonoptimal wall impedance at the design frequency. If the duct sould field modal mix is not known at all frequencies, it is *not* possible to determine whether or not a particular liner with wall impedance changes induced by bias flow will produce corresponding I.L. changes in *any* part of the spectrum, much less at a particular design frequency. As a consequence, it is not possible in this work to test this hypothesis.

### 4.4.2 Hypothesis II: Discrepancies Between Design and Actual Wall Impedances

The second possible cause of the lack of variation of I.L. to bias flow changes is the possibility that wall impedance changes are not being incurred, or if they *are* being incurred, at no values of bias flow, do they come close to the design values. The impedance measurements presented in Section 4.3 show conclusively that bias flow does indeed have the capability to induce massive impedance changes in conjunction with upward resonant frequency shifts in a manner entirely predictable from consideration of the general impedance model characteristics. However, it does remain to disprove the second part of the hypothesis, i.e. that at no value of bias flow do the measured values of wall impedance approach the design values.

Figure 73 shows a comparison of measured wall impedance values with the design values for the liner configurations tested. For the $\eta = 1.6$ liner (designation C1) excellent agreement can be seen in that the design value lies very close to 25% bias flow point on the characteristic line. For the $\eta = 1.0$

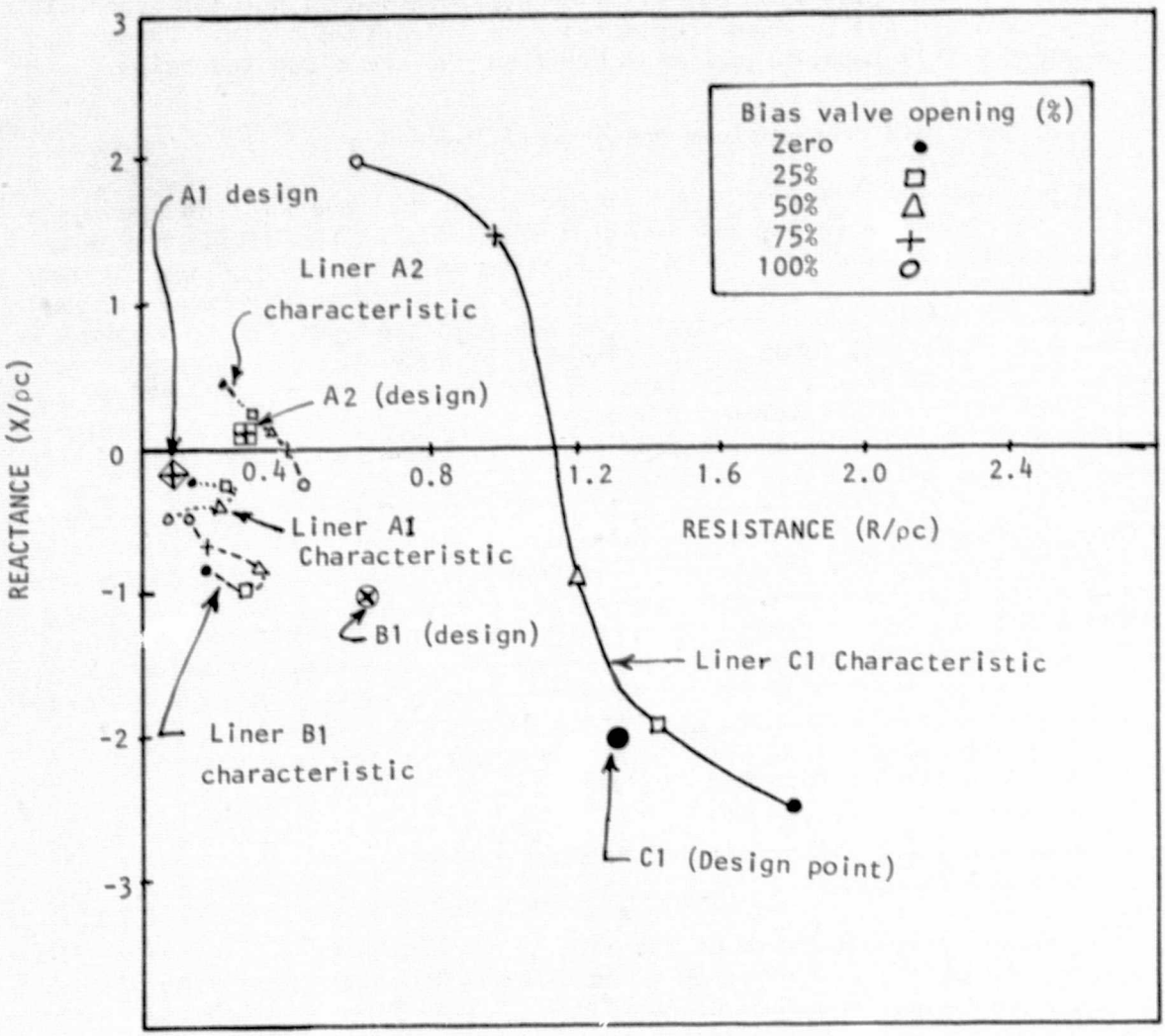


Figure 73. COMPARISON OF MEASURED WALL IMPEDANCE VALUES AND DESIGN VALUES

case (liner designation B1), the measured reactance values show good agreement, however, the measured resistance values are too low (the closest measured value is 0.3 ρc at 50% bias compared to the design value of 0.6). Inspection of the measured impedance spectra (see fig. 60, for example) shows that in this region the resistance is rising rapidly with frequency and that the design resistance value could be reached by an increase in frequency of only 200 Hz. This would correspond to a design η value of 1.1.

The liner designation A1 ($\eta = 0.25$) has the distinction of having the lowest design resistance of all, namely 0.11 ρc. This condition was closely approximated by the 100% bias flow point on the characteristic curve. However, the reactance value at this condition was more negative (-.5 ρc) than the design value (-.15 ρc) due to the increase in resonant frequency at this high level of bias flow. A small increase in frequency of 50 Hz would achieve this reactance value and correspond to a modified η value of 0.27.

This liner design highlights the difficulties associated with design impedances near the first resonance point. In a single cavity liner, resonance implies high acoustic velocities in the vicinity of the facing sheet, which absorbs energy by viscous dissipation. This implies, in turn, a peak in resistance at this frequency. Thus, very small resistances which approach zero are difficult to achieve in practice unless very large facing sheet porosities with accompanying degradation in structural integrity are permissible.

The second segment of the two-segment design for $\eta = 0.25$ was designated A2 and its design resistance was much larger (0.27 ρc) than that of liner designation A1 above. The measured bias flow characteristic for this liner almost passed through the design point at the 50% bias flow level. This close comparison is probably responsible for the insertion loss maximum observed at this bias flow level for the two-segment liner.

From the above comparison, it can be concluded that within the available range of bias flows the measured values of wall impedance do closely approach the liner design values (for liner designations A2 and C1 the values lie virtually on the bias flow characteristic). As a consequence, it is not possible to ascribe the lack of I.L. response to bias flow changes to this cause and the second hypothesis is thus invalidated.

### 4.4.3 Hypothesis III: Higher Mode Orders

The reverberant source chamber in the facility will excite all possible energy carrying modes in the hard wall entrance section of the duct. These modes and their respective cut-on frequencies have been tabulated earlier in Table III in this section. At the η value of 0.25, two higher modes are cut-on, while at $\eta = 1.0$, nineteen higher modes are cut-on. At the highest design η value of 1.6 in excess of thirty modes could exist.

The basis of the hypothesis is that there will exist higher modes in the lined section of the duct which are weakly attenuated at all levels of bias flow *and* which carry significant amounts of energy. That is to say, the specified design impedances will strongly attenuate low mode orders, but only weakly affect higher-mode orders. If equi-partition of energy is assumed, the

obvious net result will be only a very small I.L. change with change in bias flow. This phenomenon is further complicated by the fact that not only can acoustic energy be carried by an individual mode (termed self-modal energy) but can be carried also by the cross product terms between modes (cross-modal energy), which in themselves will also have an associated optimum wall impedance. For a comprehensive discussion of this aspect of modal power flow relationships, reference 4 contains a complete analysis.

The design impedances specified by NASA for the two lowest $\eta$ values (0.25 and 1.0) were based on plane wave propagation only, while the $\eta$ value of 1.6 was based on the first three two-dimensional modes of propagation, [i.e. (1,0). (2,0) and (3,0)], each in phase and with identical amplitude. It would be remarkably fortuitous if these design impedances were also the optimum values for all the remaining possible modes (defined in Table III). Thus, it appears extremely likely that higher modes carrying considerable energy will exist with the result that the measured I.L. will be largely unaffected by bias flow induced impedance changes. An *indication* of the existence of higher-order cross-modes can be seen in figure 74 where pressure and phase traverses across the duct at the design frequency for the $\eta = 1.0$ liner is shown. The characteristic pressure minima and 180 degree phase reversal clearly indicates the dominance of the first-order cross-mode. It is considered that this hypothesis is the correct one, but absolute proof can only be obtained from a complete modal analysis in the duct, which was outside the scope of this work.

The insertion loss measurements of the two segment liner (designations A1 and A2) were an attempt to evaluate the concept of phase treatment. The work of reference 4 clearly shows that successful operation at one specific frequency requires specific intermodal amplitude and relative phase relationships at the entrance of each lined segment. Thus, if the modal mix is known in the hard-wall section (which it is not in this work), the required phase relationship will exist at one particular distance from the duct entrance dependent on the mode axial wavenumbers. In addition, the second segment amplitude and phase requirements can only be met with a particular lined length of the first segment based on the modal wavenumbers within that section which are wall impedance *and* frequency dependent. Reference 4 stresses the extreme sensitivity of the phase treatment concept to relative modal amplitudes and phases and further shows that as much as 100% changes in wall impedance could be required to achieve optimum attenuations for the simple extremes of two modes either in phase or 90° out of phase. These optimum attenuations themselves were shown to vary by as much as 10 dB with less than a 30-degree phase change between the two modes at the entrance to the lined segments.

Thus, it does not appear surprising, that for the undefined multi-mode finite band width situation present in this work that the phase treatment concept shows no significant advantage over the uniform liner I.L. measurements.

### 4.4.4 Hypothesis IV: Widely Separated Modal Optima

This hypothesis can be considered as a corollary of the previous one. In essence, it postulates that in a multi-modal situation the individual modal

optima are so widely scattered on the impedance plane that it may be impossible to find an *overall* optima no matter where the liner impedance is moved about in its plane. This phenomenon makes no distinction between low and high mode orders per se, but could appear between adjacent modes for example. It was not within the scope of this work to examine this possibility analytically, however it is felt that the influence of this effect is less significant than that of Hypothesis III.

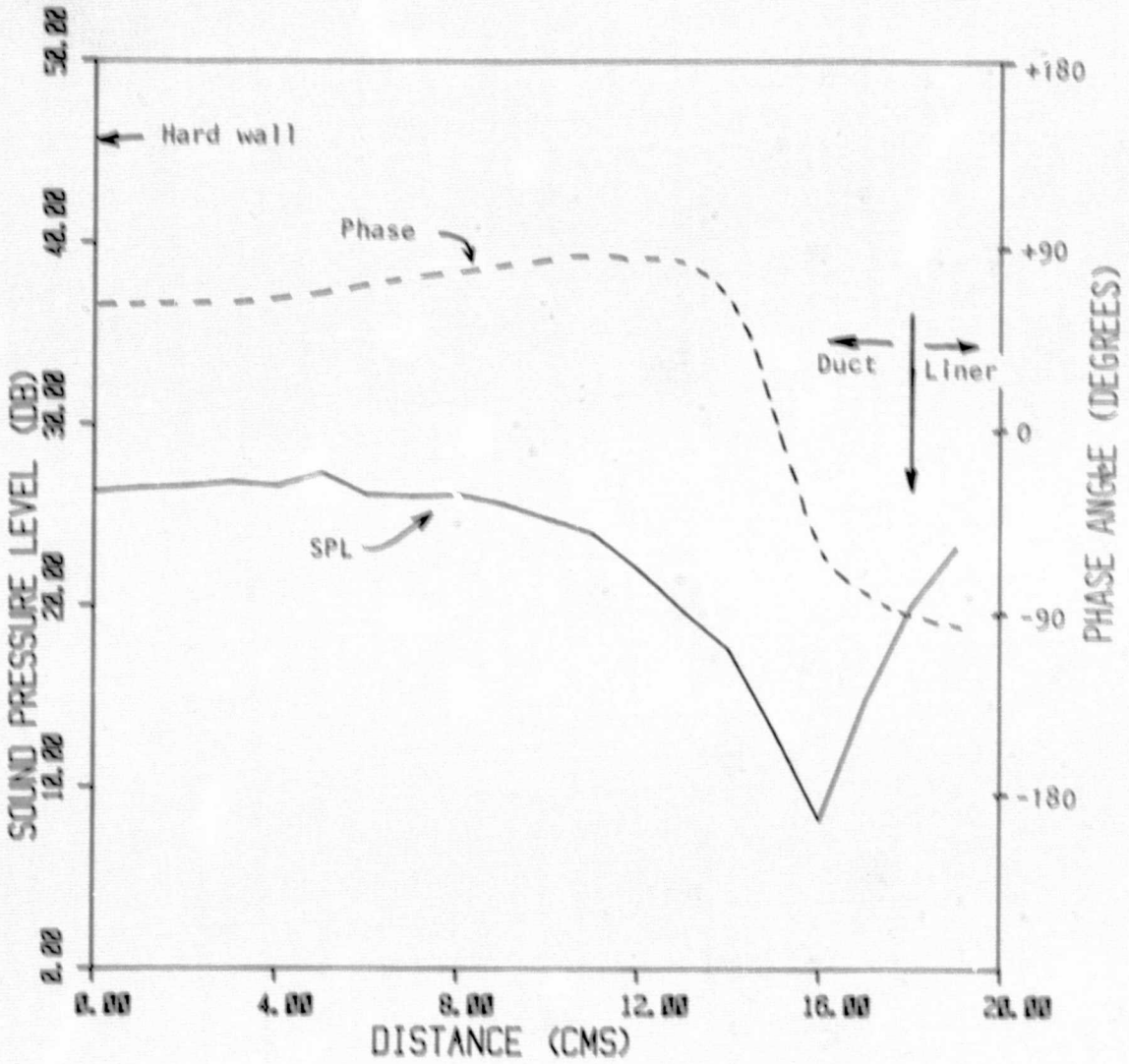


FIG. 74. SPL & PHASE TRAVERSE ACROSS DUCT FOR LINER B1 @ 2 KHz

# 5. SYSTEM CONCEPT CHARACTERISTICS AND LIMITATIONS

It is apparent from the discussion in the previous section that the basic system requirement for the existence of an insertion loss maxima within the range of wall impedance variations with bias flow was not met. The probable cause of this was the presence of higher-order energy carrying modes with low attenuation rates for the design impedances specified. These design impedances were based on the assumption that the low-mode orders contained the dominant portion of acoustic energy. This situation did not appear to exist; consequently, the systems concept for liner design optimization could not be exercised such as to evaluate its feasibility as a design tool.

Even if the wall impedance was "optimally" specified for the incident modal mix (which must be measured a priori) the range of impedance variation with bias flow is a limited quantity and a good "ball park" initial impedance choice is very critical. It is possible that other liner design configurations could be devised which would improve the range of impedance variation and thus be more effective in the execution of the concept. It is considered that the system concept is still valid *but* that refinements for initial impedance choice must be made to reflect the actual modal mix, and thus ensure a reasonable degree of confidence in operation.

The system concept appears to offer no limitations in principle to the evaluation of the phased liner concept, *provided* that the incident modal structure is known and allowed for in the initial impedance choice. Since the analysis of reference 4 indicates extreme sensitivity to intermodal wavenumber, the implication is that phased liner concept validation should be initially undertaken only with low (i.e. 1 or 2) mode orders at frequencies well away from cut-on.

The ultimate result of the system concept is the determination of the "optimized" wall impedance. The multiple microphone technique, as incorporated in the system, convincingly demonstrated its capability to perform this measurement both in the presence of multiple modes in the duct, and bias flow through the liner. The technique achieved an unprecedented degree of precision and speed in impedance evaluation over a wide frequency range by the use of narrow-band coherent transfer function analysis applied to random noise excitation in the duct.

In summary, then the system was limited in attaining the work objectives by the presence of energy carrying higher order modes. Related to this was the inability of the liners, at their design impedances, to attenuate these modes. The solution, in the form of recommendations for future work is in two parts:

(1) To reduce the duct dimensions to 18 cm square cross-section. This would enable the system to work with the existing liners in the environment of low acoustic mode orders for which they were designed. Individual power flow could be verified by a modal analysis.

(2) To develop a set of variable impedance liners which have known impedance ranges with bias flow and attempt to maximize these ranges. This would enable the concept effectiveness to be extended to cover those acoustic situations where modal mixes are unknown and the initial design choice of wall impedance happens to be far from optimum.

# 6. CONCLUSIONS

A systems concept procedure for the optimization of acoustic duct liner design for both uniform and multi-segment liners was developed and implemented using as a basis, a double reverberant chamber flow duct facility. The implementation included sophisticated computer control and acoustic analysis systems which included (1) insertion loss measurements, (2) duct liner in-situ wall impedance controls, (3) duct liner in-situ wall impedance measurements, and (4) duct air flow controls.

The validation of the systems concept was limited by the inability to optimize the insertion loss using bias flow induced wall impedance changes. This inability appeared to be a direct function of the presence of higher-order energy carrying modes which were not influenced significantly by the wall impedance changes.

The application of the bias flow concept to multi-cavity liner design, induced significant and potentially useful wall impedance changes over the test frequency range (zero to 5 kHz). However, the specified design impedances and the accompanying induced range of wall impedance appeared to be outside the optimum region for total energy insertion loss.

The multiple microphone technique for in-situ wall impedance measurements was successfully adapted to automated measurements for a multi-cavity liner with bias air flow through it. This technique as implemented with random noise excitation enabled a data base to be obtained using virtually simultaneously measured wall impedance and 'nduced insertion loss.

## REFERENCES


1. Vaidya, P. G.; and Dean, P. D.: State of the Art of Duct Acoustics. AIAA 4th Aeroacoustics Conference; Atlanta, Ga.; AIAA Paper No. 77-1279, October 1977.

2. Dean, P. D.; and Tester, B. J.: Duct Wall Impedance Control as an Advanced Concept for Acoustic Suppression, NASA CR-134998, 1975.

3. Dean, P. D.: An In-Situ Method of Wall Acoustic Impedance Measurement in Flow Ducts. *Journal of Sound and Vibration* 34(1), 1974, pp. 97-130.

4. Sawdy, D. T.; et al.: Analytical and Experimental Studies of an Optimum Multi-Segment Phased Liner Noise Suppression Concept. NASA CR-134960, 1976.